# POLITECNICO DI MILANO

SCHOOL OF INDUSTRIAL AND INFORMATION ENGINEERING

Energy Engineering Master of Science

# TECHNO-ECONOMIC ASSESSMENT OF A PUMPED HEAT ELECTRICITY STORAGE BASED ON CLOSED JOULE-BRAYTON CYCLE

Supervisor: Prof. Andrea Giostri
Co-Supervisors: Prof. Marco Binotti and Prof. Marco Astolfi

Author: Alessandro De Bortoli
Matricola: 913415

## Academic Year 2019 – 2020

# RINGRAZIAMENTI

Con il completamento di questa tesi concludo i miei cinque anni di studi in Ingegneria Energetica, iniziati con ingegneria meccanica Udine e poi spostatisi a Milano. Dopo questo lungo percorso ci tenevo a ringraziare tutte le persone che mi hanno aiutato ad andare avanti e a proseguire gli studi anche in momenti di difficoltà. Vorrei in particolare ringraziare:

I professori Giostri e Binotti che pur non essendoci mai conosciuti di persona, mi hanno dato la possibilità di scrivere questa tesi e anche per la molta pazienza, le idee e lo stimolo a portare a termine questa lavoro nonostante questo periodo difficile un po' per tutti

Il Professor Astolfi per aver partecipato alla tesi e anche per la molta passione trasmessami nel corso di Conversione dell'Energia.

Il Professor Dirk Sauer dell'università tecnica di Aquisgrana per avermi introdotto tramite un suo corso molto interessante alla tematica dell'Energy storage.

I miei genitori, la mia famiglia e tutti i miei amici per avermi sempre supportato e sopportato durante questi 5 anni, senza di voi probabilmente non sarei qui oggi.

Il mio amico Simone, che mi ha dato una mano per quanto riguarda alcune grafiche di questa tesi

Il mio amico Martino, compagno di discussioni Ingegneristiche e di stanza, senza di te la triennale sarebbe stata senz'altro più dura.

Infine un grazie in particolare a mio nonno paterno Sante, mi hai tramesso la passione per la matematica.

# INDEX

# List of Figures

# List of Tables

# EXTENDED ABSTRACT

## INTRODUCTION

While until 20 years ago the electricity supply relied mostly on dispatchable energy generation from traditional thermal power plants, today the complexity of the electricity system has increased with the integration of non-dispatchable and fluctuating renewable electricity generation. Many countries in the world have pledged to increase the share of renewable energy sources to fight climate change and global warming. European union for example has set to reach the target of 32.5% of renewable energy share in the energy final consumptions. To increase the share of renewable in the electricity sector, large-scale energy storage (ES) application will be needed in order to provide additional energy capacity to the system and supply electricity when there is no solar or wind energy generation. Current large-scale ES technologies like pumped hydro energy storage (PHS) or compressed air energy storage (CAES) though, do not represent a feasible solution to the problem due to their specific geological site requirements, plus for PHS there is concern on its high environmental impact. The is why in this thesis a novel ES technology is investigated called pumped heat electricity storage (PHES), which has the potential of becoming a promising solution to the large-scale ES challenge.

## PHES CONCEPT

Pumped heat electricity storage, or often referred to as pumped thermal energy storage or electro-thermal energy storage, is an ES system that allows to store electricity into heat. PHES takes electricity from the grid to drive a heat pump that stores thermal energy in a hot and a cold reservoir during charging, while during discharge the hot reservoir is cooled down while the cold one is heated up to drive a heat engine that generates electricity and gives it back to the grid. The basic concept of PHES is presented in Figure 0.1. On a low level of detail, the PHES is composed of a power block, the hot and cold thermal energy storages (TES) and an electric motor/generator.The efficiency of the system in storage application is called round trip efficiency (RTE) defined as the ratio of the net electrical work output over the net electrical input. PHES in literature is commonly classified based on the power block cycle, the three main categories are:PHES based on Rankine cycles, also called Compressed heat energy storage (CHEST), PHES based on transcritical $CO_2$ cyles and PHES based on closed Joule Brayton cycles

The focus of this thesis will be on PHES based on closed Joule Brayton cycles.

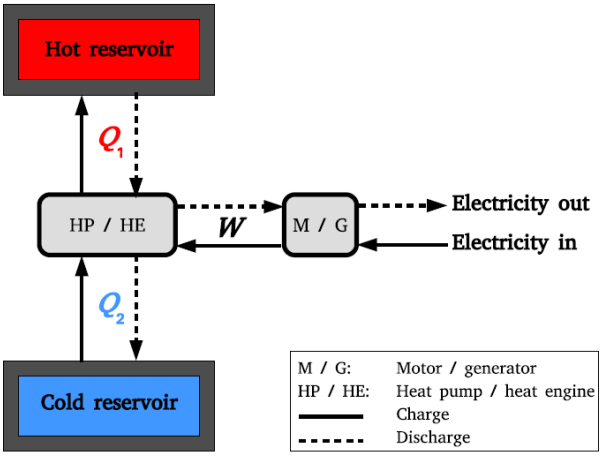


*Figure 0.1 Basic Principle of Pumped heat electricity storage* [1]

## PHES STATE OF THE ART

PHES concept was first developed by Marguerre [2] in 1924, which proposed a Rankine Based PHES which accumulated hot steam into insulated tanks. In 1979 Weissenbach [3] patented a PHES based on open air regenerative Bryaton cycles coupled with thermal reservoirs. In recent the topic gather new interest among the scientists and many publications were published (e.g. [4], [5], [6]) .

## PHES BASED ON BRAYTON CYCLES

This type of PHES is based on well-known closed Joule-Brayton cycle during discharge and on the reversed cycle during charge. The system is composed of:

- a hot and cold sensible heat reservoir, these could be in direct contact with the working fluid (packed bed storage system) or otherwise two heat exchangers are needed to exchange heat with the thermal storage unit (indirect TES)
- a set of compressor/expander machines, which could be turbomachines or reciprocating devices
- one or two auxiliary heat exchangers to exchange heat with the environment, which are needed for the dissipation of the irreversibilities generated in the cycle

In Figure 0.2 the plant scheme for a Brayton PHES is shown with an indirect liquid TES with $T_3=T_1$. Starting from point 1, in the charge phase the gas is compressed first reaching the maximum temperature ($T_2$), then it gets cooled (till point 3) heating up the hot reservoir, it is expanded (point 4)and finally it absorbs heat from the cold reservoir. During discharge the cycle is reversed and is a common closed Brayton cycle.

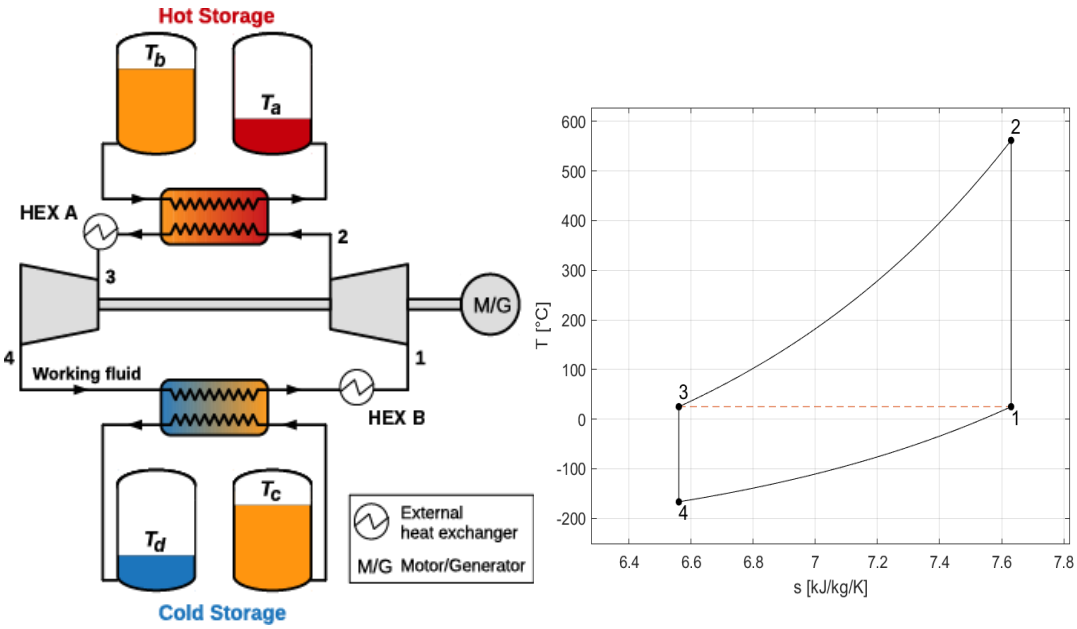


*Figure 0.2 Plant scheme* [1] *of a Brayton PHES with indirect liquid TES, arrows indicates the charge phase flow,ideal T-s diagram on the right:* $\eta_{pol}=1, \Delta T_{HEX}=0, \Delta p=0$, *with* $T_3=T_1$

A first comprehensive analysis was developed by Desrues [5], he developed a model for a PHES using packed beds, in which the hot TES operates between 1012°C (T2 ) and 25°C (T3 ) while the cold TES works between 500 °C (T1) and -70 °C (T4); the maximum pressure is 4.6 bar and the working fluid is argon. Considering a polytropic efficiency ($\eta_{pol}$) of 90% and taking into account the losses related to the operation of the packed bed TES, the RTE was 66%. Another important study is the model of White [4] who analysed the impacts of each single component irreversibility on the RTE. Howes [7] developed for the company Isoentropic Ltd [8]a small pilot system using packed beds TES and reciprocating devices as compressor and expander, he developed a preliminary analysis of 2 MW/ 16 MWh PHES and calculated an RTE of 72%. In the studies of Farres and Laughlin [1], [9] a Brayton PHES with indirect liquid TES, like the one in Figure 0.2, was investigated. They proposed to use the known technology of molten-salts employed in CSP to serve as the hot TES, while for the cold one they used a liquid hydrocarbon. Farres developed a numerical model and with the assumptions of 97% heat exchangers (HEXs) effectiveness, 1% of HEXs relative pressure drops and $\eta_{pol}$ of 90% the calculate RTE was 65% with an energy density of 46 kWh/m$^3$. The main advantage of using indirect liquid TES is that in this case the cycle can be pressurized to high pressures (134 bar in [1]) therefore using more compact and cheap turbomachines, in packed beds system this is not feasible because the packed bed tanks are at the same pressure of the cycle and for cost reason their maximum pressure cannot exceed 10 bar [10]. On the other hand, the use of indirect TES increases the complexity of the plant scheme introducing two heat exchangers with the reservoirs and also in some cases a regenerator.

## THERMAL ENERGY STORAGE

Thermal energy storage represents a key component of PHES. In Brayton PHES, which is this thesis topic, the employed TES system is a sensible heat TES (SHTES). SHTES is the most known and cheap way of storing heat, it stores energy by increasing the temperature of the storage material. The preferrable materials are the ones with a high specific heat capacity and a high density, plus the stored heat is proportional to the temperature difference between the initial and final TES temperature. Usually if solids materials are used, the TES is in direct contact with the working fluid, while if liquids materials are used heat is exchanged indirectly using a HEX. A solution for solid SHTES is the use of packed-beds system which consists of tank filled with spheres of the storage material, with a particle size of 0.5mm to 100mm [11], this solution is the most employed in PHES system because it has the advantage of being suitable for very wide operational temperature (from -200°C to 1000°C) and of having a low temperature difference between the fluid and the storage material.

Regarding SHTES with liquid materials, the most common TES architecture consists of a two-tank storage system and a HEX to exchange heat between the working fluid and the storage medium. Brayton PHES requires a hot TES that is able to reach high temperatures, therefore molten-salts are currently the most advanced technologies in the field of high temperature liquid SHTES and they have been widely tested in the field of concentrated solar power application as TES [12], for plant size from 20 to 150 MW with a storage time of 4 to 15 hours. They are composed of a of a mixture of 60% wt sodium and 40% wt potassium nitrate ($NaNO_3/KNO_3$) and are liquids from 290°C to 565°C [12] at a pressure of 1 bar. They have the advantage of having a low environmental impact and a relative low cost per unit of energy stored compared to other liquids like synthetic oils [1]. The only drawback is the solidification risk which occurs at temperatures lower than 270°C which requires that their temperature must always be kept above this limit.

Concerning the cold TES, the fluids that could be suited for PHES application the one that are liquid for temperature ranges between -100 °C to 25 °C and at a vapor pressure lower the 1 atm, this kind of fluids are all hydrocarbons or derivatives of them. In this thesis model, methanol was chosen as cold storage liquid, because of its temperature range and its quite cheap cost compared to other hydrocarbons derivatives.

## BASIC THERMODYNAMIC CONSIDERATION FOR PHES

To address the achievable RTE of Brayton PHES with indirect liquid TES the effect of each single component irreversibilities were analysed while the others were are assumed as ideal. At first the irreversibilities linked to compression and expansion processes were investigated, in a simplified way the RTE can be expressed by following formula:

$$RTE = \frac{W_{net,dis}}{W_{net,ch}} = \frac{W_{exp,id}^{dis} * \eta_{is} - \frac{W_{comp,id}^{dis}}{\eta_{is}}}{W_{exp,id}^{ch} * \eta_{is} - \frac{W_{comp,id}^{ch}}{\eta_{is}}} = \frac{WR_{ideal} * \eta_{is}^2 - 1}{WR_{ideal} - \eta_{is}^2} \quad (0.1)$$

Where WR is the work ratio , defined as $\frac{W_{comp}^{ch}}{W_{exp}^{ch}} = \frac{W_{exp}^{dis}}{W_{comp}^{dis}}$. From this basic equation it can be observed that RTE=0 when $WR_{ideal}$ is $1/\eta_{is}^2$ and that $RTE_{max} = \eta_{is}^2$ if WR $\rightarrow \infty$ therefore if $\eta_{is} = 0.9$ the maximum reachable RTE is 0.81.

The work ratio for an ideal Brayton PHES like the one shown in Figure 0.2 can be expressed as:

$$WR_{ideal} = \frac{T_2}{\tau_{is} * T_4} \quad (0.2)$$

where $T_2$ and $T_4$ are the maximum and minimum cycle temperatures, and $\tau_{is}$ is the charge compression temperature ratio. In Figure 0.3 the RTE calculated with a $T_2$ of 565°C for different values of $T_4$ and $\eta_{is} = 90\%$ is shown, as expected by the trend of the work ratio, the RTE decreases as $\tau_{is}$ and $T_4$ increase.

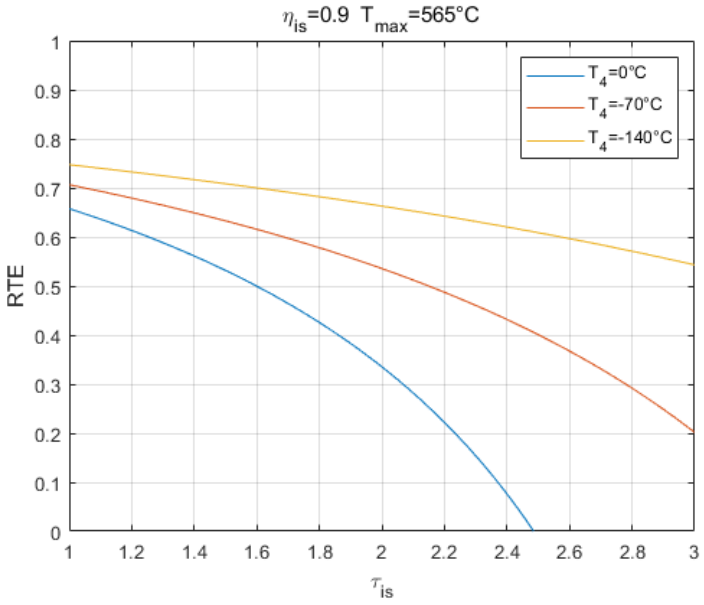


*Figure 0.3 RTE of PHES as function of $\tau_{is}$ and minimum temperature $T_4$ for a fixed maximum temperature $T_2$ of 565°C, heat transfer is considered ideal, Δp=0*

Moving to a more detailed analysis, for the real PHES cycle when considering only turbomachinery losses, the RTE is a function of τ , $T_3/T1$, polytropic efficiency $\eta_{pol}$ and τ′ (the quotation mark indicates that it refers to the discharge cycle) that is the discharge compression temperature ratio defined as T2'/T1', because in the real case charge and discharge cycle are not identical as shown in the T-s diagram in Figure 0.4. Note that in the discharge phase from point *3'c* to *3'* and from *1'e* to *1'* it occurs

the heat rejection to the environment through the two auxiliary heat exchangers HEXA and HEXB.

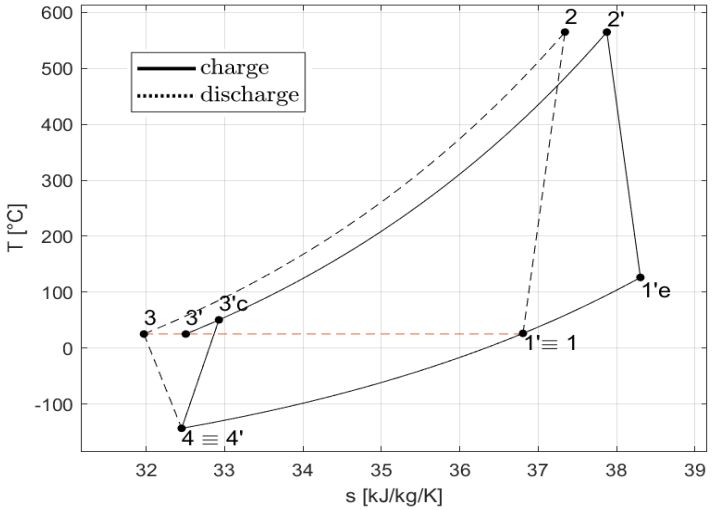


*Figure 0.4 T-s diagram of Brayton PHES with polytropic efficiency of turbomachines of 90%, diagram calculate for nitrogen, $T_3$= 25°C, $T_2$ = 565°C diagram calculated for helium*

For PHES with $T_3=T_1=T_{amb}$ (like in Figure 0.4), that there is an optimum value of $\tau'$ which maximise the RTE, which is the value that assures that both auxiliary HEXs are used and that the average temperature of the heat rejection to the environment is the lowest. However, to get a higher work ration and increase RTE, $T_1$ could be set above the ambient temperature or $T_3$ below it. If this is done clearly the heat rejection can occur only through HEXA or HEXB respectively and therefore $\tau'$ must be set so that this is made possible, so for example if $T_1$ is above ambient temperature $\tau'$, to avoid rejecting the heat at a very high temperature, must be set so that $T_{1'e} = T_{1'}$, vice versa if $T_3$ is set below ambient temperature. This can be better understood if looking at the T-s diagram in Figure 0.5 for the case where only HEX A is used.

The RTE calculated for the cycle displayed in Figure 0.5 was found to be 71% compared to 66% which is the RTE for the case displayed in Figure 0.4. Note that Brayton PHES is very sensitive to compression/expansion irreversibilities and if $\eta_{pol}$ drops from 90% to 80%, the RTE drops from 71% to 40%. Another important aspect i is that if $T_2$ and $T_3$ are fixed, the RTE decreases as $\tau$ decreases, this is associated to the compression/expansion entropy generation which is proportional to the machine pressure ratio and therefore to the charge temperature ratio. If $\tau$ reaches the minimum value of 1 this correspond to a limit case in which the cycle degenerates into an isobaric line and the net work is zero.

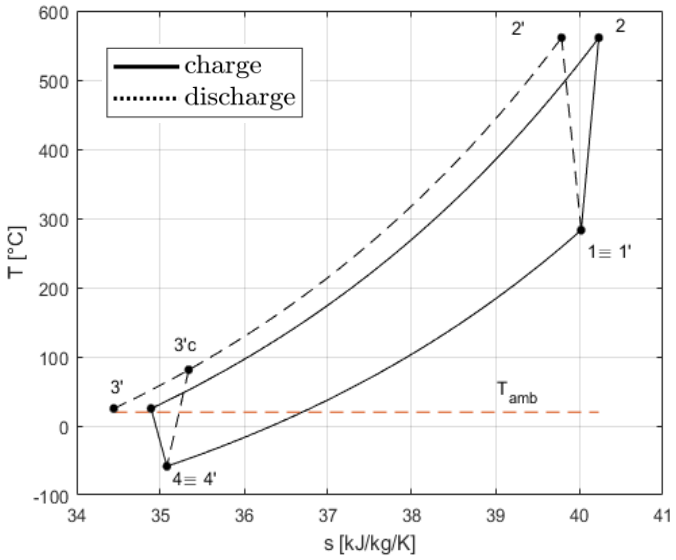


0

*Figure 0.5 T-s diagram of Brayton PHES with only turbomachinery losses and a polytropic efficiency of 90%, diagram calculated for helium with $T_2$= 565°C, $T_3$=25°C and $\tau$ =1.5*

The second most important irreversibility source for Brayton PHES with indirect TES are the ones generated in the heat exchangers with the hot and cold TES, the impact of heat transfer irreversibilities can be divide in two parts, the first related to temperature difference in the HEX due to finite heat transfer area and the second part related to pressure drops. The impact of the first can be seen in Figure 0.6. The performance of a heat exchanger is commonly determined by the effectiveness, defined as

$$\varepsilon = \frac{Q}{Q_{max}} = \frac{(mc_p)_H (T_{H,in} - T_{H,out})}{(mc_p)_{min} (T_{H,in} - T_{C,out})} = \frac{(mc_p)_C (T_{C,in} - T_{C,out})}{(mc_p)_{min} (T_{H,in} - T_{C,out})} \qquad (0.3)$$

H and C stand for hot and cold streams of the HEX. The right-hand sides are valid only if $c_p$ is constant for both fluids, this assumption is valid on first approximation for the PHES model, although the numerical model the variation of $c_p$ will be accounted for. To minimise the heat transfer losses, a PHES system is operated with counter-flow heat exchangers with balanced flow: $(m\bar{c_p})_H = (m\bar{c_p})_C$ where $c_p$ here is the average between inlet and outlet. In PHES with liquid storage, heat exchangers are used during charge and discharge, thus the inlet and outlet of heat exchangers during charge and discharge have a temperature difference of $2\Delta T$, as example $T_2$'=$T_2$-$2\Delta T$, assuming that the storage media operates between the same temperature range during charge and discharge.

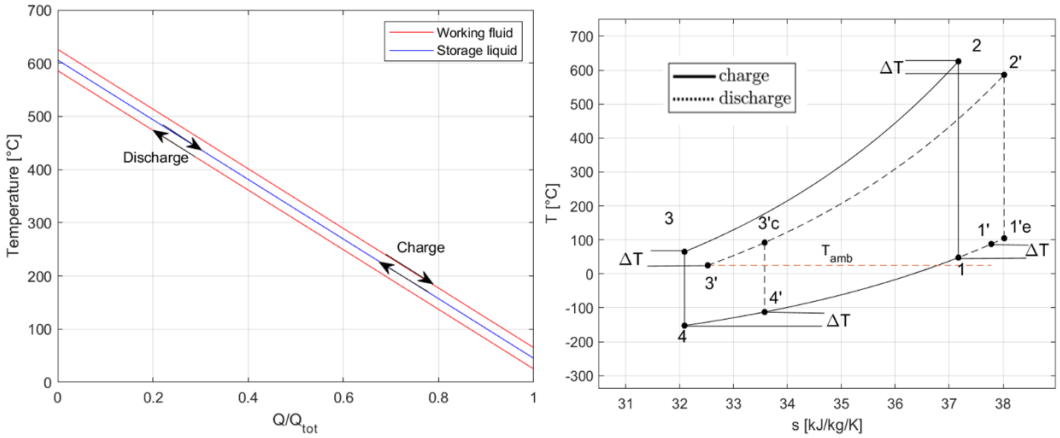


*Figure 0.6 Effect of non-ideal heat transfer for a Brayton PHES with indirect TES with ideal compression and expansion* [1]

The RTE in this case is function of τ ,θ, $\varepsilon$ and τ', but similarly to before an optimum τ' which maximises RTE can be calculated. In Figure 0.7 the RTE is plotted as function of τ for different effectiveness values and different cycle maximum temperature. To keep the RTE above 80% the effectiveness should be kept above 95% and τ above 2.5. Concerning instead the HEXs irreversibilities linked to pressure drops, relative pressure drop ($f_p$) defined as the absolute pressure drop (Δp) over the inlet pressure of the stream is considered. Again similarly to what done for the other sources of irreversibilities the RTE can be plotted as a function of τ and of $f_p$ , for an optimised value of τ', this is shown in **Error! Reference source not found.** for different values of $T_2$. Pressure drop irreversibilities have a lower impact than the other two, but still if the relative pressure if $f_p$ is 5% they account approximately for a 5% reduction of the RTE. Both the two parts of HEXs irreversibilities have the same trend RTE - τ, this is because as τ decreases the net work output of the cycle decreases but the heat transfer irreversibilities remains constant. They have an opposite trend to compression/expander irreversibilities suggesting that there is a trade off between the two.

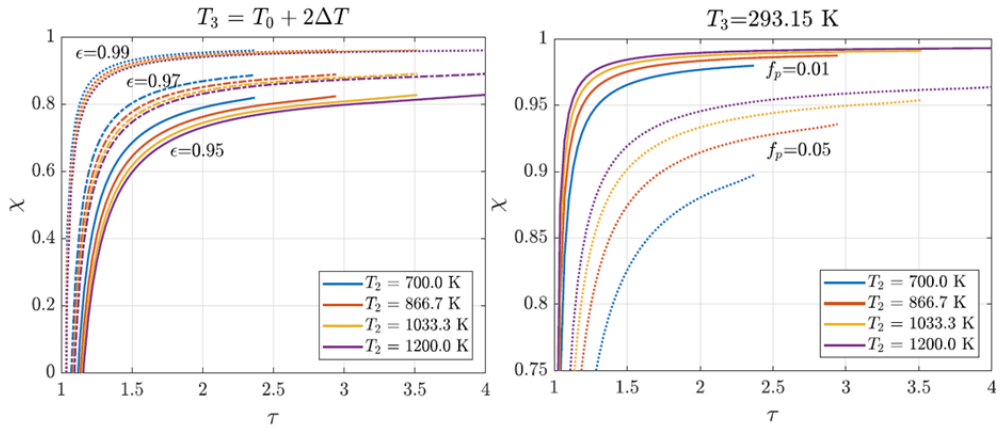


*Figure 0.7 Sensitivity of the round trip efficiency to heat transfer losses as a function of the charge temperature ratios on the left, for different heat exchanger effectiveness* [1], *τ' is optimized to*

*maximise the round trip efficiency source* [1], *Sensitivity of a Brayton PHES system in which only pressure losses are considered* [1]

## METHODOLOGY

After evaluating the analytical the limits on the RTE, to better evaluate PHES performance and cost a numerical model with Matlab® [13]was developed. The PHES types chosen is a Brayton regenerative PHES with indirect liquid TES. The choice of the TES system was done based on the consideration that so far for what regards liquid TES, it seems reasonable to investigate the integration of molten salts as hot TES in PHES, because molten salts technology is an already well studied and tested TES system in CSP application for large scale ES. Regarding the working fluids nitrogen was chosen, because of a trade-off between heat exchangers and turbomachinery cost. Other candidates were argon and helium although helium having a high specific heat capacity is associated with a high cost for turbomachines and Argon is excluded because there is no need to reduce the pressure raitos. Using indirect TES though means that there are no pressure limits relate to the TES vessels and therefore in this case between argon and nitrogen, the latter is used due to its higher specific heat capacity. In Figure 0.8 the ideal T-s diagram (identical for charge and discharge) is shown to better understand the coupling of the power cycle with the hot and cold TES: molten salts are operated between 290°C -565°C and methanol, used in the cold TES, it works between -50 °C and 25°C. Due the temperature limits of the solidification of the molten salts a regenerator is employed to ensure the compatibility with the cycle and the storage liquid materials.

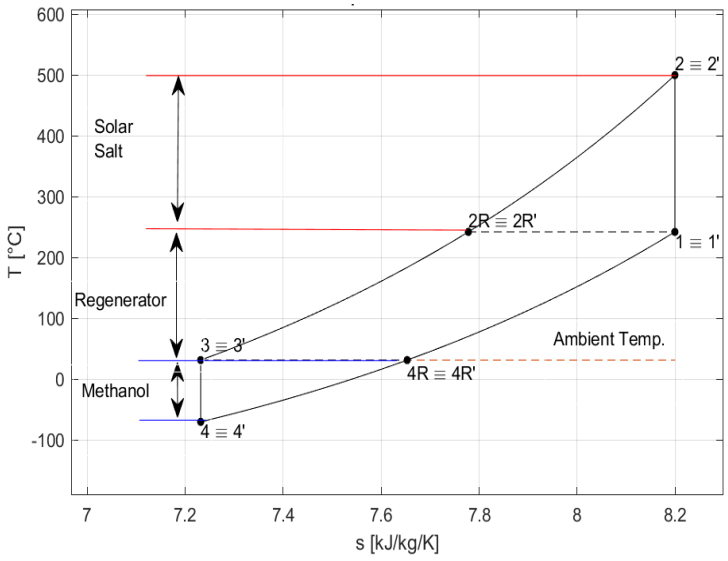


*Figure 0.8 Ideal T-s diagram for a regenerative Brayton PHES using indirect TES, $\eta_{pol}$=1, $\Delta T$ in all heat exchangers = 0, nitrogen as working fluid,*

The plant layout is shown in Figure 0.9 for the discharge phase, note that in the discharge phase, the heat caused by the components irreversibilities is dissipated to the environment through the auxiliary HEX (point 4R to 5). In Figure 0.10 the T-s charge and discharge diagram are presented. The cycle model works by first solving

the charge cycle and by evaluating the design geometry of heat exchangers, which are the same for the charge and discharge cycle, to avoid having a double cost for HEXs. For the turbomachinery instead a couple expander/compressor is used for charging and other for discharging, so that turbomachines can operate with the highest efficiency in both phases.

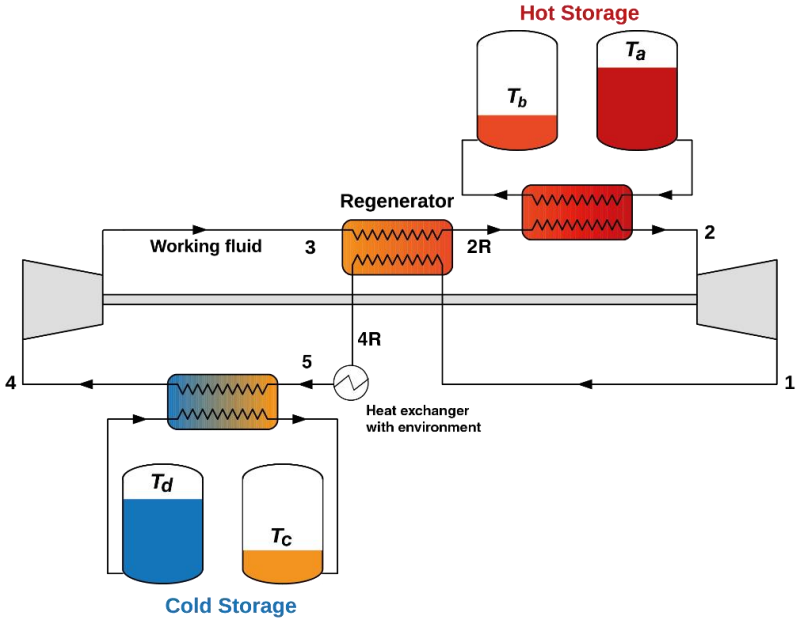


*Figure 0.9 Regenerative Brayton PHES with indirect liquid TES plant layout, arrow for the discharge cycle*

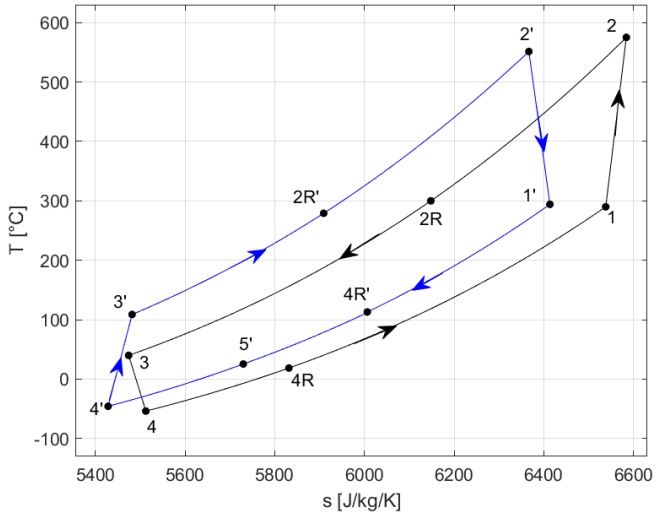


*Figure 0.10 T-s charge and discharge diagram, in black and blu respectively, for a regenerative Brayton PHES with indirect liquid TES, beta=3.88, $T_3$=40°C, Heat exchanger effectiveness of 96%, polytropic efficiency of turbomachine of 90%*

Therefore, while the HEXs during discharge operate in an off-design condition the turbomachines operate at design condition in both phases. The model is operated with

the assumption of steady state operation for all processes. Input data of the design model in charge phase are:

- Tanks temperatures of molten salts $T_a$, $T_b$ and of methanol $T_d$
- Gas maximum temperature $T_2$ and $T_3$
- Cycle maximum pressure $p_2$
- Storage tanks pressure is set to be 1 bar
- Charge compression pressure ratio ($\beta$)
- Performance of different components such as $\eta_{pol}$ of turbomachines and HEX pinch point temperature ($\Delta T_{pp}$) difference and relative pressure drop ($f_p$)
- Compressor input power is used as parameter to set the working fluid (WF) mass flow rate
- the electromechanical efficiency of the generator $\eta_{e,m}$, which comprehends also mechanical losses of the shaft bearing, is assumed to be 97% [14].

Heat leakage losses in the TES tanks and the consumption of the TES liquids is neglected. After solving the charge phase all cycle points, the geometry of the HEXs, WF and storage mass flow rates and temperatures are known. The outputs of the charge model that are taken as inputs for the discharge model are:

- HEXs geometry such as heat transfer area, tubes diameters, tubes number and length
- Tanks temperatures, which in the design model will be kept equal between charge and discharge (the reason will be explained later)
- $\eta_{pol}$ of turbomachines which is kept equal in the design model

The modelling approach for the discharge is basically the same for the charge phase only that in the discharge the cycle temperature are fixed because the HEX area is already designed and the HEX pitch point temperature cannot be set like it was done for the charge phase. Because cycle temperatures are fixed by the HEXs off-design four variables are used as control parameters of the discharge cycle, which are:

- Mass flow rate of the working fluid $m_{wf}$
- Mass flow rates of the hot and cold storage liquids, $m_{hot}$ and $m_{cold}$
- Cycle pressurization, which will set by setting the minimum cycle pressure $p_4$

The working fluid mass flow rate ($m_{wf}$) allows to set the discharge net power, while the storage mass flow rates fix the discharge time of the PHES. Between charge and discharge the tanks temperatures are assumed to be equal in order to allow the cyclic operation of the storage system.

## HEAT EXCHANGER MODELING

As already mentioned, to minimize HEXs irreversibilities, HEX in PHES system are operated with balanced flows. Since that $c_p$ of nitrogen is not constant with temperature HEXs are divided into *n* sections and for each section, an average $c_p$ is calculated between outlet and inlet. The tanks temperature plus one working fluid temperature and $m_{wf}$ are known, so to calculate the unknown temperature and the storage mass flow rate, the HEX design model is iterated on the unknown temperature so that the $\Delta T_{pp}$ is set to the desired value. Pressure drops in HEXs are set at 1% [1]. To evaluate the heat transfer area, HEXs were chosen to be of the shell and tube type with a simplified geometry with the main assumptions of purely counterflow regime and constant tube and shell flow area with no fins. To calculate the heat transfer area, the global heat transfer coefficient of the HEX was calculated with the following formula:

$$UA_{ext} = \left(\frac{1}{h_h A_{int}} + R_{cond} + \frac{1}{h_c A_{ext}}\right)^{-1} \quad (0.4)$$

where $h_h$ and $h_c$ are the heat transfer coefficient of the hot and cold stream, $R_{cond}$ is the tube wall conductive resistance, note that U is referred to the external heat transfer area $A_{ext}$. To calculate $h_c$ and $h_h$ heat transfer correlations are related to the Nusselt number, which is function o Reynolds (Re) and Prandtl (Pr) numbers through heat transfer correlations. The correlation used were for the gas side the Gnlielinski correlation:

$$Nu = \frac{\left(\frac{f}{8}\right)(Re - 1000)Pr}{1 + 12.7\left(\frac{f}{8}\right)^{0.5}(Pr^{\frac{2}{3}} - 1)} \quad (0.5)$$

where f is the friction factor calculated with the Swamee-lee explicit equation [9]. For the shell side instead the well-known Dittus-Boelter equation is used. Note that the HEXs are operated in turbulent regime in order to increase the heat transfer coefficient. Like before, the HEX is divided in *n* parts and for each part *U* and the logarithmic mean temperature difference $\Delta T_{ml}$ and *Q* are evaluated and heat transfer area is calculated by the equation :

$$Q = UA\Delta T_{ml} \quad (0.6)$$

Then the tube length and pressure drop on the gas side are computed:

$$L = \frac{A}{\pi D_{out} * N_t} \qquad \Delta p = f\frac{L}{D}\rho\frac{v^2}{2} \quad (0.7)$$

Where $N_t$ is the number of tubes, which is calculated once the cross-sectional flow area $A_f$ is known. To set the relative pressure drops at 1% the HEX model is iterated

on the $A_{f..}$ For the regenerator a similar procedure is employed only that in this case the HEX is a printed circuit HEX and it is modelled according to the model presented in [14]. Note that in this case the HEX $\Delta T_{pp}$ is set once the compression pressure ration of the cycle is set. Since heat exchangers design point is modelled in the charge phase, it is clear that in the discharge phase they work in off-design condition. Concerning the off-design procedure for HEX is the same for the design, unlike that in this case the geometry of the HEXs is fixed, so $A$, $A_{f,}$ $D$ and $L$ are known, the variation of $U$ is computed and the $\Delta T_{ml}$ will change according to equation (0.6). Concerning the pressure drop, for the off-design the variation will be accounted for by the following equation:

$$\Delta p_{off} = \Delta p_{design} \left( \frac{m_{off}}{m_{design}} \right)^2 \left( \frac{\rho_{design}}{\rho_{off}} \right) \qquad (0.8)$$

At last it is important to mention that the auxiliary HEX with the environment is modelled in a simplified way due to the fact that its only scope it to reject excess heat to the ambient. Therefore in this case the HEX can be operated with unbalanced thus allowing to reduce a lot its heat transfer area and its cost. Because of these consideration the mass flow rate of the cooling air was chosen so that $(mc_p)_{air} \simeq 4$ $(mc_p)_{wf}$ and a $\Delta T_{pp}$ of 10 K is imposed which occurs at the inlet. For the calculation of the internal heat transfer area a $U$ of 100 W/m$^2$/K [15]. To account for the worst-case scenario in which the coolant is ambient air, the power consumption of the air fan is set to 1%

## COMPRESSORS AND EXPANDERS

Compressor and expanders are turbomachines and are modelled with the polytropic efficiency defined as:

$$\eta_{comp} = \frac{\delta w_{comp,rev}}{\delta w_{comp}} = \frac{v\mathrm{d}p}{\mathrm{d}h} \qquad \eta_{exp} = \frac{\delta w_{exp}}{\delta w_{exp,rev}} = \frac{\mathrm{d}h}{v\mathrm{d}p} \qquad (0.9)$$

Note that since that the specific heat capacity ratio along the compression and expansion line is not constant, the transformations were divided in $n$ sections and starting from the inlet point equation (0.10) is integrated to calculate the output condition. In the model a polytropic efficiency of 90% is assumed. For the off-design model of the turbomachines typical characteristics maps for axial turbomachines were used [16] which relate the reduced mass flow rate to the machine pressure ratio and the machines efficiency . The off-design of turbomachines is integrated only for the discharge cycle and therefore since there a two more constraint on the model, which are that the compressor and expander must work on the turbines characteristics map, the cycle pressurization and the discharge temperature of the hot tank cannot be set like it was done in the off-design model.

## COST MODEL

The ESS cost is usually defined as power-based cost and energy-based cost, the first is normally referred to the discharge net power of the system while the second is referred to the stored electrical energy. Another important financial parameter is the levelized cost of storage, which is useful to address the financial sustainability of the ESS project through its entire lifetime.

For the turbomachines cost the formula proposed by Farres [1] for similar PHES was used:

$$Z_{comp/exp} = \frac{C_{comp/exp}\, m\, \ln\beta}{\eta_{max} - \eta} * \frac{\rho_{ref}}{\rho} \qquad (0.10)$$

where $m$ is the mass flow rate, $C_{comp/exp}$ is the cost per unit mass flow rate taken from [17], the term $(\eta_{max} - \eta)$ is to account for a higher cost as the machines isentropic efficiency increases. ($\eta_{max}$ is set to 92%), the fraction on the right instead is used to account that for an increase inlet/outlet[1] density the cost of the turbomachines decreases, because the dimension of the machines decreases as the volumetric flow rate decreases with the increase of the cycle density. The reference condition is referred to traditional gas turbines conditions.

For the HEXs the following formula were used [1], [18], [19]:

$$Z_{hot/cold} = (30800 + 1438\, A^{0.81}) \qquad Z_{AUX} = 5443 A^{0.395} \qquad (0.11)$$

$$Z_{REG} = C_{HEX}\, \rho_{metal} V_{metal} \qquad (0.12)$$

The first two are for the hot/cold HEX and the auxiliary HEX and are related to the HEX heat transfer area, while the third is used for the regenerator where $V_{metal}$ is the total steel mass of the HEXs, $\rho_{metal}$= 8000 kg/m$^3$ and $C_{HEX}$ is the cost per unit of steel mass taken as 30$/kg [1]. Note that for the power based cost a value of 400 $/kW [1] is assumed to account for all other costs like the electric motor/generator, the installation and site cost, piping etc. For what concerns the hot/cold TES costs here it is accounted only the material costs and the tanks costs, parameter used are presented in Table 0.1.

*Table 0.1 Input parameters used for the calculation of the thermal energy storage costs* [1]

| | **Material cost [$/kg]** | **Tank cost [$/m$^3$]** | **Insulation cost %** |
|---|---|---|---|
| **HOT TES (molten salts)** | 0.5 | 150 | 20% |
| **COLD TES (methanol)** | 0.3 | 50 | 20% |

[1] Inlet for compressor, outlet for the expander, for compressor $\rho_{ref}$=1.2 kg/m$^3$, for expander $\rho_{ref}$=0.5 kg/m$^3$.

The levelized cost of storage (LCOS) is calculated by the following formula:

$$LCOS = \frac{CAPEX + \sum_{t=1}^{t=L} \frac{A_t}{(1+i)^t}}{\sum_{t=1}^{t=L} \frac{E_{out}}{(1+i)^t}} \quad (0.13)$$

$$A_t = OPEX_t + c_{el} E_{in} \quad (0.14)$$

where CAPEX is the overall cost calculate as the sum of the power based and energy based costs, $A_t$ are the annual costs, sum of the OPEX cost for maintenance assumed as 15$/kW/y [20] and the cost for the charged electricity $E_{in}$, $c_{el}$ is the cost per kWh. $E_{out}$ is the total yearly output electricity. All the yearly cost are discounted by a factor of 8% and summed over the lifetime which is assumed of 20 years.

**ROUND TRIP EFFICINCY AND EXERGY ANALYSIS**

The round-trip efficiency of the system is related to the coefficient of performance (COP) for the charge cycle and the discharge cycle efficiency which are calculated as:

$$COP = \frac{W_{net,ch}}{Q_{hot,ch}} \qquad \eta_{engine} = \frac{W_{net,dis} - W_{fan}}{Q_{hot,dis}} \quad (0.15)$$

$W_{fan}$ is the consumption of the fan of the auxiliary heat exchanger $W_{net}$ is the net power and $Q_{hot}$ is the heat rate exchanged with the hot TES. The RTE is calculated as:

$$RTE = \eta_{engine} * COP * {\eta_{e,m}}^2 \quad (0.16)$$

where $\eta_{e,m}$ is the electromechanical generator efficiency (assumed to be 97%). The exergy balance of the system can be expressed by the following formula:

$$RTE = 1 - \frac{\sum W_{irr}^i}{W_{el,ch}} \quad with \quad W_{irr}^i = T_0 S_{irr}^i \quad (0.17)$$

where $W_{irr}^i$ the single component exergy loss and $S_{irr}^i$ is the entropy generation in each component calculated as shown in :

*Table 0.2 Entropy generation formulas*

| **Component** | $\mathbf{S^i_{irr}}$ |
|---|---|
| **Compressor/expander** | $m(s_{out} - s_{in})$ |
| **Heat exchangers** | $[m(s_{out} - s_{in})]_{hot,stream} + [m(s_{out} - s_{in})]_{cold,stream}$ |
| **Auxiliary heat exchanger** | $m[(s_{out} - s_{in}) - (h_{out} - h_{in})/T_0]_{hot,stream}$ |

Note that electromechanical losses and fan consumption are treated as a pure exergy loss therefore the exergy loss is equal to their electrical consumption.

**RESULTS**

At first aa validation of the model against Farres result is performed, with the same input as Farres, the obtained RTE is 65.4% with an energy density of 45 kWh/m$^3$ , which must be compared to the 65.2% RTE and 46 kWh/m$^3$ found by Farres[2].

The results of the model for a PHES of 10 MW/110MWh system are proposed in Table 0.3, input data in Table 0.4 these were chosen based on the considerations made in the preliminary thermodynamic analysis. In this example it is important to underline that the cycle has a power ratio[3] of 0.56, and that the charge and discharge time are equal.

*Table 0.3 Results of the PHES model for 10 MW/110 MWh Brayton PHES*

| **Model results** | | |
|---|---|---|
| $t_{charge}=t_{disscharge}$ | 6 | h |
| **Charge net power** | 18.9 | MW |
| **Discharge net power** | 10.6 | MW |
| **RTE** | 56.0 | % |
| $\rho_{energy}$[4] | 31 | kWh/m$^3$ |
| $\rho_{power}$ | 2.1 | MW/(m$^3$/s) |

*Table 0.4 PHES model input data*

| $T_{3,ch}$ | $T_{2,ch}$ | $p_{2,ch}$ | $T_a$ | $T_b$ | $f_p$ | $\eta_{comp/exp}$ | $\Delta T_{pp,hot}$ | $\Delta T_{pp,cold}$ | $\beta_{comp,ch}$ |
|---|---|---|---|---|---|---|---|---|---|
| 40°C | 575° C | 100 bar | 565°C | 290°C | 1% | 90% | 10°C | 2.5°C | 3.88 |

In Figure 0.11 the relative exergy losses distribution is presented and it can be seen that as expected, the compression and expansion exergy losses account for more than 50% of overall lost work[5], while the second largest source of loss are the ones in the auxiliary heat exchangers and in the regenerator, suggesting it would be more beneficial to increase its heat transfer area rather than the one of cold/hot HEX.

[2] Note that Farres when calculating energy density, it refers to the ratio of the electrical output energy over the storage fluid volume
[3] Ratio of the discharge net power over the charge power
[4] Energy density in the table is calculated considering the volume of the four tanks of the TES system, in Farres [1] this parameter was calculated considering only the storage material volume
[5] Lost work means the lost charge electrical input net work

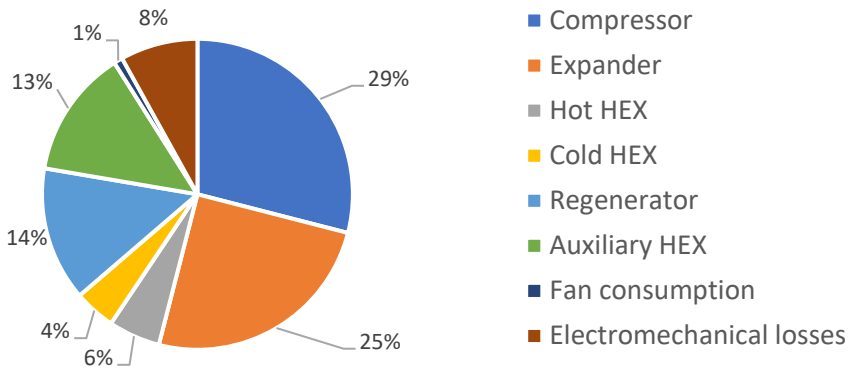


*Figure 0.11 Relative exergy losses of a regenerative PHES with liquid storage, the sum of the exergy losses accounts for 44 % of the charged net power input*

An important aspect to be investigated is the power ratio, an ESS usually must be operated with a higher discharge time and power with respect to the charge phase, because it has to discharge the electricity during the short peak period when the electricity price is higher. Therefore, an analysis was developed to compare three different discharge cycle designs. Note that this is not an off-design analysis but a design analysis of different discharge cycle designs.

The first is the refence case presented before while the other two are cases where the discharge time is halved, and the power ratio increased. Note that in the discharge cycle model to the net power output and the discharge are related, in fact the model is operated so that if $m_{wf,dis}$ is increased $m_{hot,dis}$ and $m_{cold,dis}$ (TESs mass flow rates) are increased too by the same percentage value. This is done so that even if with an increased net discharge power the hot and cold HEXs are operated with balanced flows to avoid a dramatic drop of the RTE. Therefore, when referring to an increase of the power ratio it is implied a decrease of the discharge time. The results of the three cases are presented in Table 0.5, it can be seen that in CASE B where doubling the $m_{wf,dis}$ with respect to case A does not double the $W_{net.dis}$ because the RTE decreases from 56.0% to 49.1 %, due to the increased relative pressure drops in the HEXs, which outweighs the beneficial increase of the HEXs global heat transfer coefficient. Case C was proposed as a solution to avoid losing 7 % point to double the discharge net power. In this case the solution adopted was to increase the discharge cycle pressurization of 60%which allowed to reduce the HEXs pressure drops and to have a power ratio of 1.12. Note that in from case B to case C the cycle maximum pressure goes from 130 to 188 bar.

*Table 0.5 Comparison of different Brayton PHES with liquid TES discharge cycle design case with different output power*

| | CASE A | CASE B | CASE C |
|---|---|---|---|
| **Discharge cycle control variables** | | | |
| $m_{wf,dis}/m_{wf,ch}$<br>$m_{hot,dis}/m_{hot,ch}$<br>$m_{cold,dis}/m_{cold,ch}$ | **1** | **2** | **2** |

| | | | |
|---|---|---|---|
| $p_{min.dis}/p_{min.ch}$ | 1 | 1 | 1.6 |
| **Results** | | | |
| **$W_{net,dis}/W_{net.ch}$ (power ratio)** | **0.56** | **0.97** | **1.12** |
| **$W_{net,dis}$ [$MW_{el}$]** | 10.6 | 18.5 | 20.4 |
| **Heat exchanger** | **$\Delta p/p$ [%] discharge cycle** | | |
| Hot HEX | 0.8 | 2.4 | 1.1 |
| Regenerator cold stream | 0.7 | 5.2 | 2.1 |
| Regenerator hot stream | 1.1 | 3.2 | 1.5 |
| Cold HEX | 1.2 | 5 | 1.9 |
| **RTE [%]** | 56.0 | 49.1 | 54.5 |

## OFF DESIGN OPERATION OF THE DISCHARGE CYCLE

Off-design operation was analysed, to see how it impacted the discharge cycle RTE because it could happen that the plant is requested to discharge in a longer time (i.e. at a lower net discharge power). When referring to off-design of PHES is important underlined that this means the off-design of turbomachines, since HEXs already operate in off-design between charge and discharge. The method employed for the regulation of the turbomachinery off-design is called inventory control [21], it basically consists of reducing the amount of working fluid in the cycle in order to linearly decrease its pressurization, the mass flow rate and therefore the net power. Note that as already done in the previous analysis as $m_{wf}$ is reduced also $m_{hot}$ and $m_{cold}$ are simultaneously reduced to always operate the HEXs with balanced flows. In Figure 0.12 a comparison of the T-s for the design condition and a partial load operation with $m_{wf,off}$ = 30% $m_{wf,design}$ is shown. The cycle is simply shifted to the right and its temperatures are almost constant and its efficiency does not change significantly. This is mostly related to the fact that since the pressure decreases with the same rate as $m_{wf}$ basically the reduced mass flow rate of compressor and expander remains constant and this allows the turbomachines to operate very near to their design point maintaining their efficiency constant. This is also related to the fact that in the operating range nitrogen behaves as an ideal gas with no dependence of the $c_p$ with the pressure.

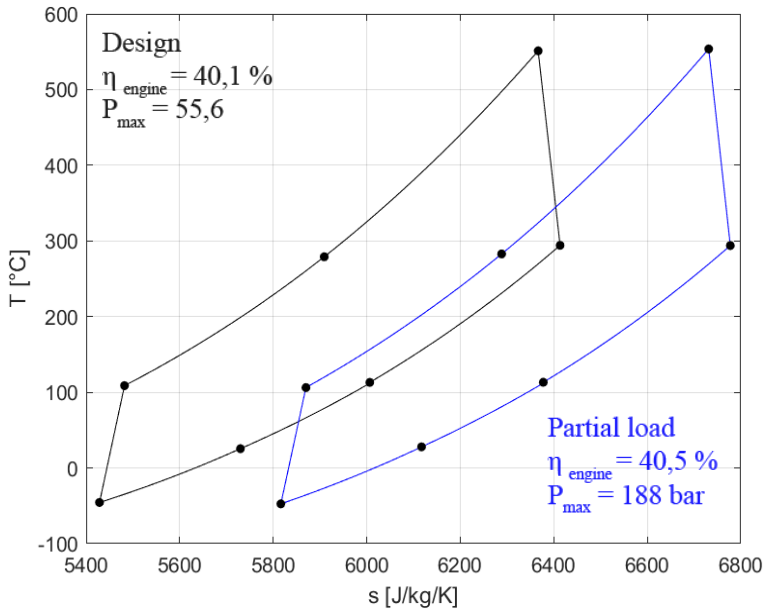


*Figure 0.12 T-s diagrams of discharge cycle of a regenerative Brayton PHES, in black the diagram of design discharge cycle, in blue the diagram in off-design operation with net discharge power of 30% of design power, inventory control mode used: working fluid mass flow rate and cycle pressure reduced of 30%, turbomachines at constant rotational speed*

Concerning the economic results, the model was used to be applied in a real case scenario, which is the Californian day ahead market. This is a significative scenario because California is a country with a high share of solar PV production, which means during that day electricity is very cheap and from 18:00 to 22:00 there is a peak in electricity demand, therefor the system was chose to a have a charge time of 6h and a discharge time of 3 h. Main data and results for the chosen system are shown in Table 0.6, the model has input data for the charge design as in Table 0.4. It can be noted that turbomachinery have a lower cost compared to HEXs and that the discharge set of turbomachines have a higher cost due to their higher pressure ratios and doubled mass flow rate compared to the charge.

*Table 0.6 Technical and cost parameters output of a regenerative Brayton PHES with liquid TES for a 114MWh / 20MW plant, specific cost referred to the net discharge power*

| **System technical specification** | | |
|---|---|---|
| **Charge net power** | 18.9 | $MW_{el}$ |
| **Capacity**[6] | 113.4 | $MWh_{el}$ |
| **Discharge net power** | 20.5 | $MW_{el}$ |
| **RTE** | 54.5 | % |
| **$\rho_e$**[7] | 31 | $kWh/m^3$ |

[6] Product of charge power and charge time
[7] Energy density in the table is calculated considering the volume of the four tanks of the TES system

| Power Based CAPEX | | |
|---|---|---|
| **Turbomachinery, ch** | 17 | $/kW_{el}$ |
| **Turbomachinery, dis** | 23 | |
| **Heat exchangers** | 80 | |
| **Generator+Extra costs** | 400 | |
| **Total** | 520 | |
| **Energy based CAPEX[8]** | | |
| **Storage materials** | 8 | $/kWh_{el}$ |
| **Tanks** | 4 | |
| **Total** | 12 | |
| **Total CAPEX[9] (6 h storage)** | 577 | $/kW_{el}$ |
| **Total CAPEX (5 days storage)** | 1770 | $/kW_{el}$ |

The total CAPEX is in line with other PHES studies, Farres and Laughlin for a similar PHES calculated an overall CAPEX of 470$/kW and 550$/kW respectively [1], [9]. Note that if the total CAPEX is calculated for a 6 hours storage the most predominant cost part is the power based one, on the other hand if the PHES should be use for a longer term energy storage for a charge time of 5 days the cost related to the TES would be the biggest part.

Finally the LCOS was calculated for this real scenario taking the average day ahead market electricity price for 2017 from [22], the buy price was taken as 18$/MWh (average from 10:00 to 16:00), while the sell price is around 70$/MWh. As can been with the assumption from Table 0.7 the resulted LCOS was calculated at 99$/MWh, the biggest component is the one associated to the CAPEX which account, the OPEX are very low, instead the most variable parameter is the cost related to the energy losses between charge and discharge, on first approximation (without discounting) this cost is simply the electricity cost 18$/MWh divided by the RTE. This suggest that there is a trad off between having a low CAPEX and a low RTE (which means $C_{el}$ is higher) or having a high CAPEX with a high RTE. With the LCOS the system cannot operate in the day ahead market without any incentives since the sell price is lower than the LCOS. In future studies though to better evaluate the performance of the storage system all the services that an ESS can offer could be studied, like the participation in the ancillary service markets in which prices higher than 100$/MWh could be reached [23]

*Table 0.7 Parameters used for the calculation of the levelized cost of storage calculation*

| | | |
|---|---|---|
| **Lifetime** | 20 | years |
| **Discount rate** | 8 | % |
| **Cycles per year** | 365 | - |

[8] Cost which contains only the thermal energy storage cost
[9] Total CAPEX includes the energy and power cost divided by the net discharge power

| | | |
|---|---|---|
| **Charging time** | 6 | h |
| **Discharge time** | 3 | h |
| **Electricity buy price** | 18 | $/MWh |
| **CAPEX** | 53.7 | $/MWh |
| **OPEX** | 13.7 | |
| **$C_{el}$** | 32.1 | |
| **LCOS** | 99.5 | |

## CONCLUSIONS

In this thesis the model of an uprising ESS technology was developed and a tecno-economic analysis of the system was done. PHES has the potential of becoming the future of energy storage competing with PHS, CAES and LAES[10]. PHES has a ten times higher energy density (around 46-100 kWh/m$^3$) than PHS and CAES, which have an energy density lower than 1.5[11] and 12 kWh/m$^3$ respectively, plus it has the advantage of having a low environmental impact and no geographical site requirement unlike CAES or PSH. Regarding the total capital costs they in the range of 454-965 $/kW [20] which are comparable to the ones of PHS (600-2000 $/kW) , CAES (400-800$/kW) and of LAES (740-1130 $/kW) [24]. Regarding the RTE it could vary between 50-70% which is comparable to that of PHS (65-87%) and of CAES (40-80%) and LAES (40-85%) [24], [25].

However, the technology success hinges upon the development of highly efficient component like turbomachinery with polytropic efficiencies higher than 90% and especially HEXs, which should have a relative pressure drops of 1% and an effectiveness above 96%. The TES represents a key component of the system and while molten salts have been widely tested, the employment of liquids for cold TES must be further studied. The calculated cost is promising and comparable to that of PHS and CAES, although to have a more realistic idea of the system costs, each component cost equation should be verified for the operational conditions of PHES. Concluding with a quote from Laughlin [9]: " Energy storage is a problem of 19th century science. No laboratory break- throughs or discoveries are required for solving it. All that is needed is fine engineering and assiduous attention to detail".

[10] Pumped hydro energy storage, Compressed air energy storage, liquid air energy storage
[11] Energy density for a heigh difference between upper and lower reservoirs of 550m

# ABSTRACT

In this thesis a techno-economic analysis of a novel energy storage technology called pumped heat electricity storage (PHES) was performed. PHES takes electricity from the grid to drive a heat pump that stores thermal energy in a hot and a cold thermal energy storage (TES) during charging, during discharge the hot TES is cooled down while the cold one is heated up to drive a heat engine that generates electricity and gives it back to the grid. In this thesis the heat pump and heat engine are chosen as regenerated closed Brayton cycle with nitrogen as working fluid. The power cycle is composed of three heat exchangers (HEX) including the regenerator, which are used both in charge and discharge, two set of turbomachinery one for the charge and another for the discharge phase, plus another HEX used to reject heat to the environment. Hot and cold HEXs with the TESs were taken of the Shell and Tube type, while the regenerator is of the printed circuit type, as regard the turbomachinery axial machines were chosen. For the hot TES molten salts are used (operational temperature range: 290-565°C) and for the cold TES methanol is employed (operational temperature range : -50 to 25°C).

A first analytical analysis on PHES achievable performance showed that when only turbomachinery irreversibilities are considered and a polytropic efficiency of 90% is assumed the highest achievable round-trip efficiency (RTE) is 71% with a maximum cycle temperature of 565°C. Moreover, to have a high RTE heat exchangers effectiveness and relative pressure drops should be kept higher than 95% and 1% respectively.

To evaluate the real performance and cost of the system a numerical model in Matlab® was developed. HEXs are designed in the charge phase while on the discharge phase they work in off-design conditions. To minimize heat transfer irreversibilities HEXs were operated with balanced flows, with HEXs effectiveness of 96% and relative pressure drops of 1%. The four turbomachines instead were modelled assuming a 90% polytropic efficiency. An exergy analysis of the system was performed and showed that 55% of the exergy losses of the system are associated to the turbomachinery and 25 % are related to HEXs irreversibilities. The obtained results for a PHES of 20.5$MW_{el}$ net discharge power and 113 $MWh_{el}$ energy capacity, are a RTE of 54.5%, specific CAPEX of 577$/kW [12] and an energy density of 31 $kWh/m^3$, The effect of the power ratio between charge and discharge was investigated showing how the HEXs off-design has a negative influence on the RTE if the net discharge power must be higher than the charge one. The partial load operation of the system was also investigated proving that cycle efficiency can be held constant if the inventory control method is employed which consists of reducing the cycle pressure and mass flow rate to reduce the net power output.

[12] referred to the net discharge power

Finally, a real case scenario was investigated and to evaluate the economic performance of the PHES, the levelized cost of the system (LCOS) was calculated. The case study was the operation on the Californian electricity market with 6 hours of charging at off peak periods and 3 hours of discharging in the peak ones. The LCOS for the 20.5 MW/113MWh system resulted to be 99 $/MWh, with one cycle per day, 20 years lifetime and a cost of the purchased electricity of 18 $/MWh. In the chosen scenario though the system did not resulted to be financially feasible, because the LCOS found was higher than the average selling prices during the peak period which is 70 $/MWh. This underlines that public policy driven investment and incentives should be planned if new large scale energy storage plants must be installed to help increase the share of renewable energy source in the electricity sector.

# 1. INTRODUCTION

In recent years it has become clear that global warning and climate change are directly linked to the raise of greenhouse gasses emission. The international panel on climate change (IPCC) estimates that human activity has caused the increase of the global average temperature of +1,0°C from preindustrial levels[26]. In December 2015 at the conference of parties (COP21) held in Paris, 196 countries signed an agreement to keep the increase of global average temperature below 2°C with respect to pre-industrial level.

In response to this the European Union developed its energy policy framework for 2030 which aims to reduce greenhouse gases emission of 40% by increasing the share of renewable energy in the final consumption to 32.5% and by improving energy efficiency of 30% [27]. As a consequence of this in 2020 Italy and all other members of European union approved their *Integrated National Energy and Climate Plan* for 2030. In Italy for example the electricity generation share of renewable energies is set to reach 55% in 2030 compared to the 34% of 2017, looking only at solar PV generation, it should reach 22% in 2030 compared to the actual 8% [28]. To reach this goal the installation of new renewable capacity alone is not enough: renewable energy sources (RES) such a solar PV or wind energy are non-dispatchable power generation sources and therefore their production cannot be controlled like traditional power plants running on fossil fuels. Because of this during periods of no RES production traditional power plants have to rump up and sustain the electricity demand. This phenomenon has already been experienced in regions with a high penetration of RES, like California, where the increase of solar PV generation has led to the so called "duck curve" [22] of electricity prices, in which wholesale market prices of electricity are very low during the day because of the high PV generation and have a peak from 5 pm to 9 pm, when the solar generation decreases and the electricity demand instead increases.

A solution to this problem is the employment of electricity storage systems (ESS), that allow to store electricity during the peak of RES generation and feed it back to the grid when there is no RES production. Because of this reason the ESS market has rapidly increased in the recent years [29]. Today pumped hydro energy storage (PHS), still accounts for 96% of the overall installed capacity mainly because it is the only ESS technology, together with compressed energy storage (CAES), employed for large scale[13] application as can be seen in Figure 1.1, which shows a classification of all energy storage technologies as function of power rating and energy capacity. In recent years though, the market focus has been on Li-ion battery storage technologies, mostly linked to behind the meter installation for residential and industrial applications. To solve the duck curve problem though, new large-scale energy storage capacity is needed as RES production increases. PHS, has the problem of high environmental impact and geographical requirement, and concerning CAES so far

[13] Power rating higher than 10 MW and energy capacity higher than 100 MWh

only two plants in the world have been built [30]. Li-ions battery are employed in some rare cases, like the big Australian ESS provided by Tesla Energy [31], but they have the disadvantage of being very expensive to store electricity with a storage capacity higher than 1 MWh.

Thus, so far there is no current energy storage technology, with a high readiness level available to boost the new installations in this specific field, this is also related to the fact that, the large scale ESS is a market with a lot of uncertainty and that is mostly dependent on stable public policy environments and incentives as underlined by the international energy agency (IEA) [29].

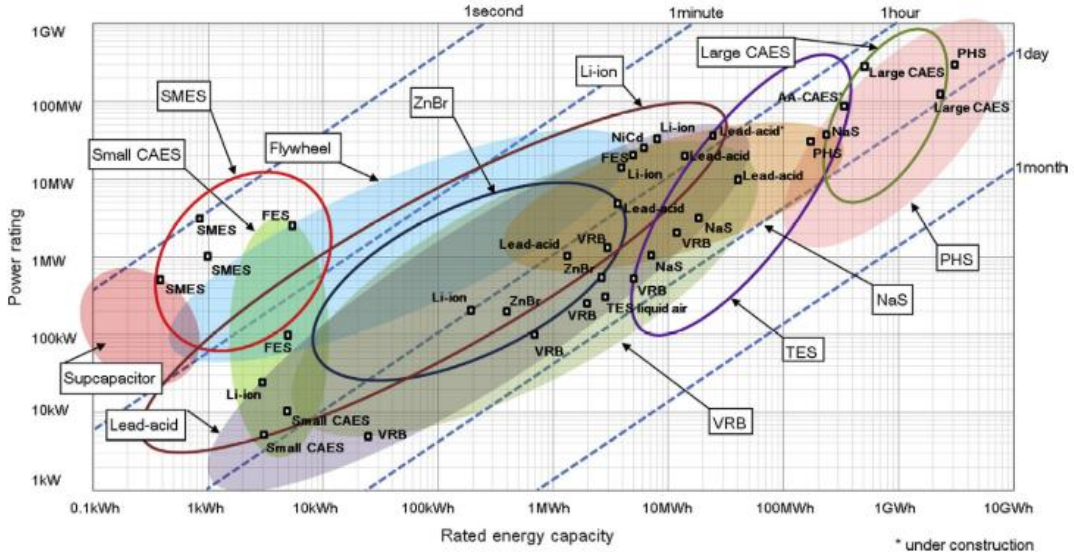


*Figure 1.1 Classification of energy storage technologies for energy storage capacity and power rating* [32]

Therefore, in this thesis a novel ESS technology called pumped heat electricity storage (PHES) is investigated. At first a literature survey on PHES and thermal energy storage will be developed, secondly the thermodynamic performance of the ESS will be investigated with a numerical model of the system. Finally, an economic analysis will be presented with a real case scenario of operation.

# 2. CONCEPT AND LITERATURE REVIEW

## 2.1.BASIC PRINCIPLE

Pumped heat electricity storage (PHES) or also called pumped heat thermal energy storage (PTES) is a quite new technology that allows to store electricity in the form of thermal energy.

PHES takes electricity from the grid to drive a heat pump that stores thermal energy in a hot and a cold reservoir during charging, during discharge the hot reservoir is cooled down while the cold one is heated up to drive a heat engine that generates electricity and gives it back to the grid. The basic concept can be seen in

Figure 2.1. On a low level of detail, the system is composed of five subsystems: a hot and a cold reservoir, a heat pump and a heat engine plus an electric motor/generator. The heat is stored in insulated tanks, that do it using sensible or latent heat depending on the power cycle chosen.

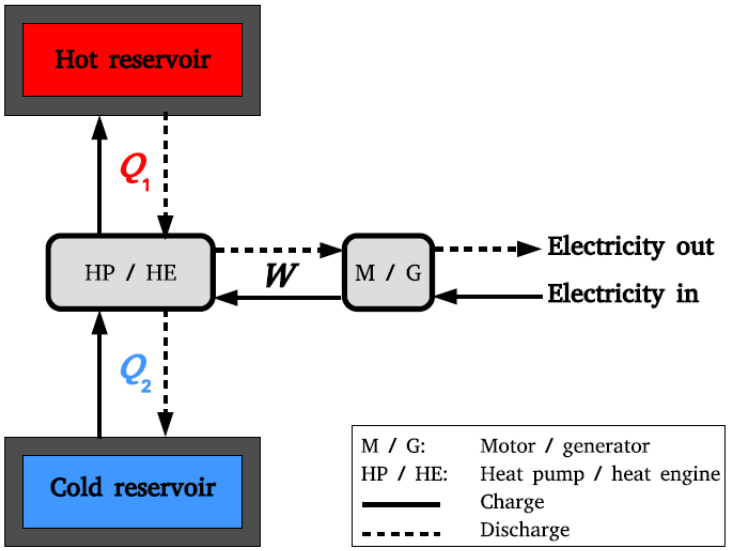


*Figure 2.1 Basic Principle of Pumped heat electricity storage* [1]

The main advantages of this technology are that it needs no geographical requirements (caverns or water reservoirs) like pumped hydro energy storage (PHS) or compressed air energy storage (CAES) and that unlike other upcoming energy storage technologies like hydrogen, it is composed of well-known and studied components available in the market today. Thus the technology has the potential to become a competitive solution in the field of energy storage from the large scale to the small scale and could also be used not only to store electricity but also coupled with a high temperature heat and/or cold demand[33] .

To understand the maximum performance of the system, the most simple configuration that could be imagined, is one based on a direct and a reversed Carnot cycle; assuming the reservoirs have infinite heat capacity and that the machines are

reversible and operate between $T_{hot}$ and $T_{cold}$ the efficiency results in the product of the Carnot efficiency (2.1) and the heat pump efficiency (2.2) therefore :

$$\eta_{engine} = \frac{(T_{hot} - T_{cold})}{T_{hot}} \quad (2.1)$$

$$\eta_{pump} = \frac{T_{hot}}{T_{hot} - T_{cold}} \quad (2.2)$$

$$\eta_{PTES,reversible} = \eta_{pump} * \eta_{engine} = 1 \quad (2.3)$$

PHES is one rare example of thermodynamic cycle in which, even though energy is converted from electricity to heat and vice versa, when considering all reversible processes, it results in an overall round trip efficiency (RTE) of 100%.

In reality, PHES round trip efficiency is lower than one due to irreversible processes used to drive the heat pump (HP) and the heat engine (HE), the main sources of irreversibilities are caused by compression, expansion and heat transfer processes moreover there are heat leakage losses in the tanks and pressure drops losses.

Going from the ideal concept to the real implementation, PHES can be categorized in three main groups based on the type of thermodynamic cycle and consequently on the working fluid adopted. The three main categories are:

- Compressed heat energy storage (CHEST), bases on water-steam or/and ammonia sub critical Rankine cycle, also called latent PHES
- PHES based on transcritical $CO_2$ Rankine cycle
- PHES based on Brayton cycle with monoatomic or biatomic gasses

In Figure 2.2 the different thermodynamic cycles used, for the three concepts are presented (assuming the same working fluid is used). According to [34] the main trade off for PHES system is between the heat storage ratio and the back-work ratio. Heat storage ratio is defined as the ratio between the heat delivered to the hot source and the compression work while charging: $\frac{Q_{hot}^{ch}}{W_{comp}^{ch}}$ and the back-work ratio is defined as the ratio of expansion work over compression work during charge: $\frac{W_{exp}^{ch}}{W_{comp}^{ch}}$ .

Comparing the three types of PHES, if we assume to have the same amount of compression work during charge, a high back work ratio means having a higher expansion work and a therefore lower energy stored in the hot reservoir, in this case

so the major source of loss are the irreversibilities in the turbomachinery. On the contrary having a high heat to storage ratio means having for the same compression work a higher heat stored in the hot reservoir and therefore in this case the major source of losses are the heat transfer irreversibilities with the hot reservoir. In Figure 2.2 a plot for these two ratios is presented, as we can see heat storage ratio is inversely proportional to the back work ratio; the Brayton PHES has a high back work ratio and low heat storage ratio, vice versa for the latent PHES, while transcritical PHES lays in the middle of the two.

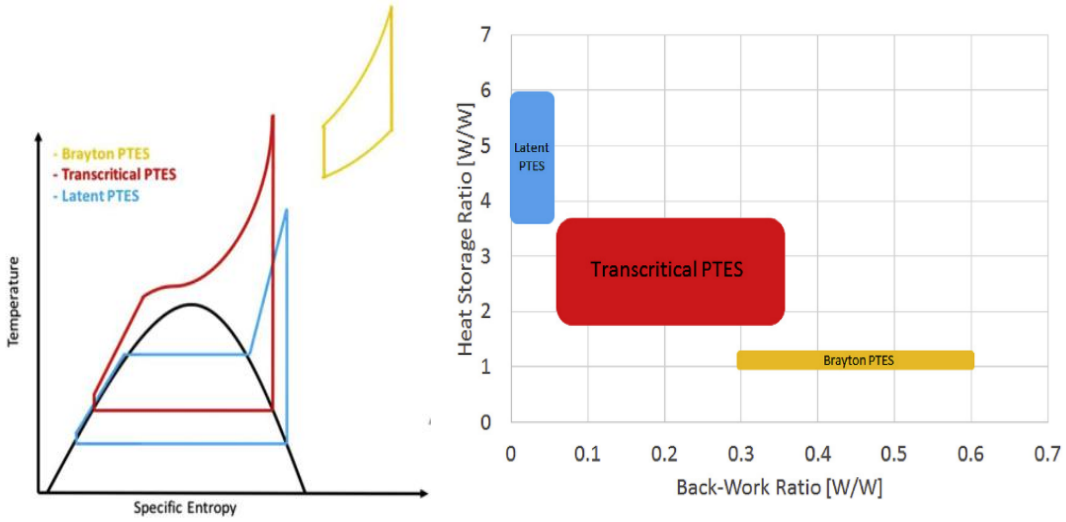


*Figure 2.2 Thermodynamic cycles of PHES concepts plot of heat storage ratio ad Back-work ratio*

It is important to mention that so far only a small pilot plant (150 kW/600kWh), based on Brayton-PHES, in collaboration with the University of Newcastle was installed [35]. Concerning Rankine cycles and CO2-cycle there is only a European project called CHESTER's project [36] that is part of the program horizon 2020 to integrate the CHEST concept with a district heating system.

## 2.2. TERMINOLOGY AND NOTATIONS

In this small paragraph some key parameters and rating criteria will be defined, these concepts will be recalled many times later on in the thesis, therefore this paragraph has the scope to clarify to the reader the terminology and notations specific of energy storage.

### STORAGE CAPACITY AND SIZE DEFINITION

Normally the size of an energy storage system (ESS) is expressed by the rated net discharge power (in MW) and the ESS capacity (in MWh). The Capacity of the system is defined as :

$$Capacity = W_{el,ch} * t_{ch} \tag{2.4}$$

where $t_{ch}$ is the charge time and $W_{el,ch}$ is the net electricity input power. As example the size of the storage is usually expressed in the following form: 20MW/100MWh.

### ROUND TRIP EFFICIENCY

The round-trip efficiency RTE is defined as the electrical energy output during discharge and the electrical energy input during the charge phase:

$$RTE = \frac{W_{el,discharge}}{W_{el,charge}} \tag{2.5}$$

It is a key parameters of energy storage plants which defines the overall efficiency of the system, plus it has an impact on the annual costs of the plant, in fact it determines the marginal cost at which electricity can be supplied during discharge:

$$C_{el,discharge} = \frac{C_{el,charge}}{RTE} \tag{2.6}$$

where $C_{el}$ is the electricity cost ($/kWh).

### ENERGY DENSITY

Energy density in the field of static energy storage application is commonly defined as:

$$\rho_E = \frac{W_{el,discharge}}{\sum V_{storage}} \tag{2.7}$$

Where $W_{el,discharge}$stands for the electricity output during discharge, $\sum V_{storage}$ denotes the total volume of the tanks (reservoirs), $\rho_e$ is usually measured in kWh/m$^3$. Clearly it is desirable to have a high energy density in order to reduce the storage plant cost, since the lower the volume of the tanks is, the lower the overall capital cost of the plant.

**POWER DENSITY**

The power density is defined as:

$$\rho_P = \frac{W_{el,discharge}}{\dot{V}_{max}} \tag{2.8}$$

where $\dot{V}_{max}$ is the maximum volumetric flow rate of the working fluid in the cycle. A high power density is preferred because it usually means a lower cost for the turbomachinery, since having a low volumetric flow rate means using more compact devices

**WORK RATIO**

The work ratio is a key parameter in evaluating PHES performance. For the heat pump (charge phase) it is defined as:

$$WR = \frac{W_{comp}}{W_{exp}} \tag{2.9}$$

basically, it is the ratio of expansion over compressor work, vice-versa for the heat engine (discharge phase). It is the inverse of the back-work ratio defined in [34] and mentioned in paragraph 2.1 . Expressing the net work during charge as a function of the work ratio it results:

$$W_{net} = W_{comp} - W_{exp} = W_{comp}\left(1 - \frac{1}{WR}\right) \tag{2.10}$$

note that WR is always greater than 1, for a given net work having a high WR means having more compact machine to produce the same network, it also means having a lower amount of work processed in the turbomachines and therefore a lower impact of the irreversibilities in the expansion/compression process.

## 2.3. STATE OF THE ART OF PHES

The first concept of PHES was first proposed by Marguerre in 1924, the system was a Rankine-based PHES which accumulated hot steam in insulated tanks. The concept came out again after the oil crisis in 1979 when Weissenbach proposed a patent [3] in which an open air regenerative Brayton cycle plus a thermal reservoirs was used to store electricity. In 2008 Howes developed a patent for a PHES system using reciprocating devices and two reservoirs [8] and several other patents were published ([37], [38], [39]). Only during recent years though, the topic has become again a theme of interest, since the development made in the field of thermal energy storage (mainly related to the use in CSP application) and also because of the increasing demand of energy storage. As a matter of fact, the number of scientific papers related to the topic has risen in the last years [40].

In the following paragraphs the state of the art of the technology for the three different categories will be presented, along with a summary table for each technology reporting the most important parameters for the different PHES models that were found in literature. It is important to mention that the focus of the thesis is on PHES based on Brayton cycle, therefore that section will be more detailed.

### 2.3.1. PHES BASED ON WATER-STEAM RANKINE CYCLE

Rankine-PHES also called compressed heat energy storage (CHEST) is based on subcritical Rankine cycle, with a working fluid that could be water or an organic fluid depending on the application. In the simplest configuration the cold reservoir is the ambient, so no cold storage is needed. While charging, saturated steam is compressed to produce high temperature superheated steam, that then gets de-superheated, condensed, and subcooled in order to transfer heat to the hot storage unit. During discharge the cycle is a common Rankine cycle where steam is evaporated to run a steam turbine, the steam then condenses at ambient temperature and enters the preheating section of the cycle. In Figure 2.3 it is shown the T-s diagram of the cycle and the plant scheme during charging and discharging.

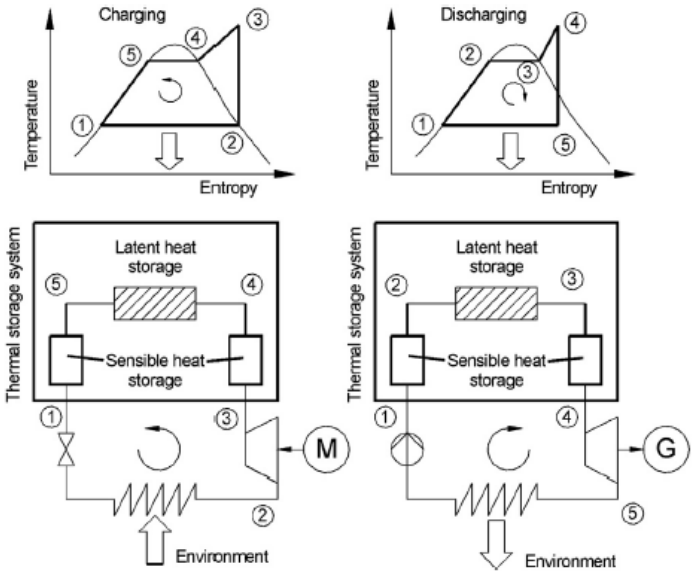


*Figure 2.3 Plant scheme and T-s diagram of CHEST concept source:*[41]

For a Rankine cycle the two most important parameters to estimate the capacity specific cost are the maximum pressure and temperature. In [41] a cycle using water steam at a maximum pressure of 100 bar and temperature of 400°C were chosen and the calculated RTE was around 70% (taking into account only turbomachinery irreversibilities), going to higher maximum temperature would increase the RTE but also increase the cost of material that must resist to higher temperature and higher pressures. For what regards the storage system, with an evaporation pressure and temperature of 100 bar 400°C, 50% of the heat is required at constant temperature, therefore the heat storage system must include a sensible and a latent heat storage unit as shown in Figure 2.3. The use of Nitrate salts, as phase change material for the latent heat storage, has been proven an optimal solution to this problem as demonstrated in [42]. Clearly the melting temperature of the phase change material is important because it fixes also the evaporating temperature and pressure of the steam cycle, since in order to minimize heat transfer losses the temperature difference between steam and salts will be in the order of 5-10 K. Together with the storage system, in CHEST cycle the process that requires a particular design is the compression of steam, which is not a conventional process in current steam cycle operation. To limit the compressor outlet temperature a particular stage compression design is suggested in [41] where a stage is composed of a compression, then the superheated steam is cooled down to saturated steam by injection of condensate and send to the next compression stage. Another disadvantage of using steam as a working fluid is the high specific volume of steam at low pressure that requires therefore high volumetric flow rate in the compressors. A solution to the last problem could be the integration of a saturated Rankine cycle with ammonia, as bottoming cycle that operates between ambient temperature and a middle temperature where water steam specific volume is sufficiently high, in [41] it was chosen a condensation temperature of ammonia of 80°C at 42bar. In Figure 2.4 a) this alternative solution is

presented, as we can see during the discharge phase the steam cycle is operated as before, with the ambient as cold reservoir.

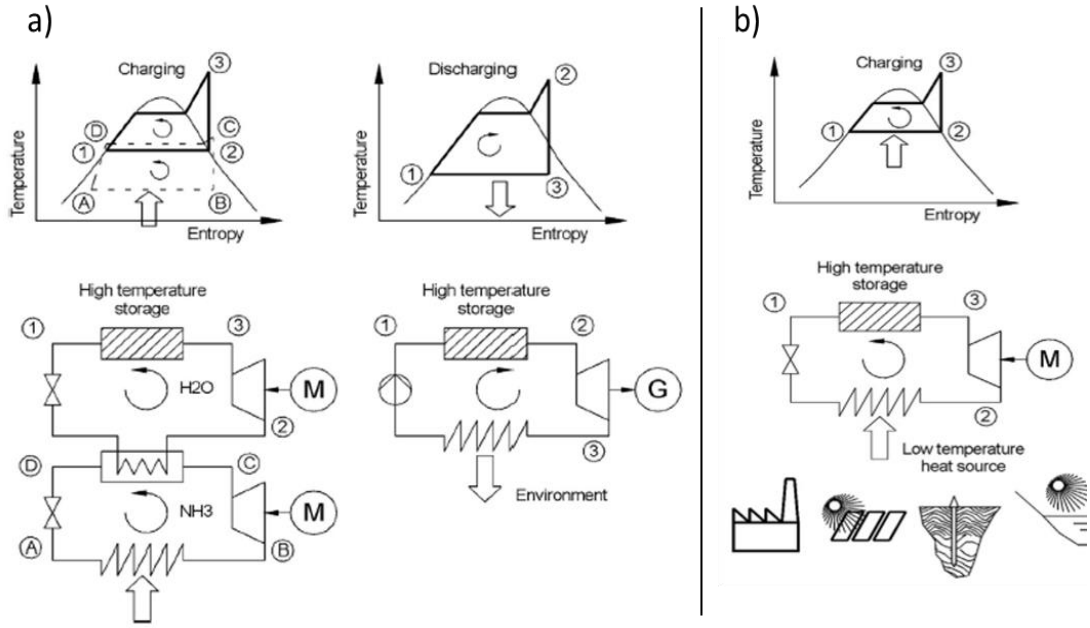


*Figure 2.4 Rankine-based PHES: a) using a bottoming ammonia cycle,b) integrating an external heat source* [41]

Another solution would be to integrate the CHEST concept with a low temperature heat source, it could be waste heat, solar thermal or geothermal heat, that allows the production of low temperature saturated steam. If the external heat source is able to produce saturated steam at 88°C, in point 2 as shown in Figure 2.4 b), the heat input from the external source compensate the irreversibilities of the cycle so that the net work is the same during charge and discharge phase, therefore in this particular case the RTE is 100%.

In the work of Peterson [43] a solution using an organic Rankine cycle with propane was proposed. The cycle operated between a maximum temperature of 50°C and a minimum temperature of -15°C. The RTE considering all the major losses of the system was calculated to be 50%. A similar concept is what the European project called Compressed Heat Energy Storage for Energy from Renewable sources (CHESTER) as part of the Horizon 2020 is trying to implement. In particular it plans to integrate the CHEST concept with a seasonal thermal energy storage that provides heat for a district heating system in Spain, although since the scale of the project is around 1MWe, for the discharge phase an organic Rankine cycle is used.

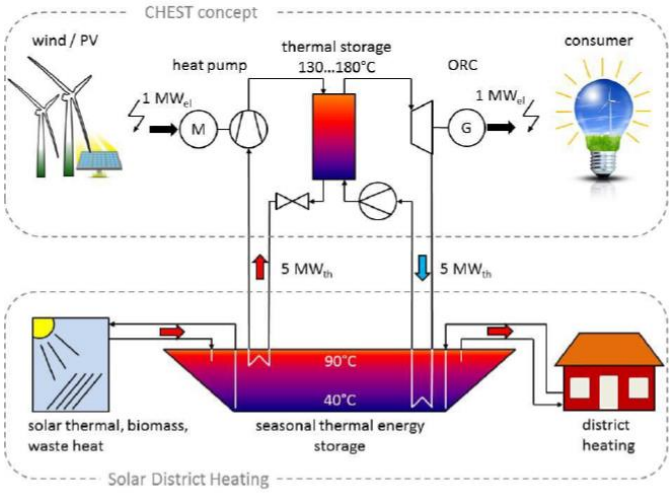


*Figure 2.5 CHESTER project concept and scheme source:* [36]

Advantages of the CHEST concept is that it uses the well-developed technology of steam Rankine cycles and that therefore has the potential of being used for large size storage system: power greater than 100 MW and several hours of storage. Another advantage is the limit on the maximum temperature and pressure around 400°C and 100 bar that means low energy density, but also lower cost for turbomachinery and for the steam generator. The biggest challenges are represented by the design of the latent heat hot reservoirs and also by the compression process of steam.

### 2.3.2. PHES BASED ON CO2-CYCLE

To minimize the cost of the storage system in PHES, liquid water could be used as storage medium. In this case heat is stored in pressurized tanks, that due to cost consideration can reach a maximum temperature of 200°C at 15.5 bar. For the cold reservoir, which in this case use latent heat, a salt water ice slurry is used that allows to have a minimum temperature of -21°C [44], which is the melting temperature of the slurry. To match such temperatures a $CO_2$ Rankine cycle is the appropriate solution due to its low critical temperature (31 °C). Working with $CO_2$ and using transcritical cycle eliminates the need of a latent heat storage unit, since that in this case there is no evaporation at constant temperature like in CHEST. In Figure 2.6 the T-s diagram of the $CO_2$ cycle is presented.

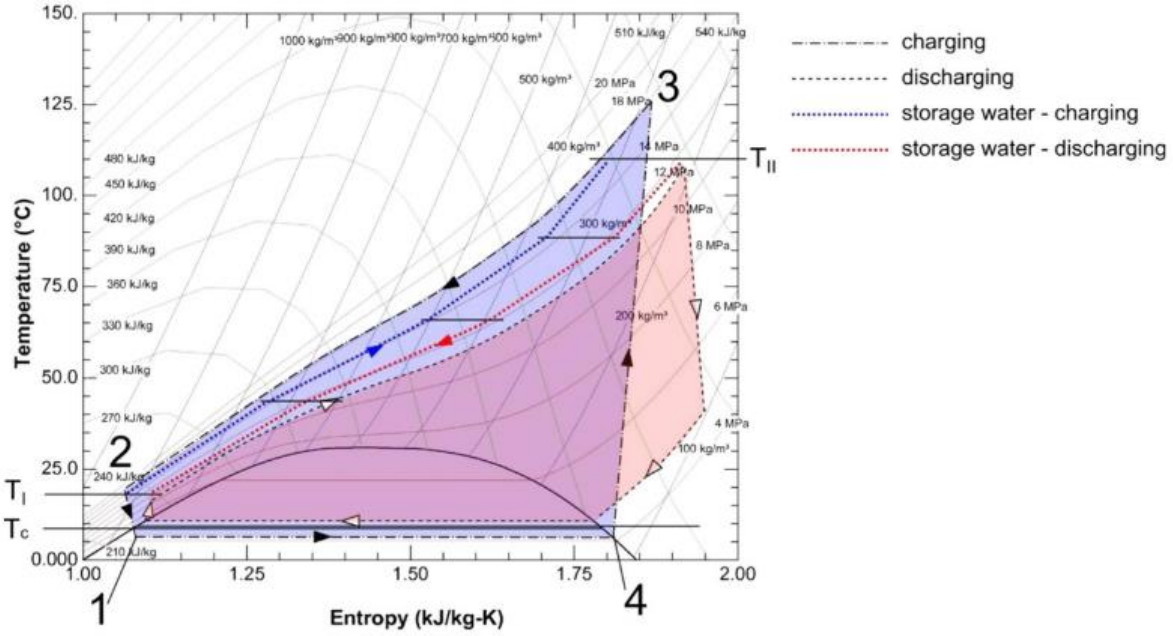


*Figure 2.6 T-s diagramm of PHES based on $CO_2$ transcritical rankine cycle* [44]

In [45] the concept of a commercial plant of 50 MW rated power and maximum temperature and pressure of 123°C, 140 bar and a minimum temperature of -3°C was estimated to reach an RTE of 65%. In Figure 2.7 the plant scheme is presented, on the cold side an energy balance system is needed to balance the heat exchanged with the cold TES during charge and discharge, since as can be noted from the T-s diagram in Figure 2.6 the heat absorbed and transferred to the cold storage is not constant.

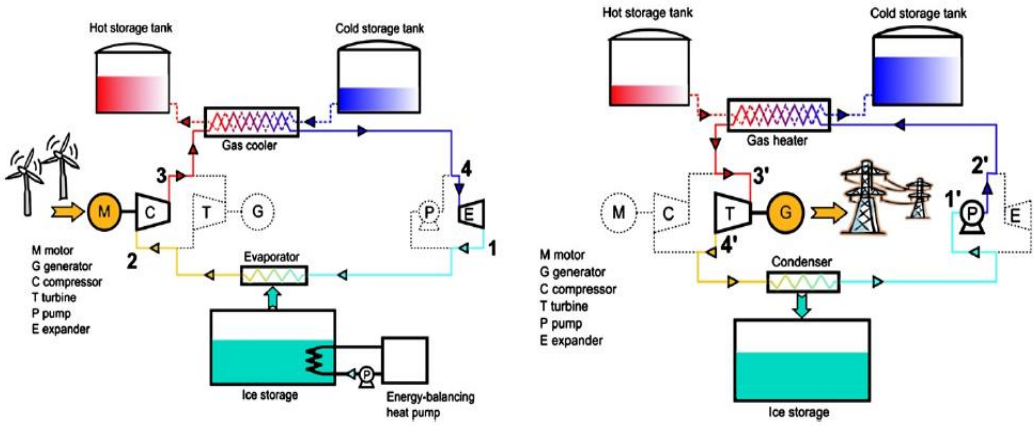


*Figure 2.7 Plant scheme of PHES based on $CO_2$ cycle*

The advantages of using this type of PHES system are mainly related to the low temperature requirements, low cost and good thermodynamic performance of the water as storage system, low environmental impact of the working and storage fluid. The main disadvantage is that during transcritical phase change $CO_2$ has a big change

of the specific heat and therefore particular attention must be paid on the design of the $CO_2$-water hot heat exchanger.

### 2.3.3. POWER TO HEAT TO POWER (PHP)

In this paragraph a small variant of CHEST is proposed, this concept uses an electrical heating system to convert electricity into heat instead of a heat pump, this has the main drawback of being limited by the efficiency of the reversible Carnot cycle operating between the maximum and minimum temperature of the real cycle and since that Joule heating means directly converting electricity into heat it results:

$$W_{el,charged} = Q_{stored} \tag{2.11}$$

$$\eta_{PHP,max} = \frac{W_{el,charged}}{W_{el,discharged}} = \frac{Q_{stored}}{W_{el,discharged}} = 1 - \frac{T_{min,cycle}}{T_{max,cycle}} \tag{2.12}$$

The power cycle can be chosen based on the size of the plant: for small size ($W_{discharge}$ < 5 MW) organic Rankine cycles are to be preferred, while steam Rankine cycle would be used for big size power plants due to the higher efficiency. An advantage for this technology is that it has no geographical restriction. So far, the most developed technology for thermal energy storage is the one used for concentrated solar power (CSP) that is used to drive a steam Rankine cycle. The most used storage medium for this application are the molten salts. In the Germasolar solar tower power plant in Spain molten nitrate salt is cycled between 560°C and 290°C to operate a steam turbine of 19.9 MW with a cycle efficiency of 42%. [44] In Figure 2.3 it is shown the integration of PHP concept with the molten salt technology running a Rankine cycle.

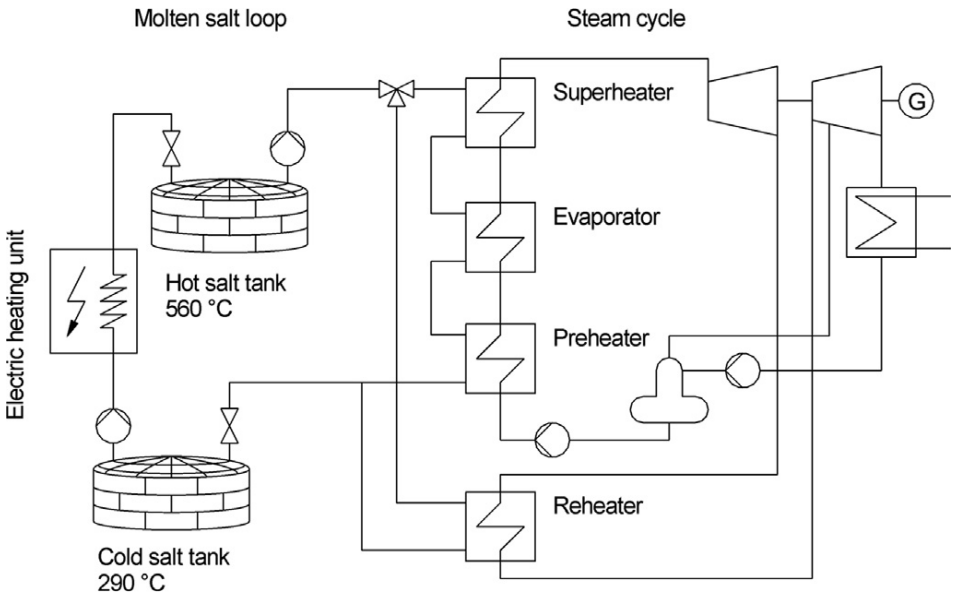


*Figure 2.3 PHP integration with molten salts storage tanks* [46]

In [44] the costs for a future 8h PHP-system with a thermal storage cost of 15 $/kWh$_{thermal}$ are estimated to be 206 $/kWh$_{el}$ and 1650 $/kW$_{el}$. A further cost reduction could be obtained if the PHP system is integrated with an existing power plant running a coal-fired steam Rankine cycle; it could be a good idea to use this concept to convert coal power plants into big thermal storage systems, this could help increase the lifetime of the plant, since some components of the plants like turbine, pump and condenser could be reused, while the boiler would have to be turned into an electrical heater. This would also to save some of the jobs related to the running of coal power plants. This option has been of particular interest in Germany, where the government has decided to shut down coal power plants by 2038, here coal accounts for the 30% of the electricity production [47].

### 2.3.4. PHES BASED ON BRAYTON CYCLE

This type of PHES is the most studied in literature, it is based on well-known Joule-Brayton cycle during discharge and on the reversed cycle during charge. The system is composed of:

- a hot and cold sensible heat reservoir, these could be in direct contact with the working fluid (packed bed storage system) or otherwise two heat exchangers are needed to exchange heat with thermal storage unit
- 2 pairs of turbomachines consisting in a compressor and an expander set each, one pair for charging and one pair for discharging
- one or two auxiliary heat exchangers to exchange heat with the environment

In Figure 2.8 the plant scheme for a packed bed PHES and the ideal cycle (assuming turbomachinery efficiency of 100%) on the T-s diagram are presented, during charging the gas flows counter clockwise and while discharging it flows clockwise. Starting from point 1, in the charge phase the gas is compressed first, reaching the

maximum temperature ($T_2$), then it gets cooled (till point 3) heating up the hot reservoir, it is expanded (point 4) and finally it absorbs heat from the cold reservoir. During discharge the cycle is reversed and is a common closed Brayton cycle.

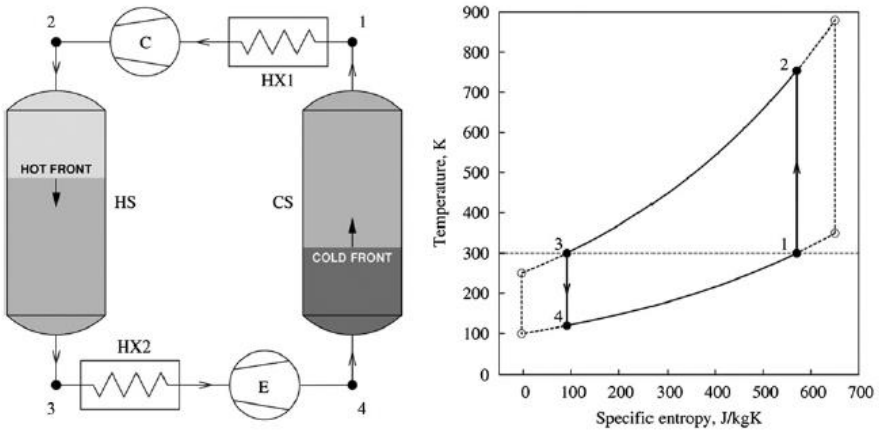


*Figure 2.8 Brayton-PHES, plant scheme on the left, ideal T-s scheme on the right, Dashed horizontal line indicates ambient temperature* [4]

When taking into account only irreversibilities of turbomachinery, drawing the T-s scheme it is clear from Figure 2.9 that between charging and discharging, the heat exchanged with the cold storage is different, in particular :

$$Q_{hot}^{dis}(2' - 3'c) < Q_{hot}^{ch}(2 - 3) \quad Q_{cold}^{dis}(1'e - 4') > Q_{cold}^{ch}(1 - 4) \qquad (2.13)$$

This would result in cycle temperatures increasing after every cycle, to avoid that as shown in Figure 2.8 two auxiliary heat exchangers (HX1 and HX2) are introduced to cool down the gas in the charge phase from $T_{1'e}$ to $T_{1'}$ and from $T_{3'c}$ to $T_{3'}$.

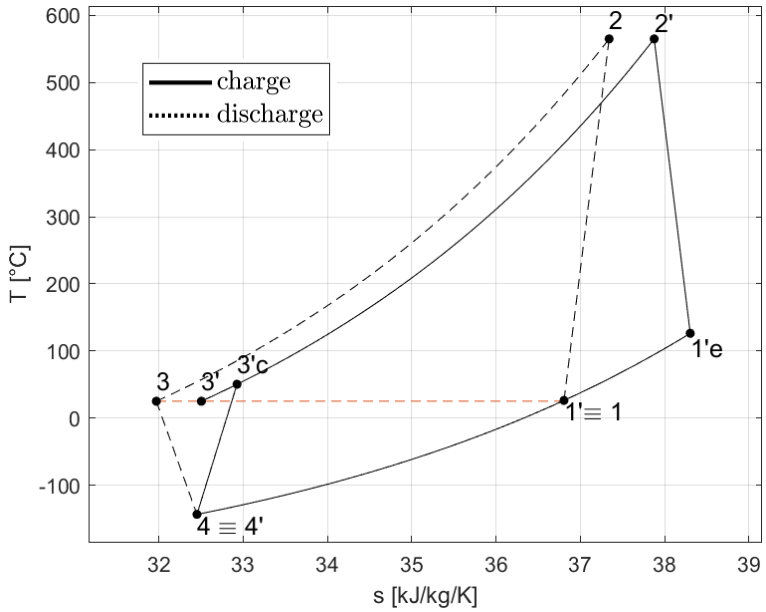


*Figure 2.9 T-s scheme of Brayton PHES with non-ideal compression and expansion, in red charge and black discharge phase, dashed line stands for ambient temperature*

A first comprehensive analysis of the Brayton cycle PHES was developed by Desrues [48]. In his study a preliminary analysis trying to estimate the RTE for different maximum temperatures was presented, introducing only turbomachinery irreversibilities. In Figure 2.10 the result of this analysis can be observed, as expected for a cycle with a low work ratio the turbomachinery efficiency has a high influence on the RTE. To reach a high RTE with the lowest cost two approaches are suggested: either employing a high maximum temperature and low turbomachinery efficiency or high turbomachinery efficiency and low maximum temperature. They developed then a PHES model, in which the hot tank operates between a 1012°C ($T_2$ ) and a of 25°C ($T_3$ ) while the cold tank works between 500 °C ($T_1$) and -70 °C ($T_4$); the maximum pressure is 4.6 bar and the working fluid is argon. After the preliminary analysis, they developed a model for the packed bed, using a simplified geometry and analysed the related losses, due to the moving thermal front and taking into how this influence turbomachinery efficiency. Considering only compression/expansion irreversibilities (assuming 0.9 polytropic efficiency) and the irreversibilties related to the packed bed operation (like pressure drops and irreversibilities related to the moving thermal front in the tanks) the RTE they got was 66% with a volumetric energy density of around 28 kWh/m$^3$, which is a value ten times higher that the energy density of pumped hydro energy storage.

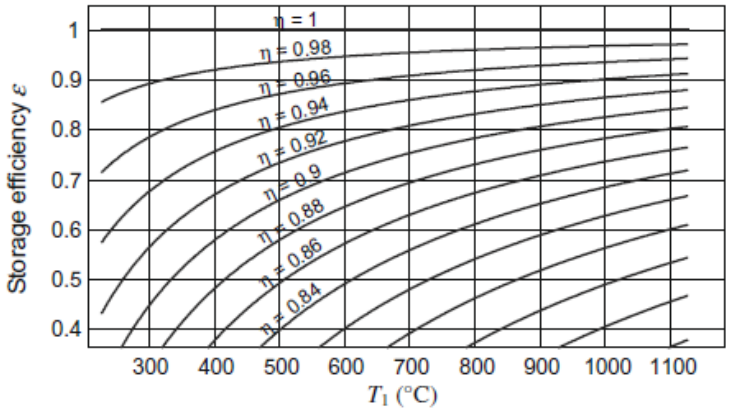


*Figure 2.10 PHES Round trip efficiency as function of maximum cycle temperature and turbomachinery polytropic efficiency* [48]

In [48] an alternative solution is proposed since its rather inefficient to cool down a gases at high temperature, Desrues et al. proposed to change the discharge pressure ratio in order that $T_{1',e}$ is equal to $T_{1'}$ and thus only to use one auxiliary heat exchanger, which works at quite lower temperature.

The heat exchangers have also another important function that is to keep the inlet temperature of turbomachinery constant during charge when the thermal front approach the end of the vessel, this is also referred to as exit loss in the work of [4]. Ni and Caram [49] in fact analysed a model with similar parameters of Desrues, using exponential matrix solutions to investigate deeper into the packed system . They found out that the RTE goes down if the tanks are used completely, for example if the hot tank is all brought to the maximum temperature. If only 50% of the packed bed is brought to the maximum temperature, with a $\eta_{pol}$=0.9 they got a RTE of 72.2%. White [4], whose model is depicted in Figure 2.8, underlined that to increase the energy and power density it is important to increase the isentropic temperature ratio ($T_2/T_1$). Moreover, he made an impact analysis of all losses on the RTE, including pressure and heat leakage losses (due to non-ideal insulation of the reservoirs). He noticed that the optimal discharge pressure ratio is the one that allows an equal distribution of the exergy dissipated in the two auxiliary heat exchangers. Mc Tigue et al. [10] developed an optimization of White model and stated that using reciprocating devices, with reasonable mechanical (92%) and electrical (97%) losses, the RTE could achieve 70% while if using turbomachinery with common efficiencies ($\eta_{pol}$=85%) the RTE could not be higher than 50%. Howes [7] developed a prototype, for the company Isoentropic Ltd. [8], of a reciprocating device investigating the problem of friction, valve pressure and heat losses of the machine. He then used the results to do a preliminary analysis of 2MW PHES and considered feasible that the RTE can reach 72% with current technology.

Regarding the working fluid, in early studies [4], [7], [48] argon is used, mainly to reduce the pressure ratio since it is a monoatomic gas, it is important to mention that

the maximum temperature of the cycle is related to the pressure ratio, therefore in order to reach higher temperatures the pressure ratio must be increased. High pressures are a problem because of the direct contact with the storage system, i.e. the two packed ped tanks are at the same pressure as the working fluid therefore, higher pressures would result in higher costs for the vessels. In a recent study of Benato [50] where a different plant scheme is proposed a comparison between argon and air is done, resulting in an better performance of air. In this study to decouple the maximum temperature and the pressure ratio an electrical heater is used after the compressor in charge phase, this allow to lower the requirements for the compressor and use air as a working fluid. In another study of Wang [51] the comparison between argon and helium was developed, the main advantage is that helium has a ten time higher specific heat capacity than Argon, this results in an overall better thermodynamic performance. The drawback it is the higher cost for turbomachinery since a higher heat capacity requires a higher number of stages of compression and expansion. Wang also pointed out another problem of packed bed storage, that is that that during discharge the power output decreases because of the moving thermal front. In his model working with Helium, for a 10 MW/4h PHES the RTE calculated was 56.9%.

The advantages of using a packed bed system as TES are that they allow a compact and therefore cheaper solution of the storage system and moreover they are suited to operate on a wider range of temperatures than liquid TES. On the other hand having the TES in direct contact with the gas, present some problems, mainly related to the thermal front, that increase the complexity and the management of PHES, moreover the limits of maximum pressure is around 10 bar [10], limiting the achievable power density that is around 240 $kW/m^3s^{-1}$ in White model. This results in a cost increase for both turbomachinery and the two auxiliary heat exchangers.

For these reasons in some others papers [1], [9] for the TES an indirect liquid TES is proposed, the hot and cold storage consist in this case of two tanks each, during charge the hot storage is heated from $T_b$ to $T_a$ while the cold one is cooled from $T_c$ to $T_d$. The plant scheme is presented in Figure 2.12, while the ideal T-s scheme is the same shown in Figure 2.11. In this layout the heat exchange with the TES is done indirectly using a liquid-gas heat exchanger, plus since the temperature range of the two liquids is limited, a regenerator is used. It is important to underline that regenerative heat transfer does not increase the RTE of the system when comparing two identical thermodynamic cycle as mentioned in [52],[9]. The main advantage of using an indirect TES configuration is that now the cycle can be pressurized to ten times the pressures of the packed bed PHES, thus increasing the power density. For the liquid of the hot TES in [1], [9] molten-salts are used, with allowed temperature range of 290°C-565°C, while for the cold TES in [9] n-hexane, at 1 bar is liquid from -95 to 77°C and in [1] methanol is used, at 1 bar is liquid from -98°C to 15 °C. Concerning the working fluid, Nitrogen and Argon are adopted respectively in [1] and [9]. In the doctoral thesis of Farres [1] he calculated the RTE of a regenerative, liquid storage PHES to be 65%, plus he got a volumetric energy density of 46 $kWh/m^3$ and a power density of 3 $MW/(m^3/s)$. In the model he takes a maximum

cycle temperature of 587 °C and -76°C respectively and a maximum pressure of 134 bar during charge. For his calculation he considered $\eta_{pol}$=0.9, relative pressure losses ($\Delta p/p$) of 1% and 98 % effectiveness for all heat exchangers.

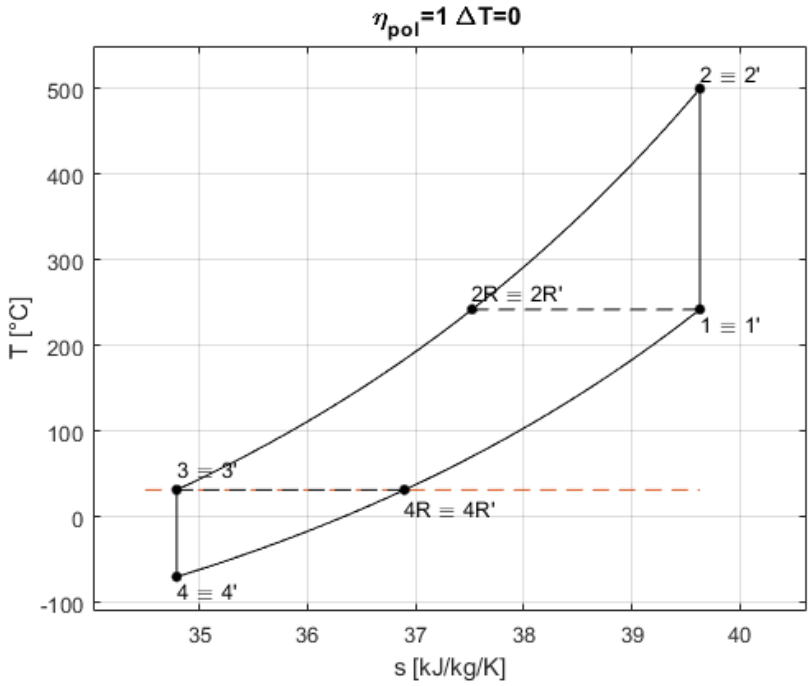


*Figure 2.11 Ideal T-s scheme of a regenerative Brayton PHES*

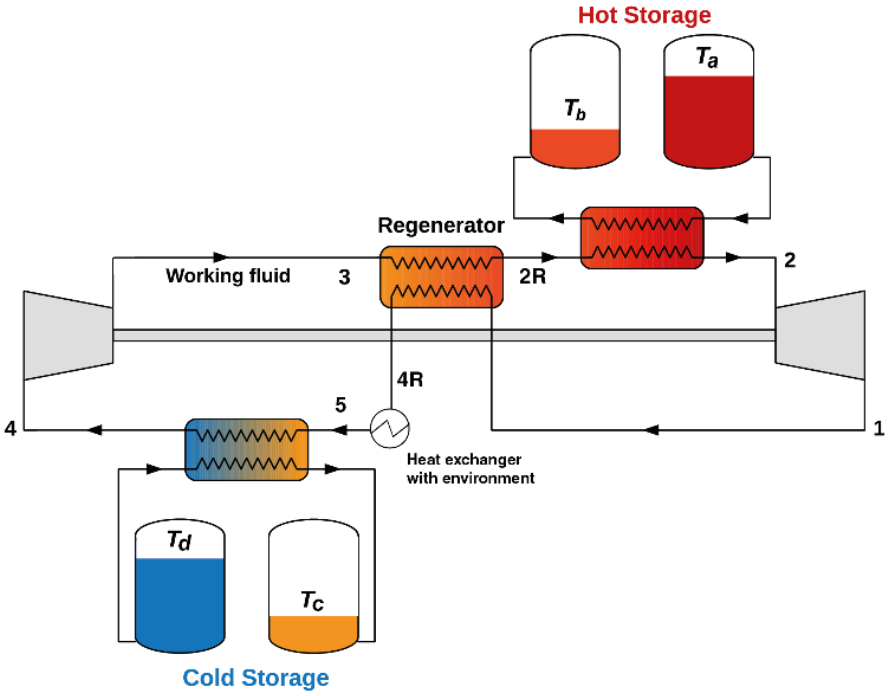


*Figure 2.12 Plant scheme of PHES with liquid thermal energy storage, arrows indicate the flow during discharge phase [1]*

In Table 2.1 a summary of the relevant parameters for all the different Brayton PHES models reviews is presented:

*Table 2.1 Summary of different Brayton PHES models with key parameters*

| **Model author** | **Working fluid** | **T2/T4 [°C]** | **T3/T1 [°C]** | **βc / βD** | **RTE [%]** | **Size MW/MWh** | **Additional information** | **Energy density [kWh/m3]** |
|---|---|---|---|---|---|---|---|---|
| Desrues et al. [6] | argon | 1000/-70 | 25/500 | 4.6/ βD to get T1=T1' | 66.7% | 100/600 | Solid TES | 27.9 |
| Ni and Caram [15] | argon | 1000/-70 | 25/500 | 4.6/ βD to get T1=T1' | 60%-100% | -/- | Analysis of losses of the thermal front | - |
| Mc Tigue et al. and White [5],[13] | argon | 505/-150 | 37/37 | 10.5/- | 50-70% | 2/16 | Model optimisation performed | 50 |
| Wang et al. | Argon and helium | -/- | -/- | 10/7 | 56.9% helium 39.9% argon | 10/40 | Comparison of argon and helium | 33 |
| Howes[11] | argon | 500/-166 | -/- | 12/12 | 72% | 2/16 | Prototype of a reciprocating device used | 50 |
| Farres [2] | Nitrogen | 590/-75 | 20/20 | 4.3/5.5 Pmax =134 bar | 65% | 2.5/25 | Liquid TES | 46 |

## 2.4. THERMAL ENERGY STORAGE

An important part of the system is the heat storage system. In this chapter a review on the state of the art of thermal energy storage will be presented.

It is commonly acknowledged that there are three ways of storing heat, they are listed in increasing energy density, but also technical and design challenge required:

- Sensible heat TES
- Latent heat TES
- Thermochemical TES

A part from a good integration with the rest of the system, TES has to met the following technical characteristics [52]:

- High volumetric energy density
- Good heat transfer performance between working fluid and the TES
- Stability and safety over the lifetime of the application
- Low exergy losses due to heat transfer and heat loss with the environment
- Low cost per unit of exergy stored

It is important to mention that there are two ways of integrating the thermal storage with the power cycle, this can be another classification criterion:

- Direct storage concept, in this case the heat carrier and storage material are the same medium, this is a cost-effective solution if the pressure if the medium does not need to be pressurized avoiding the use expensive pressure vessels.
- Indirect storage concept, in this case heat carrier and storage material are separated, this requires the use of a heat exchanger or a tube register within the storage medium

Concerning the direct storage concept another important property is thermal diffusivity, which is the ratio of thermal conductivity over the product of density and specific heat capacity, the higher this property the quicker the material reacts to a temperature difference and therefore the quicker the system can be sustain charge and discharge cycles.

### 2.4.1. SENSIBLE HEAT TES

Sensible heat TES (SHTES) is the most known and developed method for storing heat. It consists of heating or cooling a liquid (like oil or water) or solid material (rocks, ceramics, concrete etc.). Heat is absorbed increasing the temperature of the medium, depending on the mass of material m, specific heat capacity $c_p$ and the temperature change:

$$Q = \int_{T_i}^{T_f} mc_p dT \qquad (2.14)$$

Where $T_f$ and $T_i$ are the final and initial temperature of the medium respectively. Therefore, to have high energy density the TES material should have high specific heat capacity and density. SHTES has the advantage of being the cheapest among the three type of TES and of using safe materials, the only disadvantage is the low energy density reached:20-100 kWh/m$^3$.

In Table 2.2 a list of the most common material used SHTES is presented along with some key parameters. For low temperature TES, water is the most used application mainly because it is the cheapest option and has a high specific heat capacity (4.2 kJ/kg/K). The only limit is the temperature range (0-100°C, until 200°C if it can be pressurized [44]).

Above 100°C synthetic or diathermic oils and Molten Salts are used. Oils have a range of operation from 200-400°C [53], depending on the type, to increase the maximum temperature the storage system could be pressurized, but this often increases costs. Oils where use in early stages of development of CSP technology, they were used both as storage medium and heat transfer fluid. The main problem of using oil for TES is the thermal stability, as a matter of fact in 1999 there was an explosion in SEGS-1 concentrated solar power plant related to the storage unit [53].

Molten salts are used because they are liquid at atmospheric pressure (low cost for the tanks) in the range between 260°C to 550°C [9],the upper limit is the decomposition limit of the salt, while the lower one is the freezing temperature. Typically the salts consists of a mixture of 60% wt sodium and 40% wt potassium nitrate ($NaNO_3/KNO_3$) [53] and are widely used in the CSP sector [53]. They have the advantages of being compatible with steel and not presenting toxicity and explosion problems [9] plus of having a lower cost per unit of energy stored compared to synthetic oil as shown in Table 2.2. The only drawback is that they need to be kept at a temperature higher than the freezing point (with a certain safe margin) and therefore safety-heating system are required.

Concerning cold storage the fluids for temperature ranges between 180 K to 300 K and a vapor pressure lower the 1 atm are all hydrocarbons or derivatives of them [9], they are well suitable for cold TES. The only major disadvantage it is the high volatility of their price linked to the oil market, plus some special adjustments have to be made in order to prevent safety issues like toxicity and explosion problems.

A liquid TES system can be implemented easily by employing a two tank solution and a heat exchanger, to further reduce costs a single tank could be used with a moving partition to separate the cold and hot side, the two options are shown in Figure 2.13, in a simpler configuration there could no partition and in this case there would be a temperature gradient between the bottom and the upper part of the tank,

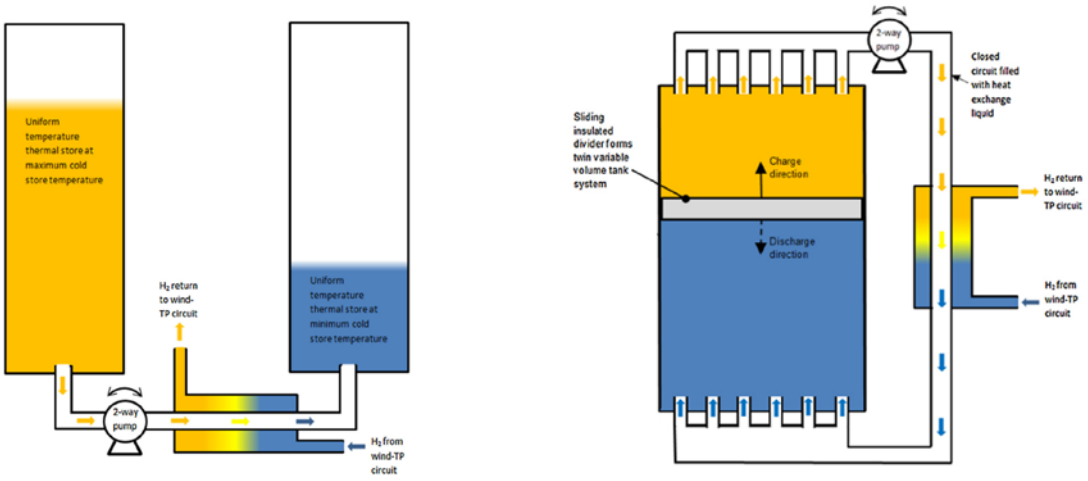


*Figure 2.13 Liquid TES system: two tank on the left, single tank with separator on the right* [54]

*Table 2.2 Sensible heat storage common materials and basic parameters Liquid materials on the top solid on the bottom* [55]

| **Storage medium** | **Temperature** | | **Average density [kg/m3]** | **Average thermal conductivity [W/m/K]** | **Average heat capacity [kJ/kg/K]** | **Volume specific heat capacity [kWht/m3]** | **Media costs per kWht [$/kWh]** |
|---|---|---|---|---|---|---|---|
| **Liquids** | Cold (°C) | Hot (°C) | | | | | |
| **Mineral oil** | 200 | 300 | 770 | 0.12 | 2.60 | 55 | 4.2 |
| **Synthetic oil** | 250 | 350 | 900 | 0.11 | 2.30 | 57 | 43.0 |
| **Silicone oil** | 300 | 400 | 900 | 0.10 | 2.10 | 52 | 80.0 |
| **Nitrite salts** | 250 | 450 | 1825 | 0.57 | 1.50 | 152 | 12.0 |
| **Nitrate salts** | 265 | 565 | 1870 | 0.52 | 1.60 | 250 | 3.7 |
| **Carbonate salts** | 450 | 850 | 2100 | 2.00 | 1.80 | 430 | 11.0 |
| **Liquid sodium** | 270 | 530 | 850 | 71.00 | 1.30 | 80 | 21.0 |
| **Solids** | | | | | | | |
| **Sand-rock-mineral oil** | 200 | 300 | 1700 | 1.00 | 1.30 | 60 | 4.2 |
| **Reinforced concrete** | 200 | 400 | 2200 | 1.50 | 0.85 | 100 | 1.0 |
| **NACL (solid)** | 200 | 500 | 2160 | 7.00 | 0.85 | 150 | 1.5 |
| **Cast iron** | 200 | 400 | 7200 | 37.00 | 0.56 | 160 | 32.0 |
| **Cast steel** | 200 | 700 | 7800 | 40.00 | 0.60 | 450 | 60.0 |
| **Silica fire bricks** | 200 | 700 | 1820 | 1.50 | 1.00 | 150 | 7.0 |
| **Magnesia fire bricks** | 200 | 1200 | 3000 | 5.00 | 1.15 | 600 | 6.0 |

On the bottom of Table 2.2 we can find materials used as solid state SHTES they have the advantage of being cheap, have a very high density and high thermal conductivity although they have a lower specific heat capacity compared to liquids. A technological solution involving materials in the solid state could be the construction of massive block with channels in which flows the heat transfer fluid (HTF) as proposed in the model of Desrues [5], this option has the advantage of reducing the pressure drop but has a low heat transfer performance. Plus the TES structure has to sustain mechanical and thermal stresses, in this cases Concrete is the preferred material for this application [52].

Another solution could be the use of a packed bed system, that consists of a tank filled with spheres of the storage material, the HTF then passes between the particles and gets cooled/heated, a scheme is presented in Figure 2.14. The heat transfer performance increases as the diameter of the particle decreases, because it increases the chances of developing turbulent flows and reduces the pressure drops. Particle size can be in the range of 0.5 to 100 mm [52]. This configuration has the advantage to be suitable for a large temperature range (from -200°C to up 1000°C [11]) therefore it was chosen in the most of PHES studies. As seen before a drawback is the non-homogeneity of the temperature in the tank, due to the thermal front that results in an exergy loss in case of PHES application.

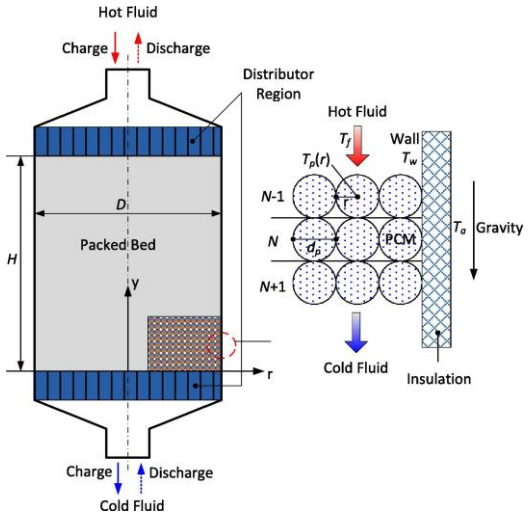


*Figure 2.14 Schematic diagram of packed bed thermal storage system* [56].

### 2.4.2. LATENT TES

Latent TES (LTES) is the storing of energy by absorbing and releasing heat with a change in the physical state of the material. This is why the materials employed are called phase change materials (PCMs). At first the PCM store energy with SHTES until it reaches the phase change temperature and then it absorbs heat at constant temperature with the formula:

$$Q = m * L \qquad (2.15)$$

where m is the mass and L is the phase change enthalpy required per unit of mass. The phase change can be solid-solid, when the material undergoes a change in the crystalline structure, solid-liquid, or liquid-gas. Liquid-gas phase change is not used in LTES because from liquid to gas there is a high change in volume. LTES has the main advantage of having a higher volumetric energy density (50-150 kWh/m$^3$ [57]) and that it works at constant temperature, allowing to minimize the temperature difference with the heat transfer fluid [53] in cycles where there is a constant temperature evaporation/condensation section.

The first requirement for a PCM is to have a suitable phase change temperature, moreover the following characteristics should be seeked in a good PCM:

- High phase change enthalpy
- Good thermal stability at low pressure
- Small volume change during the phase change process
- High thermal conductivity both in solid and liquid phase
- Low cost per unit of energy stored

In Figure 2.15 a classification of PCM is presented, currently the most used materials are water-ice mixtures, salt hydrates and paraffins. Water-ice slurry could be used in transcritical $CO_2$ PHES for the cold TES, in this case the phase change temperature could be reduced, by employing a eutectic mixture with salt.

The main technological challenge is that PCMs has in general a lower thermal conductivity (<1 W/m/K)), thus requiring special design to increase the heat transfer performance by increasing the heat transfer surface, the most common techniques are: encapsulation of the PCM in a solid material or in the heat transfer fluid and enhancement using a conductive structure made of metal [53].

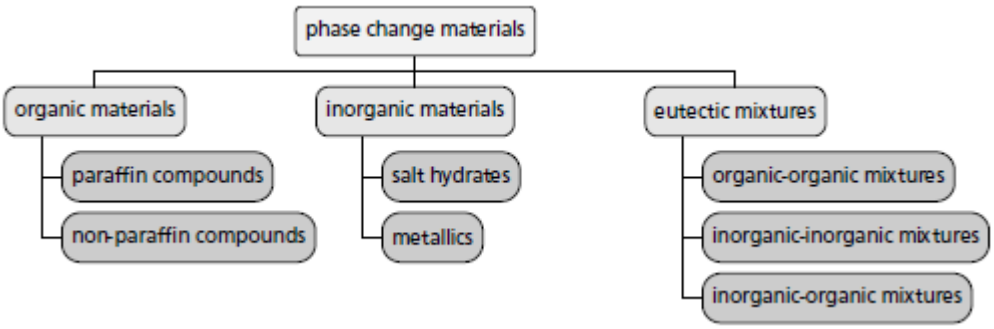


*Figure 2.15 Classification of PCMs* [52]

### 2.4.3. THERMOCHEMICAL TES

In a thermochemical TES a reversible endothermic chemical reaction is used to store energy in the form of chemical compounds, the heat is then released by recombining the two products (B and C) and the opposite exothermic reaction takes place. Such reaction can be expressed in the following form:

$$A + \Delta Q \leftrightarrow B + C$$

The heat stored is than equal to the enthalpy of reaction $\Delta Q$, which is far greater than the enthalpy of fusion and higher than the heat capacity stored in sensible heat, thus allowing to reach energy density in the order of 100-400 kWh/m$^3$[52]. The most studied reactions are presented in Table 2.3, as it can be seen the choice of the reaction depends on the temperature at which the reactions occurs.

| Reaction | | Temperature (°C) | Energy Density (kJ/kg) |
|---|---|---|---|
| Methane steam reforming | $CH_4 + H_2O = CO + 3H_2$ | 480–1195 | 6053 |
| Ammonia dissociation | $2NH_3 = N_2 + 3H_2$ | 400–500 | 3940 |
| Thermal dehydrogenation of metal hydrides | $MgH_2 = Mg + H_2$ | 200–500 | 3079 (heat)<br>9000 ($H_2$) |
| Dehydration of metal hydroxides | $CA(OH)_2 = CAO + H_2O$ | 402–572 | 1415 |
| Catalytic dissociation | $SO_3 = SO_2 + \frac{1}{2}O_2$ | 520–960 | 1235 |

*Table 2.3 Some chemical reactions for thermal energy storage* [58]

It is worth to mention that a Swedish company called SaltX Technologies has developed a concept for thermochemical TES using a special nanostructure of salts inside a water solution, they have a installed pilot plant in cooperation with a power plant in Berlin and also in China [59]. This technology has the potential of becoming a solution to store excess renewable electricity into heat and store it at ambient temperature. Plus, the technology could be employed to be used for long term energy storage.

While uncharged the storage medium is composed of a mixture of water and nano coated-salt, during charging heat is supplied and the reaction take place at 500°C, evaporating the water in the mixture, the salt is now charged. During the discharge phase water is reinjected in the salt and the reaction releases heat at 450°C with an efficiency of 85% (electrical to heat); the special nanostructure adopted allows the TES to have a high lifetime [59].

The main advantage of thermochemical TES is that the compounds when stored can be kept at ambient temperature allowing to reach higher efficiencies than SHTES or LTES, because in this case there are no heat losses with the environment during the storing time. Although this thermochemical TES seems promising, the technology is not yet mature and is still on the research and small prototypes level.

## 2.5. COMPARISON WITH OTHER ENERGY STORAGE TECHNOLOGIES

### 2.5.1. PUMPED HYDRO ENERGY STORAGE

Pumped hydro energy storage PHS is the most predominant and mature energy storage technology, it accounts for almost 97% of installed energy storage capacity (153 GW with a total stored energy of 9000 GWh in 2017) [47] . The concept is simple: energy is stored in the form of potential energy by pumping water from a lower reservoir to an upper reservoir. During discharge the water goes back to the lower reservoirs driving a turbine. The typical plant layout is presented in Figure 2.16, the energy stored is given by the formula $E=\rho Vg*(H_{upper}-H_{lower})$ where the first two terms are the density and volume of water in the upper reservoirs, g is the gravity acceleration constant and the last term id the height difference between the reservoirs. The RTE is around 70- 80%, the major sources of losses come from the operation of pumps and turbines, and by now PHS is the only ES technology that has proven to be capable of having a capacity up to 1 GWh and power that can reach 500 MW . Other advantages of PHS are the long lifetime (30-60 years), low OPEX cost, low levelized cost of storage(for definition see 4.6.3) and black start capability. The main drawback is related to the high environmental impact and geographical restrictions of PHS, since large volumes and heights are required, and the low energy density 0.5-1.5 $kWh/m^3$. The capital cost is around 470€/kW-2170€/kW[60] because of the big infrastructure like dams, tunnels and pipes that must be built. Nonetheless the IEA forecasted that new installations for a capacity of 26GW will be made in the years 2018-2023 [47].

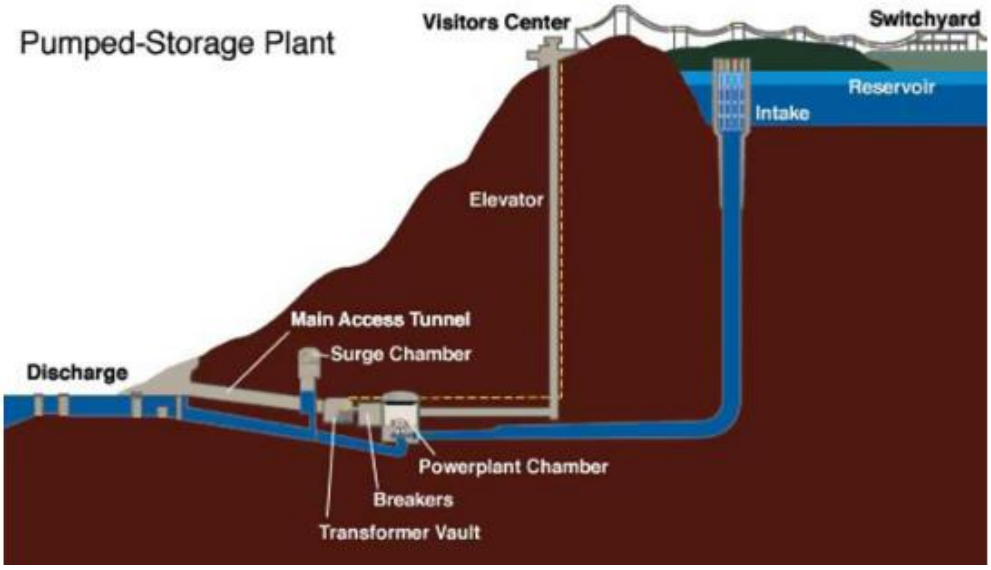


*Figure 2.16 Pumped Hydro plant scheme*[24]

Most efforts in research on PHS is now focused on the integration with renewables power plants in particular wind and PV in order to reduce the fluctuations of their production curve and increase the profitability of the plants [61].

### 2.5.2. COMPRESSED AIR ENERGY STORAGE

Compressed air energy storage (CAES) stores energy in the form of compressed air inside large underground caverns. During charge air undergoes a series of compressor with intermediate cooling, the maximum pressure is around 70 bar in current plants. During discharge air is heated up in burner where natural gas is injected, and the flue gasses are expanded in a high pressure and low pressure turbine with another burner in between, before going to the stack heat is recuperated, the scheme of the plant is depicted in Figure 2.17 and this layout is called diabatic-CAES (because it uses a fuel to heat up air). Currently the are only two installed CAES plants one in Germany (built in 1978) and one in USA (built in 1991) and they both use the diabatic-CAES concept. Since this process involves the use of a fuel, when calculating efficiency, we need to subtract to the output electricity, the one that could be generated if the fuel would have been in used in a power plant. Based on the assumed efficiency of the conversion of the fuel, D-CAES has a RTE between 33-63%, these values refer to the USA plants that has a recuperator [44].

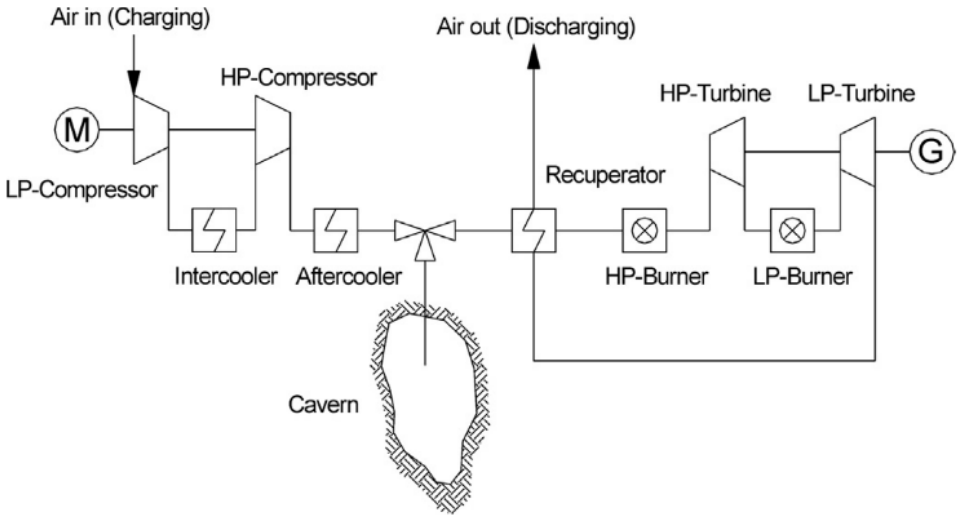


*Figure 2.17 Diabetic-CAES plant scheme*

The energy density is between 1.4-2.8 kWh/m$^3$, the total energy stored can reach the order of 1 GWh and a discharge power up to 300 MW. To avoid the consumption of fossil fuels and the production of $CO_2$ plant scheme involving a TES were developed, the concept is known as adiabatic-CAES (A-CAES). In this case the TES is used to store the heat released during compression and gives it back during discharge to heat up the compressed air. The RTE of the system are calculated to be in the range of 60-70%, although no A-CAES concept has been built yet.

### 2.5.3. LIQUID AIR ENERGY STORAGE

Liquid air energy storage (LAES) is a technology that could be classified as PHES, in the sense that it stores energy in the form thermal energy. It has some similarities with CAES only that in this case after compression air is liquefied. A plant scheme for charge and discharge is presented in Figure 2.18. During charge ambient air is undergoes a series of intercooled compressions, the heat is recuperated and stored in a liquid TES (mineral oil), air is then cooled down below air critical temperature of 133 K using a cold storage system made of propane and methanol air is the expanded via a throttle valve or a cryo-expander, the liquid fraction is stored in an insulated tank at atmospheric pressure, while the gas fraction is heated up and ejected in the atmosphere. During discharge the cycle is reverse air is pumped to high pressures using a cryo-pump and the is heated up by both the cold and hot TES and then undergoes a series of expansions and intermediate reheating. Although it has a more complicated system LAES is a more developed technology than PHES, mainly because it takes some of the technology from the air liquefaction technology used in the chemical industry. Recently a small pilot plant 350kW/2.5MWh was built by the company Highview in England, the obtained RTE was around 8% although it is suggested with bigger scale plants efficiency could reach 50% [1], in 2018 the first grid scale plant (5MW/15MWh) was commissioned near Manchester. In the work of Georgiou et al. [62], who performed a techno economic assessment of LAES, a CAPEX cost of 5000 $/kW and an OPEX of 890 $/kWh were calculated, the overall LCOS was estimated to be 410 $/kWh. The main advantage of LAES is the capability of reaching high energy density and of being suitable for large scale energy storage greater than 100MWh because also the RTE benefits from a scale up of the plant size [63].

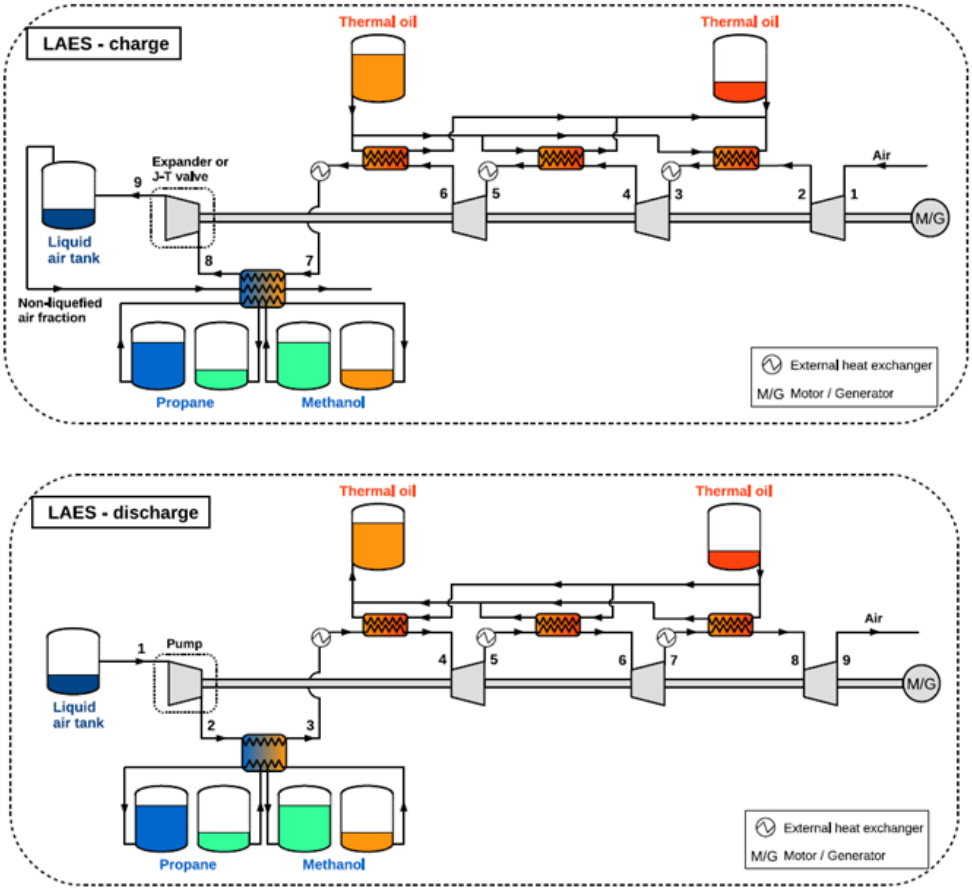


*Figure 2.18 Liquid air energy storage plants scheme on the top during charge on the bottom during discharge* [1]

### 2.5.4. COMPARISON WITH PHES

In Table 2.4 a comparison of the most important rating criteria for different technology is presented. To present a more detailed comparison also Li-ion and flow batteries were included in the table. The data for PHES were taken from Smallbone et al. [20] and McTigue et al.[10], it must be underlined that since being the technologies in the early stage of development the data for LAES, PHES and flow batteries must be taken with caution, especially the costs. Looking at the table it can be stated that PHES has the potential of becoming a viable solution for energy storage since it has a comparable RTE to PHS: the optimistic value is around 70% [10], with the advantage of having an energy density that is ten times higher and also it has no geographical restriction for the plant site.

*Table 2.4 Energy storage technology comparison* [30],[10],[20],[24]

| **Energy storage technology** | **Energy density [kWh/m$^3$]** | **Capital costs [$/kW]** | **Price per energy unit stored [$/kWh]** | **Round trip efficiency [%]** | **LIifetime (years)** |
|---|---|---|---|---|---|
| **PHS** | 0.5-1.5 | 600-2000 | 5-100 | 65-87 | 30-60 |
| **CAES** | 3-12 | 400-800 | 2-200 | 40-95 | 20-60 |
| **LAES** | 50 | 900-2000 | 260-530 | 40-85 | 20-40 |
| **PHES** | 46-100 | 454-965 | 58-120 | 50-70 | 25-30 |
| **LI-ION BATTERIES** | 250-670 | 740-1130 | 1000-1500 | 95 | 20 |
| **FLOW BATTERIES** | 16-60 | 600-1500 | 120-1000 | 20-50 | 5-30 |

# 3. BASIC THERMODYNAMIC CONSIDERATION FOR PHES

In this chapter some basic thermodynamic consideration for the Brayton PHES will be presented to better understand the influence of different loss parameters on the RTE. On each paragraph a single source of losses will be analysed while the other components will be assumed to be ideal. On the first paragraph a simple analysis of a PHES based on Carnot cycle will be shown.

## 3.1. PHES BASED ON CARNOT CYCLES

In [45] heat transfer irreversibilities were taken into account for a PHES based on Carnot cycles, a temperature difference ($\Delta T$) between the reservoirs and the heat pump (HP) and heat engine (HE) was introduced.

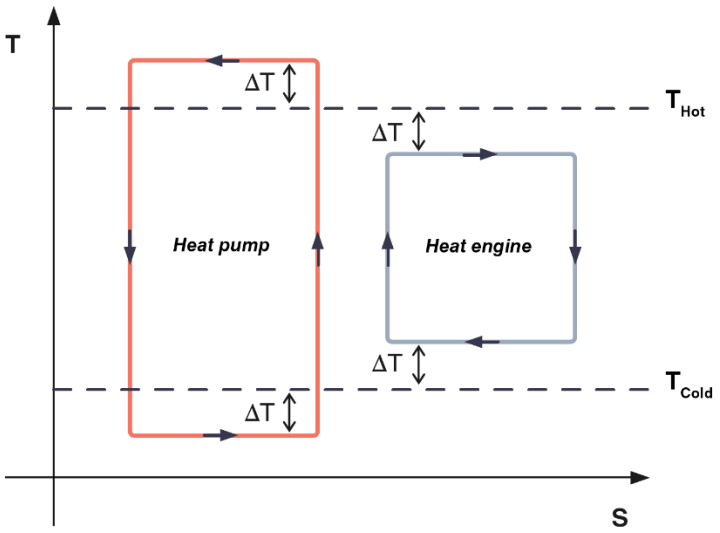


*Figure 3.1 PHES with Carnot cycle as a heat pump and heat engine, with a temperature difference with the hot and cold reservoirs, artwork from:*[64]

The RTE of the system is expressed by the following equation:

$$RTE = \left(\frac{(T_{hot} - \Delta T)}{(T_{hot} - \Delta T) - (T_{cold} - \Delta T)}\right) * \left(\frac{(T_{hot} - \Delta T) - (T_{cold} - \Delta T)}{(T_{hot} - \Delta T)}\right) \quad (3.1)$$

where the first term is the HP coefficient of perfomance and the second the HE efficiency, $T_{hot}$ and $T_{cold}$ are the temperatures of the hot and cold reservoirs respectively. HP and HE are reversible Carnot cycles. In Figure 3.2 the RTE is plotted for different values of $\Delta T$, it can be seen that with a temperature ratio of 2 and a $\Delta T$ of 10 K the RTE is around 75%, secondly the RTE increases as the temperature ratio of the reservoirs increases, this is because the $\Delta T$ is fixed and it clearly has a higher impact when $T_{hot}$ and $T_{cold}$ are almost equal.

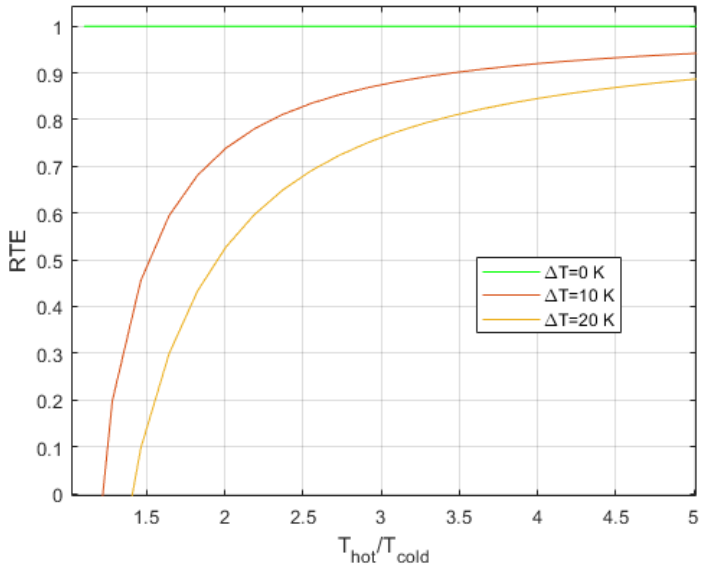


*Figure 3.2 RTE of PHES based on Carnot cycles with heat transfer irreversibilities(Δp=0 , $\eta_{is}$=0)*

## 3.2.COMPRESSION AND EXPANSION LOSSES

A simple expression for an estimation of the RTE of a Brayton PHES was proposed in [4], this formula is the most general one and can be applied to a PHES where the turbomachinery are the largest sources of irreversibilities. In Figure 3.4 ease the reader the plants scheme of PHES and its ideal T-s diagram are presented.

Assuming that heat transfer with the reservoirs is ideal and taking into account only irreversibilities in expansion and compression by scaling the ideal compression work ($W_{comp,id}$) by $1/\eta_{is}$ and the ideal expansion work ($W_{exp,id}$) by $\eta_{is}$ , where $\eta_{is}$ is the isentropic efficiency of the turbomachines. The RTE results then in:

$$RTE = \frac{W_{net,dis}}{W_{net,ch}} = \frac{W_{exp,id}^{dis} * \eta_{is} - \frac{W_{comp,id}^{dis}}{\eta_{is}}}{W_{exp,id}^{ch} * \eta_{is} - \frac{W_{comp,id}^{ch}}{\eta_{is}}} = \frac{WR_{ideal} * \eta_{is}^2 - 1}{WR_{ideal} - \eta_{is}^2} \qquad (3.2)$$

Where WR is the work ratio , defined in section 2.2 as $\frac{W_{comp}^{ch}}{W_{exp}^{ch}} = \frac{W_{exp}^{dis}}{W_{comp}^{dis}}$. From this basic equation it can be observed that RTE=0 when $WR_{ideal}$ is $1/\eta_{is}^2$ and that $RTE_{max} = \eta_{is}^2$ if WR $\rightarrow \infty$, therefore if $\eta_{is}$ = 0.9 the maximum reachable efficiency is 0.81. This basic calculation underlines that is very important to have both a high WR and a high efficiency in turbomachines, as can be seen in Figure 3.3 where equation 3.2 is plotted.

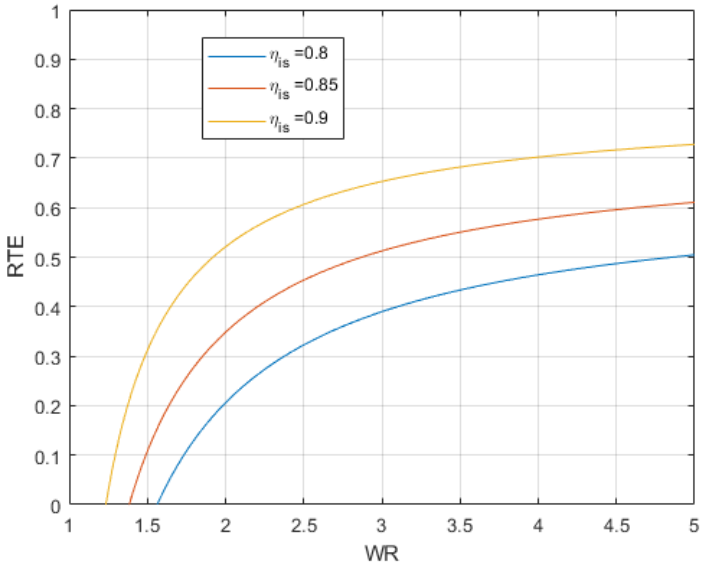


*Figure 3.3 Round trip efficiency as a function of work ratio for Brayton PHES with only turbomachinery losses,*

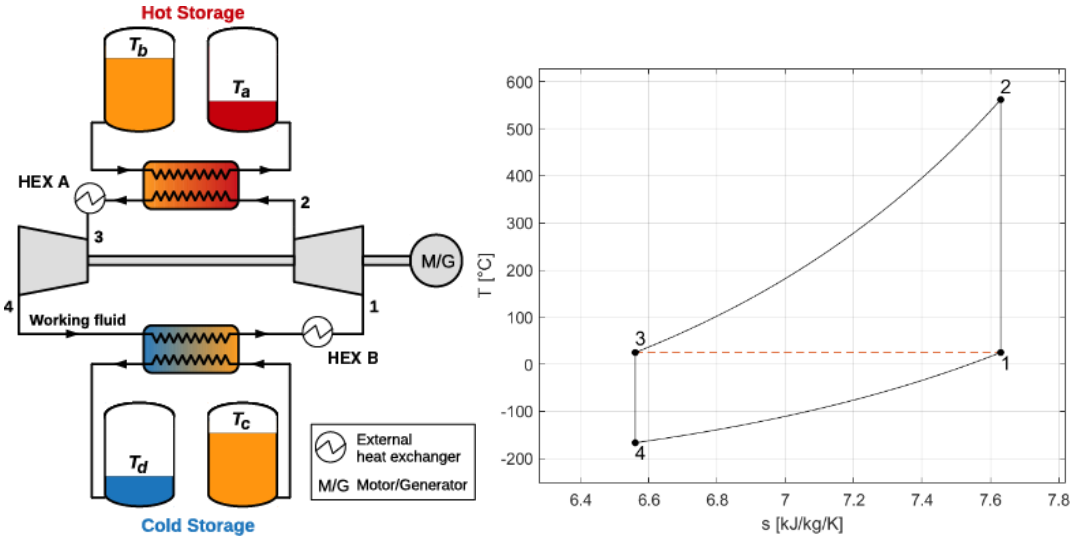


*Figure 3.4 Plant scheme* [1] *of a Brayton PHES with indirect liquid TES, arrows indicates the charge phase flow,ideal T-s diagram on the right: $\eta_{pol}$=1,$\Delta T_{HEX}$=0, $\Delta p$=0, with $T_3$=$T_1$*

For an ideal Brayton cycle, as the one shown in Figure 3.4 under the assumption of perfect gas with constant $c_p$, noting that for the ideal Brayton cycle $T_2/T_1 = T_3/T_4$ the work ratio can be expressed as:

$$WR_{ideal} = \frac{(T_2 - T_1)}{(T_3 - T_4)} = \frac{\tau_{is}}{\theta} \tag{3.3}$$

where $\tau_{is}=T_2/T_1$ is the charge isentropic expansion temperature ratio and $\theta = T_3/T_1$, so the WR increases as $\tau_{is}$ increases and $\theta$ decreases. If $T_1$ is fixed increasing $\tau_{is}$ means

increasing the maximum temperature of the cycle and decreasing θ results in the decrease of the minimum temperature of the cycle. In Figure 3.5 the RTE as a function of $\tau_{is}$ and θ is presented for a cycle with $T_3$=25°C and a isentropic efficiency of turbomachines of 90%. It is important to note that $\tau_{is}$ is related to the pressure ratio by the isentropic transformation formula:

$$\tau_{is} = \beta^{\left(\frac{\gamma-1}{\gamma}\right)} \tag{3.4}$$

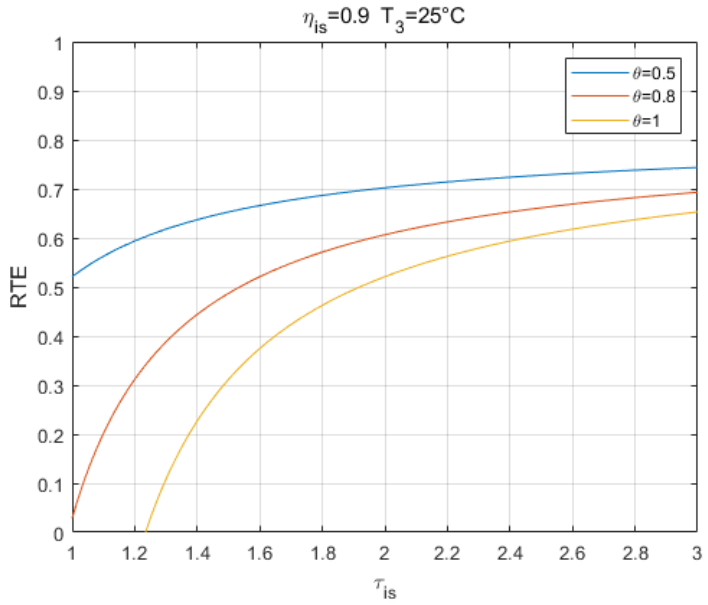


*Figure 3.5 Round trip efficiency of ideal PHES as a function of $\tau_{is}$ and θ ,calculated with the equation proposed in* [4]

It is clear that in reality the cycle constraints are the maximum and minimum temperature ($T_2$ and $T_4$) and therefore the work ratio can be rearranged and written as a function of $\tau_{is}$, $T_2$ and $T_4$:

$$WR_{ideal} = \frac{T_2}{\tau_{is} * T_4} \tag{3.5}$$

So once the maximum and minimum temperature are fixed the WR ratio increases as $\tau_{is}$ decreases, i.e. when T1 increases. In Figure 3.6 the RTE calculated with a $T_2$ of 565°C for different values of $T_4$ is shown, as expected by the trend of the work ratio, the RTE decreases as $\tau_{is}$ and $T_4$ increase.

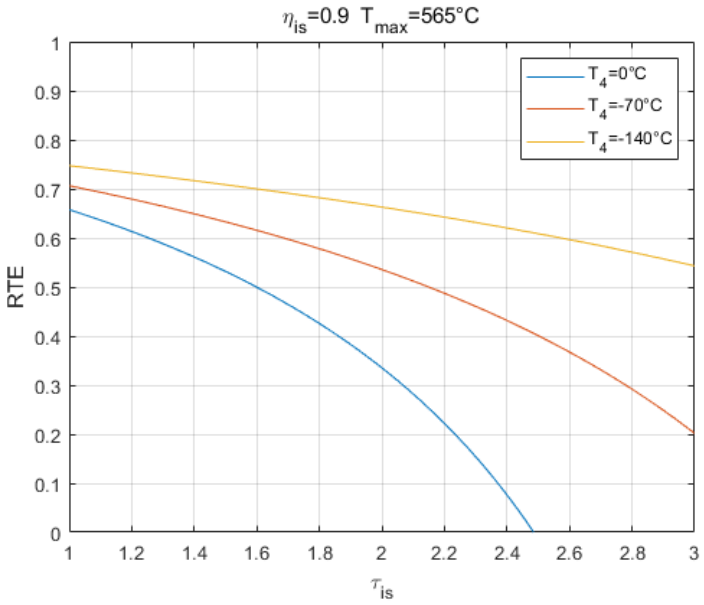


*Figure 3.6 Round trip efficiency of ideal PHES as a function of $\tau_{is}$ and minimum cycle temperature $T_4$, efficiency calculated with the equation proposed in* [4]*, for a maximum cycle temperature $T_2$ of 565°C*

It is important to underline that when comparing two types of different Brayton PHES configuration the first element of comparison must be the work ratio, in order to understand which one has the better performance on first approximation.

Moving to the real PHES cycle when considering only turbomachinery losses, the RTE is a function of $\tau$ ,$\theta$, polytropic efficiency of turbomachiens ($\eta_{pol}$) and $\tau'$ (the quotation mark indicate that it refers to the discharge cycle) that is the discharge compression temperature ratio defined as T2'/T1', because in the real case charge and discharge cycle are not identical. As explained before in the real system two heat exchangers are required to balance the heat exchanged with the reservoirs. In Figure 3.7 the T-s diagram of the cycle is shown, with $T_3$=$T_1$=25°C, during charge and discharge, in a) $\tau'$ has the highest value ($\tau'_{max}$) , in this case the heat rejection occurs only in heat exchangers A, in Figure 3.7 b) $\tau'$ is minimum ($\tau'_{min}$) and the heat rejection occurs in heat exchanger B. The calculations and graphs were made for helium under the assumption of ideal gas behaviour. In [1] an optimum discharge temperature ratio, the optimal value resulted to be a value in between of $\tau'_{min}$ and $\tau'_{max}$ , because the optimum RTE is when the average temperature at which the heat rejection occurs, is the minimum. Although there is an optimum RTE if both heat exchangers are used, when $T_3$=$T_1$ the work ratio is low and this penalizes the RTE.

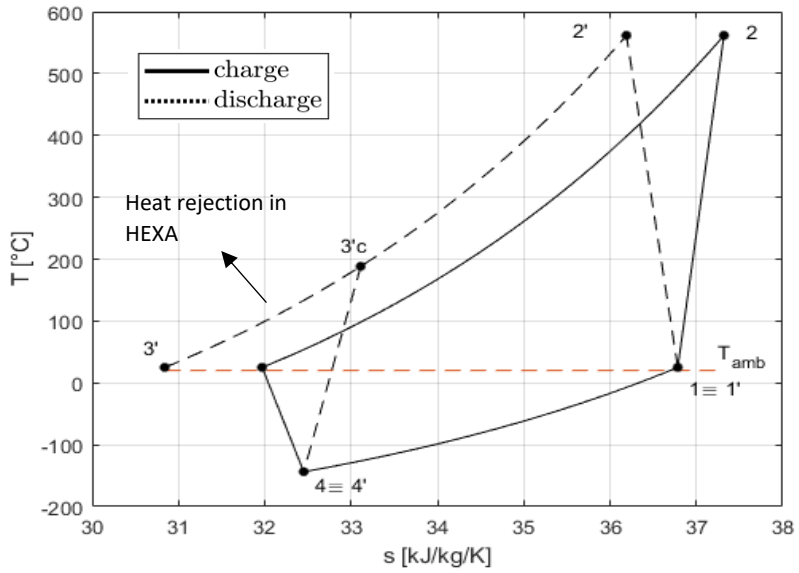


a) Heat rejection through HXA $\tau = 2.8$ $\tau' = \tau'_{max}$

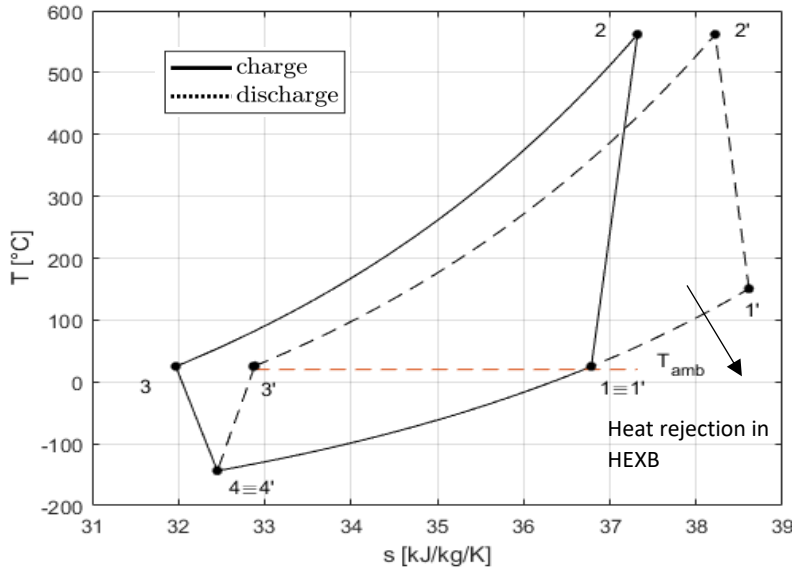


b) Heat rejection through HXB $\tau = 2.8$ $\tau' = \tau'_{min}$

*Figure 3.7 T-s diagrams of Brayton PHES with two different discharge temperature ratio with $T_3=T_1$, diagrams calculated for helium, $\eta_{pol}=0.9$ and maximum temperature =565°C*

The advantage of using only one heat exchanger is that the work ratio could be increased by varying $\tau$ : so if only the HXA is used $T_1$ could be set above ambient temperature (Figure 3.8 c) ), while if HXB is used $T_3$ could fall below ambient temperature (Figure 3.8 d) ).

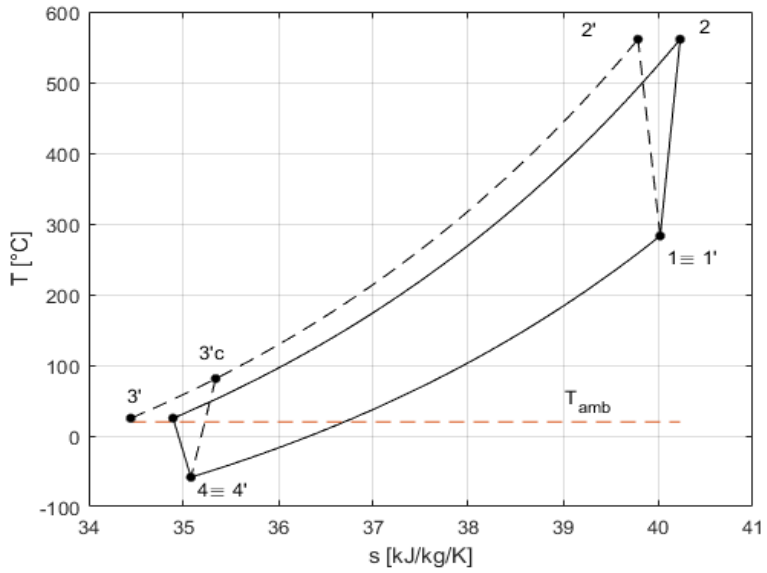


c) PTES with $T_1$ above ambient temperature and $\tau = 1.5\ \tau' = \tau$

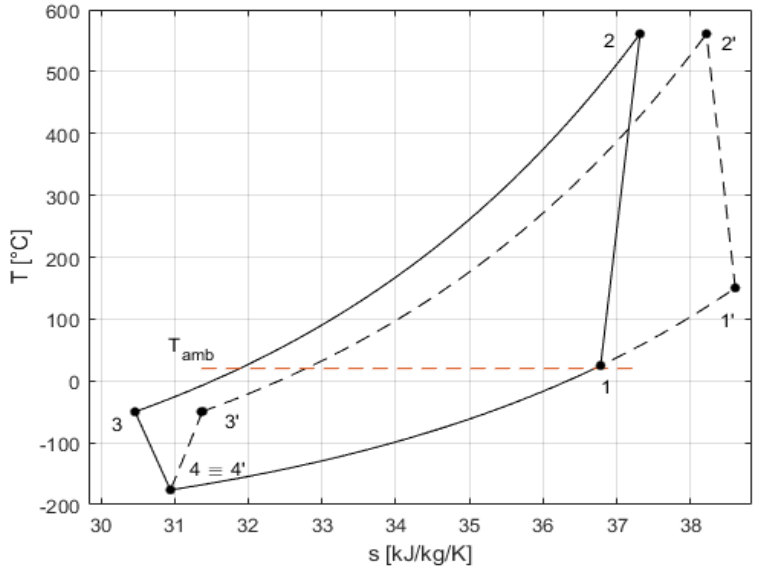


d) PTES with $T_3$ below ambient temperature $\tau = 2.8\ \ \tau' = 2$

*Figure 3.8 T-s diagrams of Brayton PHES with $T_3/T_1$ <1, diagrams calculated for helium, $\eta_{pol}$=0.9*

To evaluate the RTE for the four cases proposed a simple MATLAB® code was used, with the following assumptions:

- Ideal gas behaviour, the calculation were done for helium although it is important to mention that when assuming ideal gas behaviour the working fluid has no influence on the RTE, if the comparison is done for the same $\tau$
- Polytropic expansion and compression which follows the equation for the calculation of expansion and compression ratio:

$$\tau_{exp} = \beta^{\left(\frac{\gamma-1}{\gamma}\right)\eta_{pol}} \quad (3.6)$$

$$\tau_{comp} = \beta^{\frac{\left(\frac{\gamma-1}{\gamma}\right)}{\eta_{pol}}} \quad (3.7)$$

Where *y* is the specific heat capacity ratio and $\beta$ the pressure ratio

- Neglecting pressure and heat transfer losses
- Same maximum temperature of 565°C and ambient temperature of 25°C

RTE results then to be for the four different cases: a) 55%, b) 65%, c)71% and d) 68%. It is important to underline that as mentioned in [65] the cycle with $T_3$=$T_1$, since it has the lowest work ratio is also the most sensible to a decrease of the polytropic efficiency of turbomachines, this effect can be seen in Figure 3.9 where the case a) in particular is really sensitive to $\eta_{pol}$, this is also due to the fact that $T_{3'c}$ is already high due to the high $\tau'$, instead case c) and d) are less sensitive due to the higher work ratio. Nonetheless since Brayton PHES is most sensitive to turbomachinery efficiency even in case d) a reduction of 5% of $\eta_{pol}$ results in a reduction of the RTE of 10%.

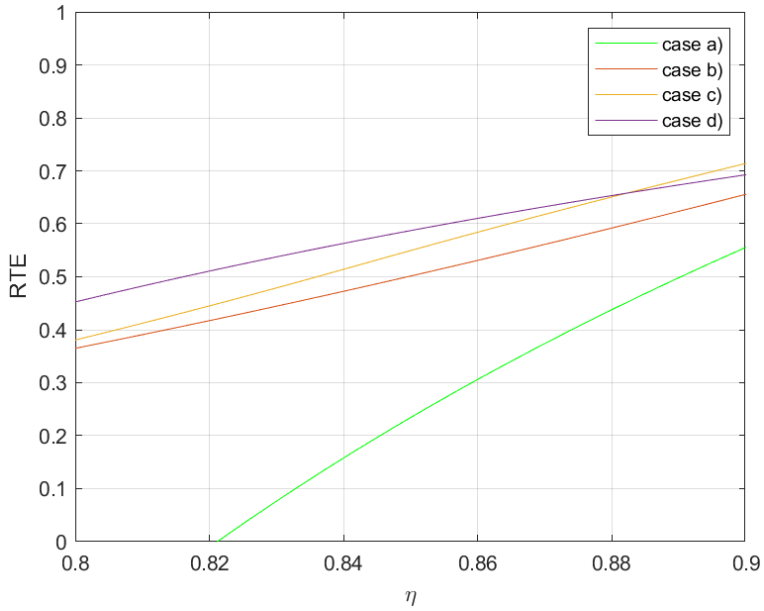


*Figure 3.9 RTE sensitivity to polytropic efficiency for four cases of PHES system*

Additionally, it is important to investigate how sensitive is the RTE to the variation of τ, for case c) and of $T_3$ for case d). In case c) since $T_2$ and $T_3$ are fixed the ideal work ratio can be rearranged to the form: $WR_{ideal} = \frac{T_2}{T_3}$, so also the WR is fixed and is not dependent from τ. Nonetheless it can be seen in Figure 3.11 that the RTE decreases as τ increases, to explain this one must recall that entropy generation in

turbomachines is proportional to the logarithm of the pressure ratio and therefore as τ increases irreversibilities increases. Plus, as the irreversibilities increases the average temperature of heat rejection to environment increases. The maximum efficiency can be reached when τ=1, i.e. when the net work is zero, clearly this is a limit case. For case d) instead it can be seen from Figure 3.11 that RTE increases as $T_3$ decreases, this can be explained again by looking to the ideal work ratio, that increases as T3 decreases. Keep in mind that for case d), for a given $T_{max}$, τ is kept fixed.

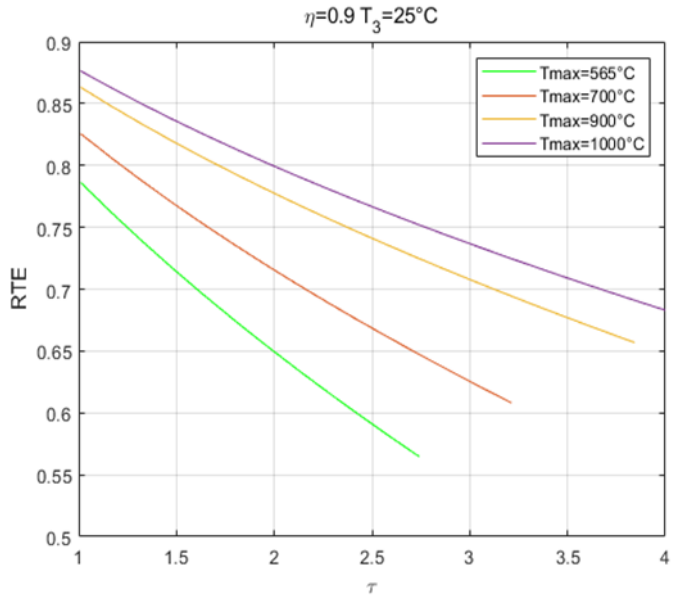


*Figure 3.10 CASE c) sensitivity to τ of Brayton PHES with T1 above ambient temperature and τ′=τ*

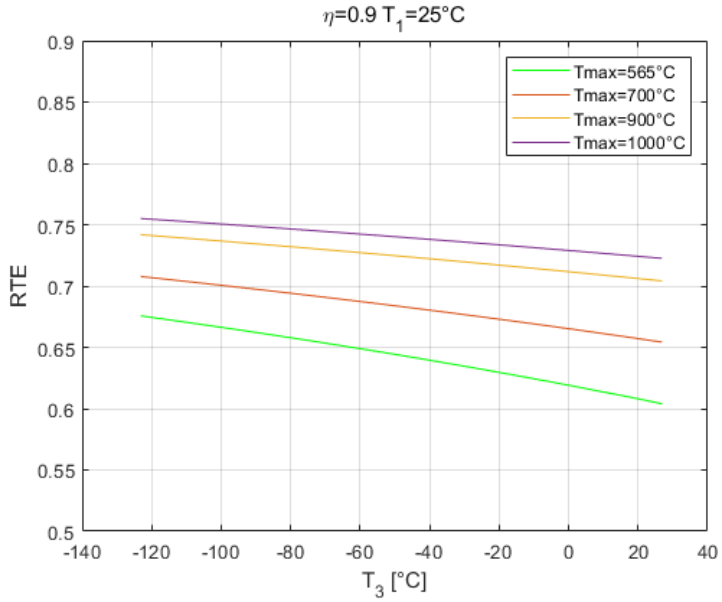


*Figure 3.11 CASE d) RTE sensitivity to $T_3$ for a Brayton PHES with $T_3$ below ambient temperature and $\tau'=\tau'_{min}$*

## 3.3.HEAT EXCHANGERS

The other bigger sources of losses are heat transfer losses and pressure losses that occurs in heat exchangers, this analysis is valid for a PHES with liquid system that adopts two heat exchangers with two reservoirs. The analysis is performed for a indirect storage system using four storage tanks, two for the hot and the two for the cold side.

### 3.3.1. HEAT TRANSFER LOSSES

The performance of a heat exchanger is commonly determined by the effectiveness, defined as

$$\varepsilon = \frac{Q}{Q_{max}} = \frac{(mc_p)_H (T_{H,in} - T_{H,out})}{(mc_p)_{min} (T_{H,in} - T_{C,out})} = \frac{(mc_p)_C (T_{C,in} - T_{C,out})}{(mc_p)_{min} (T_{H,in} - T_{C,out})} \qquad (3.8)$$

H and C stand for hot and cold streams of hot exchanger. The right-hand sides are valid only if $c_p$ is constant for both fluids. To minimise the heat transfer losses, a PHES system is operated with counter-flow heat exchangers with balanced flow [1]: $(m\bar{c_p})_H = (m\bar{c_p})_C$ where $c_p$ here is the average between inlet and outlet. If stream are balanced the temperature difference is equal in every point of the heat exchanger and the $\Delta T = T_{H,out} - T_{C,in} = T_{H,in} - T_{C,out}$ can be calculated as :

$$\Delta T = \left(\frac{1}{\varepsilon} - 1\right)(T_{H,in} - T_{H,out}) \qquad (3.9)$$

In PHES with liquid storage, heat exchangers are used during charge and discharge, thus the inlet and outlet of heat exchangers during charge and discharge have a temperature difference of $2\Delta T$, as example $T_2' = T_2 - 2\Delta T$, assuming that the storage media operates between the same temperature range during charge and discharge. The effect of non-ideal heat transfer can be seen in Figure 3.12 on the left the T-Q diagram and on the right the T-s diagram are presented.

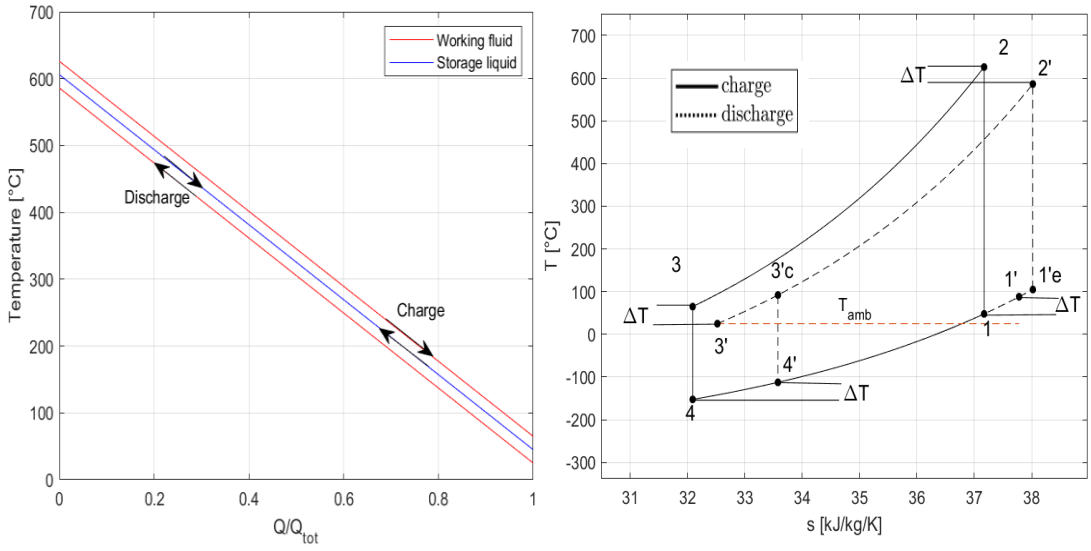


*Figure 3.12 Effect of non-ideal heat transfer for a Brayton PHES with indirect TES with ideal compression and expansion, T-s diagram calculated for helium*

In this case RTE depends on $\tau$ ,$\theta$, $\varepsilon$ and $\tau$', for $\tau'$ a maximum and a minimum can be defined, similarly as what done before, recalling that the limits cases are when all heat is rejected through HEXA (3'to $T_{amb}$) or HEXB (1' to 1) . After doing this, the sensitivity to heat transfer losses can be addressed as shown in Figure 3.13. The impact of the heat transfer losses is lower than that of turbomachinery if heat exchanger effectiveness is kept higher than 97% and $\tau$ is greater than 1.5 , instead it can still account for a loss greater than 20% if heat exchanger effectiveness is not kept greater than 95%. Additionally, it must be underlined that heat transfer losses have an opposite trend with respect to turbomachinery losses, because when $\tau$ decreases the net work decreases too but the heat transfer exchanged with the reservoirs does not.

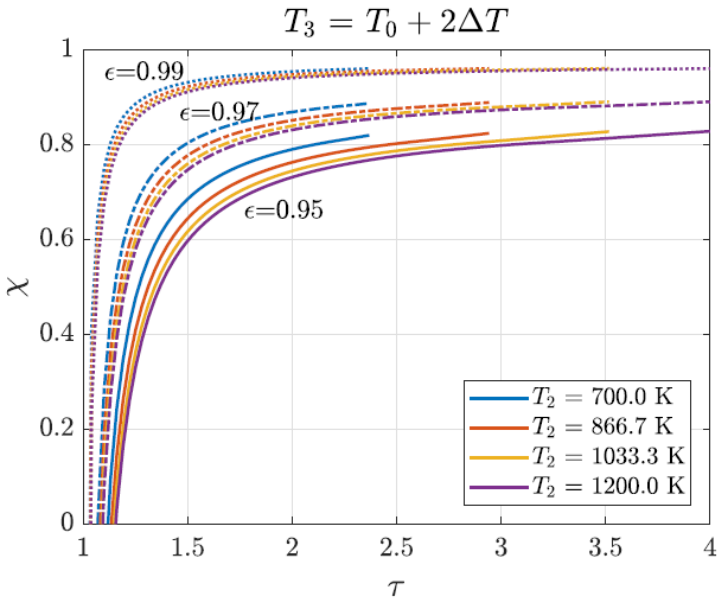


*Figure 3.13 Sensitivity to heat transfer losses as a function of the charge temperature ratios, for different heat exchanger effectiveness* [1]

### 3.3.2. PRESSURE LOSSES

Pressure losses in heat exchangers are usually accounted for by the pressure drop as a fraction of inlet pressure:

$$f_p = \frac{\Delta p}{p} \tag{3.10}$$

This is done because the exergy loss generation due to pressure drops is proportional to $f_p$ and not to the absolute pressure drop. It is important to notice that the pressure drop in the heat exchanger also reduces the expansion pressure ratio and increases the compression pressure ratio.

As done for the other losses an optimum $\tau'$ as a function of $f_p$, $\tau$ and $\theta$ can be derived maximizing the RTE efficiency and a sensitivity analysis can be developed. In Figure 3.14 similarly to heat transfer losses, pressure losses do not decrease as $\tau$ decreases and therefore the RTE decreases as $\tau$ decreases. It must be noted that if the $f_p$ can be kept below 1%, pressure losses have a low impact on the RTE.

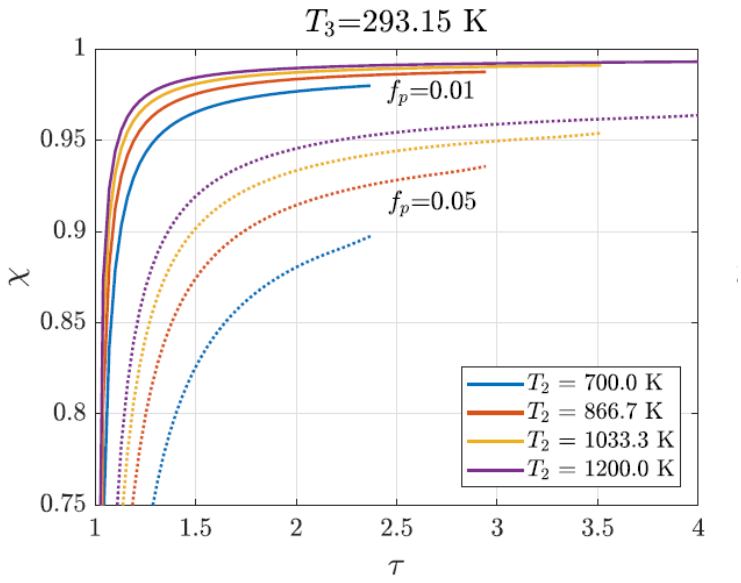


*Figure 3.14 Sensitivity to pressure drop irreversibilities of a Brayton PHES with indirect TES system in which only pressure losses are considered* [1]

# 4. METHODOLOGY

The scope of this thesis is to develop a model for the Brayton PHES system with liquid TES, in order to evaluate cycle performance and do an estimate of cost for this technology. The model was developed using Matlab R2019b [13] and taking the working fluid and cold storage properties data from NIST software REFPROP 9.1 [66], molten salts properties were taken from [67].

Considering the type of Brayton PHES, to the author knowledge for the indirect TES Brayton PHES there is only a paper of Laughlin [9] and a doctoral thesis of Farres [1]. Plus SHTES based on Molten Salts technology has already being proven feasible and tested in CSP power plants with power capacity from 20 MW to 150 MW with 4 to 12 hours of storage [68]. This is not the case for packed-bed system which are currently under development phase [68]. These are the main two reasons why it was chosen to investigate this kind of Brayton PHES.

## 4.1. WORKING FLUID CHOICE AND COMPATIBILITY WITH LIQUID STORAGE MEDIA

The choice of the working fluid for the PHES application is limited to gases that are stable and that are in the gas phase in a temperature range from -100°C to 600°C, this operational temperature range is imposed in this particular application by the hot and cold liquid TES as it will be explained later. As shown in chapter 2.3.4, in the literature the proposed candidates are monoatomic gases like helium and argon or biatomic gasses such as nitrogen. In a closed Brayton cycle the main trade-off in which the choice of the working fluid matters are the turbomachinery cost and the heat exchangers cost. The cost of turbomachinery is generally associated with the number of stages required (assuming ideal gas):

$$N = \frac{\Delta h_{total}}{\Delta h_{stage}} = \frac{c_p \Delta T_{total}}{k_{is} \frac{U^2}{2}} \qquad (4.1)$$

Where $\Delta h$ is the enthalpy change, $k_{is}$ is the stage loading coefficient, and $U$ is the rotor blade speed. When $k_{is}$ and $U$ are fixed the number of stages $N$ is proportional to the $c_p$, this suggests that, for the same $\Delta T_{total}$, helium would require five time the stages of a nitrogen turbomachine ($c_{p,He} \simeq 5200$ J/kg/K and $c_{p,N2} \simeq 1100$ J/kg/K). This is the main reason why Helium is not chosen as working fluid. Another aspect to be considered is the pressure ratio, monoatomic gasses have the lowest pressure ratio for a given temperature ratio, this is the reason why argon is chosen for PHES systems employing a packed bed TES.

Regarding the cost of heat exchangers, the most important properties to be considered are the specific heat, thermal conductivity and density of the working fluid. A higher $c_p$ is desirable because it means that for the same temperature difference of the fluid,

a lower mass flow rate is required to exchange the same heat. A high thermal conductivity is preferable because it means having a higher global heat transfer coefficient and therefore a reduced heat transfer area. Regarding the density having a higher density it is advantageous because it reduces the volumetric flow rate required and therefore it reduces the size of the HEX however this means also having a higher pressure drop in the HEX. All these consideration can be summarised, as done in paper [69] which demonstrates that the most important parameters when considering heat transfer performance is the fluid molar mass. Upon these considerations among the three fluids Helium has the best heat transfer properties because it has the lowest molar mass. Between argon and nitrogen, the latter is preferred because of its higher $c_p$ and of its higher thermal conductivity.

*Table 4.1 Working fluid properties at 1 bar and 300 K* [70]

| **Property** | **He** | **Ar** | **$N_2$** |
|---|---|---|---|
| **Molar mass [kg/kmol ]** | 4 | 39.9 | 28 |
| **cp kJ/kg/K** | 5.194 | 0.524 | 1.04 |
| **k x$10^6$ kW/mK** | 150 | 18 | 26 |
| **ρ kg/$m^3$** | 0.16 | 2.4 | 1.1 |

Based on the above considerations Nitrogen was chosen as working fluid since Helium would require a high cost for turbomachinery and argon has a lower heat transfer performance than nitrogen. Unlike PHES using packed-beds argon here is not chosen as working fluid also because there is no need of reducing the maximum cycle pressure to reduce TES cost.

In chapter 3 a simplified thermodynamic analysis for PHES was presented, it must be noted that in that analysis the working fluid is assumed to transfer heat to the hot TES in a temperature range that goes from around 600°C (point 2) to ambient temperature (point 3). While this is feasible for PHES using packed bed TES, which as shown in 2.4.1 have a wide operating temperature range, this is not for a system using liquid TES, because Molten Salts which have been chosen for the hot TES, have an operational temperature range that goes from 290°C to 565°C [1]. When looking to the T-s diagram in Figure 4.1 it is clear that if $T_3$ would have to be increased till 290°C, this would mean decreasing the work ratio of the cycle and therefore obtaining poor values for the RTE.

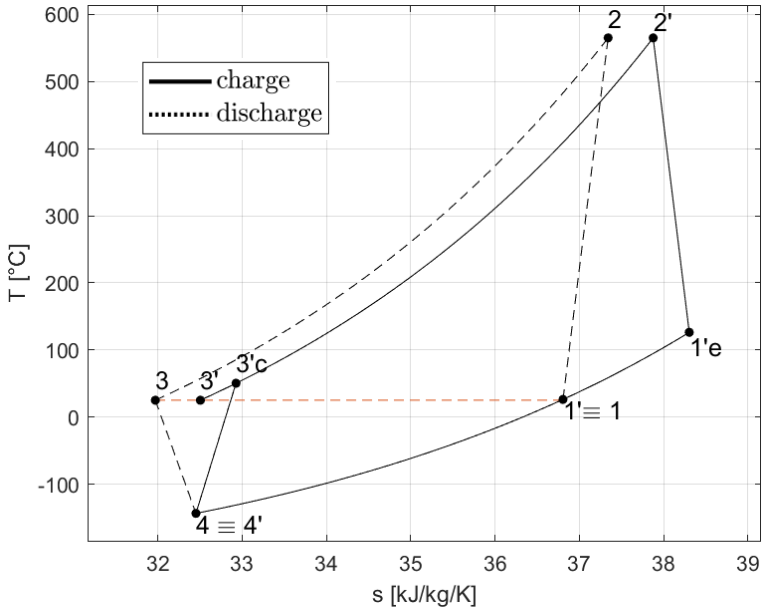


*Figure 4.1 T-s diagram of PHES system using helium as working fluid, considering only turbomachinery irreversibilities with polytropic efficiency η=0.9, T-s diagram for helium*

To solve this problem, in this system a regenerator is employed. This allows to keep $T_3$ at around ambient temperature and to increase $T_1$ above it, respecting the compatibility with the molten salts, if $T_{2R}$ is higher than the solidification temperature of the molten salts, moreover as seen in 3.2 increasing $T_1$ above ambient temperature has the positive effect of increasing the work ratio of the charge cycle. The match with the liquid TES is shown in the T-s diagram of the ideal cycle, proposed in Figure 4.2. For the cold TES fluid that are liquid in the temperature range of -100°C to 25°C at atmospheric pressure are all hydrocarbons derivatives [9]. In the model methanol was chosen as the cold TES fluid, because it adapts well to the cycle requirements ( at 1 bar it is liquid from -90 °C to 60°C), plus it is has the advantage of being a quite cheap material, well kwon in the chemical industry [1], although to the author knowledge, there is no paper reporting its employment in the energy storage sector.

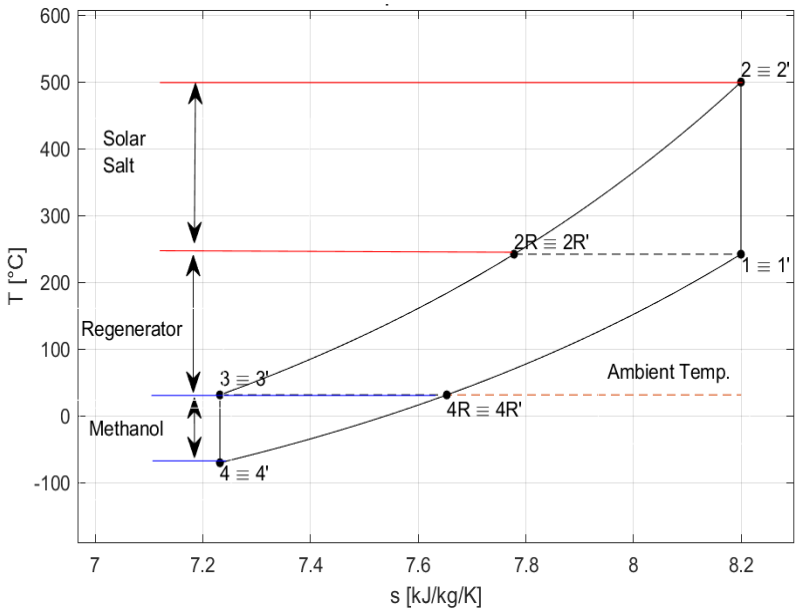


*Figure 4.2 Ideal T-s diagram for a regenerative Brayton PHES using indirect TES, $\eta_{pol}$=1, $\Delta T$ in all heat exchangers = 0, nitrogen as working fluid,*

## 4.2.MODEL INPUT DATA AND MAIN ASSUMPTIONS

The cycle model works by first solving the charge cycle and by evaluating the design geometry of heat exchangers, which are the same for the charge and discharge cycle, in order to avoid having a double cost for HEXs. For the turbomachinery instead a couple expander/compressor is used for charging and other for discharging. Therefore, while the heat exchangers during discharge operate in an off-design condition the turbomachines operate at design condition in both phases. Plant scheme and T-s diagram are presented in Figure 4.4 and Figure 4.4 . The model is operated with the assumption of steady state operation for all processes. Input data of the design model in charge phase are:

- Tanks temperatures of molten salts $T_a$, $T_b$ and of methanol $T_d$
- Gas maximum temperature $T_2$ and $T_3$
- Cycle maximum pressure $p_2$
- Storage tanks pressure is set to be 1 bar
- Charge compression pressure ratio (β)
- Performance of different components such as polytropic efficiency of turbomachines and heat exchanger pinch point temperature difference and relative pressure drop
- Compressor input power is used as parameter to set the working fluid mass flow rate
- the electromechanical efficiency of the generator $\eta_{e,m}$, which comprehends also mechanical losses of the shaft bearing, is assumed to be 97% [14].

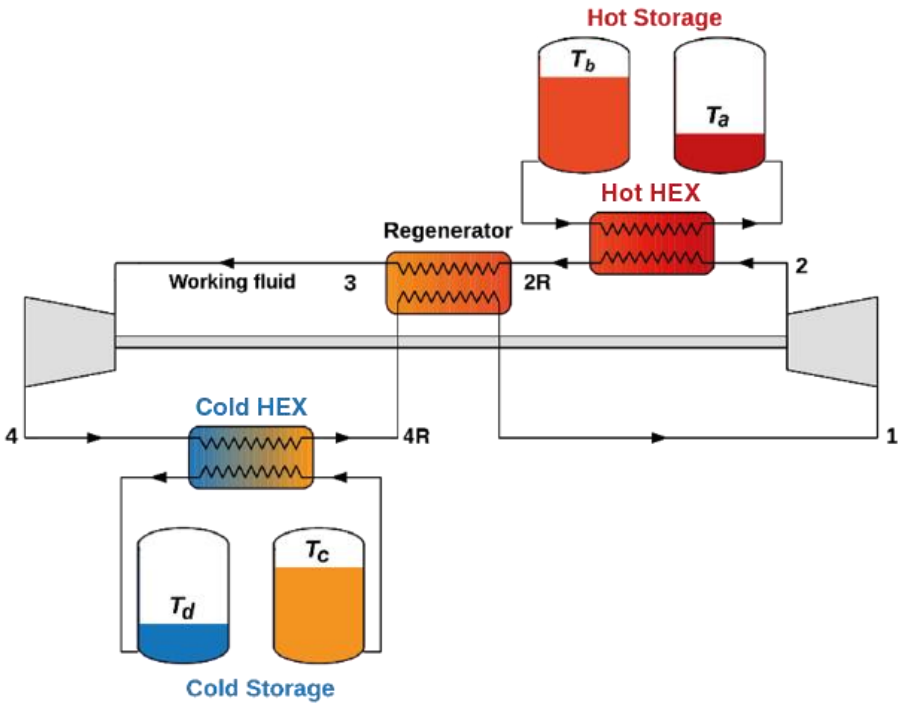


*Figure 4.3 Plant scheme of a regenerative Brayton PHES with liquid TES*

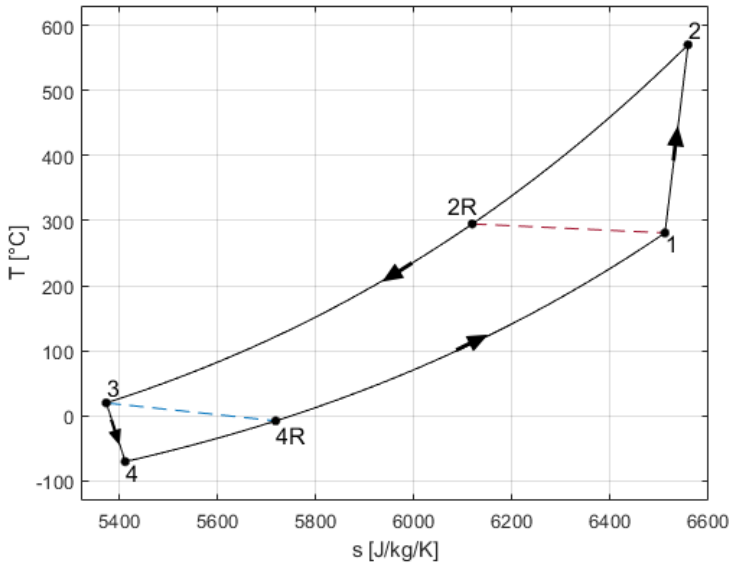


*Figure 4.4 T-s diagram of regenerative Brayton PTES during charge, βcomp=3.88, T2=575 °C and T3=40 °C, nitrogen as working fluid, regenerator effectiveness 96.4%*

Regarding the consumption of the pump for the molten salts and methanol, with the assumptions of a pressure drop of 1 bar [71] and a pump efficiency of 70% their power consumption is negligible (for a rated charge power of 18MW the pumps consumption is around 30 kW).

It is important to underline that heat losses from the hot and cold TES are neglected [1],[12].

After solving the charge phase all cycle points, the geometry of the heat exchangers, working fluid and storage mass flow rates are known. The outputs of the charge model that are taken as inputs for the discharge model are:

- Heat exchangers geometry such as heat transfer area, tubes diameters, tubes number and length
- Tanks temperatures, which in the design model will be kept equal between charge and discharge (the reason will be explained later)
- Polytropic efficiency of turbomachines which is kept equal in the design model
- Net power input to evaluate the RTE

The plant scheme and T-s diagram of the discharge phase are presented in Figure 4.5 and Figure 4.6. The discharge model works similarly to the charge one only that in this case the HEXs operate in off-design condition. Because of this aspect, in the discharge model the temperature differences in the heat exchangers cannot be chosen and must satisfy the heat transfers laws that governs HEXs which will be explained in chapter 4.3.2. Practically this means the cycle temperatures are determined by the off design of the heat exchangers.

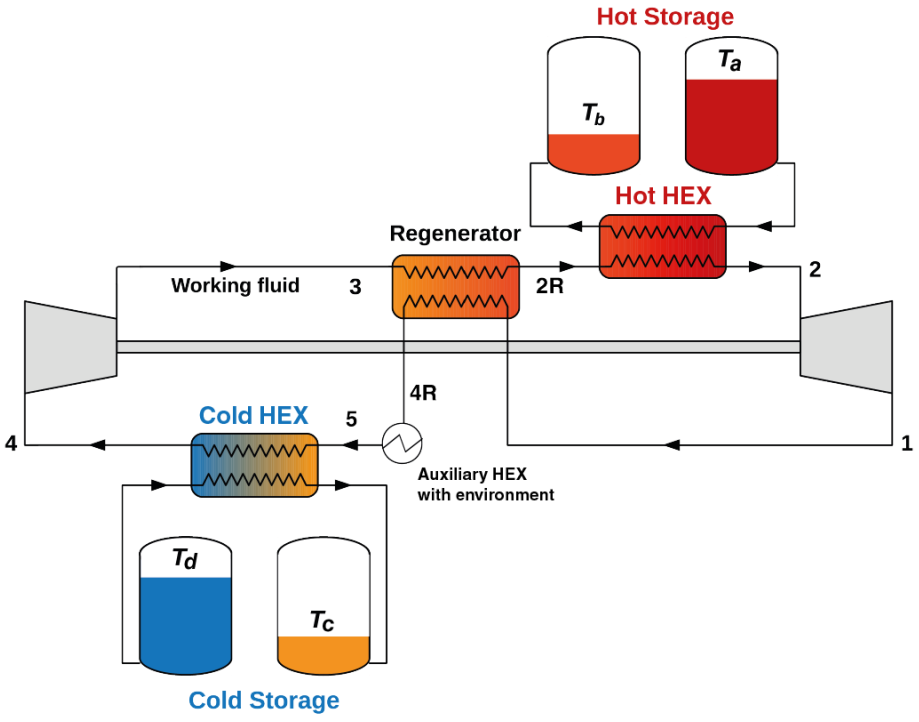


*Figure 4.5 Plant scheme of a regenerative Brayton PTES with liquid TES in the discharge phase, source:*[1]

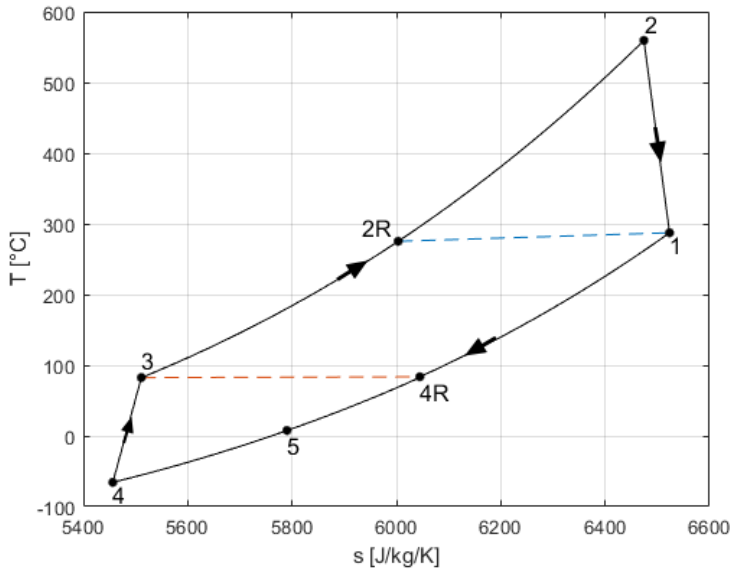


*Figure 4.6 T-s diagram of a regenerative Brayton PHES during discharge phase, nitrogen as working fluid, , βexp=4.7, regenerator effectiveness 93%, T2=555°C, $T_5$=30°C*

Since basically all cycles temperatures are fixed by the off design of heat exchangers and by fixing the tanks temperatures, four variables are used as control parameters of the discharge cycle, which are:

- Mass flow rate of the working fluid $m_{wf}$
- Mass flow rates of the hot and cold storage liquids, $m_{hot}$ and $m_{cold}$
- Cycle pressurization, which will set by setting the minimum cycle pressure $p_4$

It is important to mention that the three mass flow rates control variables are set by imposing an equal percentage increase/decrease with respect to the charge phase values. This is done to ensure that similarly to the charge phase, also in the discharge phase heat exchangers are operated with balanced flows, i.e. the $\Delta T_{\text{inlet}} \simeq \Delta T_{\text{outlet}}$ which is the strategy that allows to minimize heat transfer irreversibilities.

The working fluid mass flow rate is directly related to the net discharge power on the generator shaft:

$$W_{net,dis} = m_{wf,dis}\left[\left(h_{1,dis} - h_{2,dis}\right) - \left(h_{3,dis} - h_{4,dis}\right)\right] \qquad (4.2)$$

Whereas the mass flow rates of the cold and hot TES are directly related to the heat exchanged with the TES:

$$Q_{hot,dis} = m_{hot,dis}(h_a - h_b) \qquad Q_{cold,dis} = m_{cold,dis}(h_d - h_c) \qquad (4.3)$$

From these equations it can be seen that a variation of the three control variables allows to set the net discharge power and therefore to change the charge and discharge time.

This can be understood by doing a first principle consideration applied to the hot and cold TES. Doing an energy balance for the hot TES it results:

$$E_{hot,dis} = m_{hot,dis}(h_{a,dis} - h_{b,dis})t_{dis} = m_{hot,ch}(h_{a,ch} - h_{b,ch})t_{ch} = E_{hot,ch} \qquad (4.4)$$

Where *t* is the charge and discharge time, the same balance can be written for the cold TES. Clearly under design condition the charge and discharge cycle must be operated repeatedly with steady state condition, and therefore even if all three parameters of the balance could be different between charge and discharge, the enthalpy change and therefore the temperatures of the tanks have to be kept the same, in other words the tanks energy must be fully discharged during the discharge phase, otherwise after one complete cycle (charge and discharge) the hot/cold tank would have to be cooled/warmed to the initial tanks temperature and this would result in an exergy loss.

Another important aspect to be considered in the discharge cycle is the auxiliary heat exchanger with the environment (points 4R-5), as already mentioned in 2.3.4, this HEX is needed in order to balance the heat exchanged with the cold TES which otherwise would be different between charge and discharge and to assure cyclic steady state operation of the PHES. This can be observed when comparing point 4 and 4R on the T-s diagram of the charge and discharge cycle (Figure 4.4 and Figure 4.6) .

Depending on the site of the storage system the coolant could be water or ambient air, but in both cases since here the goal is just to cool down the working fluid, this HEX will be operated with unbalanced flows: $(mc_p)_{coolant} >> (mc_p)_{wf}$ which allows to reduce considerably the heat transfer area and therefore to reduce the HEX cost. This heat exchanger will be modelled in a simplified way: on the working fluid side a 1% relative pressure drop is assumed, while the pinch point temperature difference of 10 K is imposed. Since the HEX is operated with unbalanced flows, the pinch point ($\Delta T_{pp}$) is located at the hot stream outlet and therefore temperature $T_5$ is:

$$T_5 = T_{amb} + \Delta T_{pp} \qquad (4.5)$$

where $T_{amb}$ is the ambient temperature, To calculate the required mass flow rate of the coolant air the approach temperature difference is set to 50 K (in order have $(mc_p)_{coolant} \simeq 4\ (mc_p)_{wf}$) and the coolant air mass flow rate in design condition is calculated applying the energy balance to the HEX. For the calculation of the heat transfer area a global heat transfer coefficient of 100 W/m$^2$/K is adopted with respect to internal area [15]. Plus, to account for the worst-case scenario in which the coolant is ambient air, the power consumption of the air fan is set to 1% of the thermal duty of the HEX.

In the off design model only the pressure drops on the working fluid side are modelled as explained in 4.3.3. The rest of the HEX is assumed to work at fixed $\Delta T_{pp}$, while the cooling air mass flow rate will change as the thermal duty of the HEX changes. The fan consumption in off-design is assumed to be like in the design 1% of the thermal duty, therefore it will linearly increase/decrease with the HEX duty.

Practically the condition expressed in (4.5) set a limit to the discharge temperature of the cold TES ($T_{c)}$ which is related to $T_5$ by the cold HEX: $T_c = T_5 - \Delta T_{cold}$, so assuming ambient temperature of 293K, $\Delta T_{pp}$=10K and $\Delta T_{cold}$= 5K temperature $T_c$ would result 298K.

## 4.3. HOT AND COLD HEAT EXCHANGERS

Hot and cold heat exchangers (HEX) are a key component since they couple the PHES cycle with the hot and cold TES. Their performance can be measured as seen in 3.3.1, by the effectiveness which is strictly linked to the pinch point temperature difference. Hot and cold HEX will be a counterflow HEX with balanced flows ($m_{hot}c_{p,hot} \simeq m_{cold}\ c_{p,cold}$), this allows to minimize the heat transfer irreversibilities, plus to avoid having a high variation between charge and discharge working fluid temperatures as shown in 3.3.1, which would affect the RTE, temperature difference should be kept lower than 10 K. It is important to underline that the design of the HEXs is done in the charge phase.

### 4.3.1. BASIC DEISGN CALCULATION

The first step in HEX design is to define the operating and process conditions of the hot and cold stream, taking as example the hot HEX, at first the following parameters are known:

- for the cold stream (liquid-side): $T_a$,$T_b$ ,$p_a$ and $p_b$
- for the hot stream (gas-side): the mass flow rate ($m_{wf}$), $T_2$ and $p_2$

In order to solve the problem and calculate the molten salts mass flow rate and point 2R the following assumptions are made:

- fractional pressure losses ($f_p$)=1% for the gas-side, therefore $p_{2R}$ is known
- no heat losses towards the environment
- pinch point temperature difference ($\Delta T_{pp}$) is set to a desired value

Since the specific heat ($c_p$) of molten salts and working fluid is not constant in the HEX temperature range, it is not known beforehand whether the pinch point is at the hot inlet, cold inlet or in the middle of the HEX. To solve this at first an iteration variable is set called $\Delta T_{ap}$, with an initial guess, it allows to calculate the outlet temperature of the hot side and then the liquid mass flow rate applying the first law balance to the HEX:

$$T_{2R} = T_b + \Delta T_{ap} \tag{4.6}$$

$$m_{liquid} = \frac{m_{wf}(h_2 - h_{2R})}{(h_a - h_b)} \tag{4.7}$$

After that to get the value and position of the pinch point, the HEX is divided in a number *n* of parts with a fixed temperature difference for the cold stream (the stream for which both temperatures are known) and in each part the $c_p$ assumed is held constant at the average value between inlet and outlet. Starting from the inlet where both temperatures are known (as example in the hot HEX the hot inlet conditions are known) for each *n* parts the first law balance is applied to calculate the hot stream outlet temperature. Once the process is completed the value of $\Delta T_{pp}$ and its position are known, and the function is iterated on $\Delta T_{ap}$ to get the desired value of $\Delta T_{pp}$. In figure Figure 4.7 the T-Q diagram of the hot HEX is shown with an imposed temperature difference of 5K, note that in this case the $\Delta T_{pp}$ is at the cold inlet.

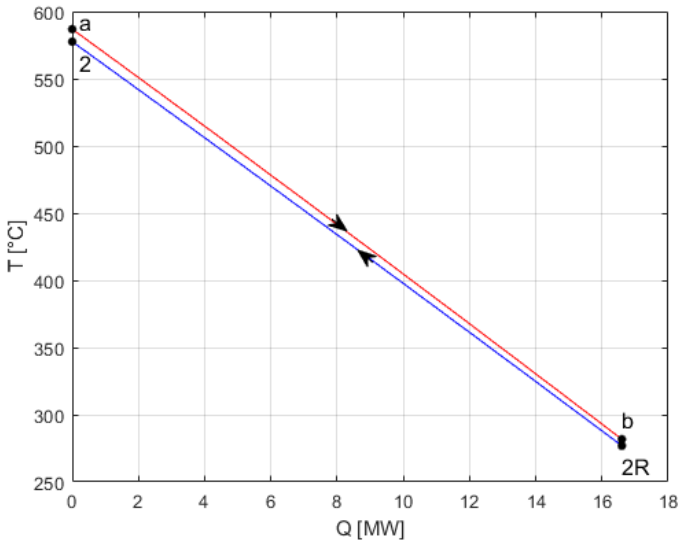


*Figure 4.7 T-Q diagram for hot heat exchanger during charge, $\Delta T_{pp}$= 5 K, cold stream: molten salts, hot stream: nitroge.*

### 4.3.2. HEAT TRANSFER ANALYSIS

The second step is the evaluation of heat transfer performance and the geometry definition for the HEX under the operating points calculated in 4.3.2.

For the gas-liquid heat exchangers it was chosen a shell and tube type, the geometry is a simplified one and is the same described in the work of [72] in which the properties of molten-salts were tested in a shell and tube heat exchanger. The HEX geometry is presented in Figure 4.8, the gas flows on the tube-side while the liquid flows on the shell side. Main assumptions on the HEX geometry are:

- purely counterflow regime
- constant tube and shell flow area with no fins

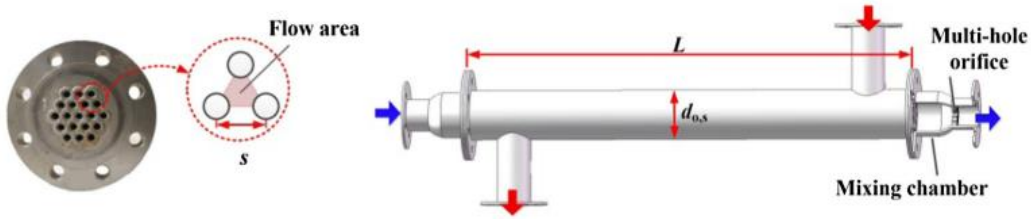


*Figure 4.8 Shell and tube hea exchanger geometry chose for the hot and cold HEX*

The two parameters that influence the heat transfer performance for each stream side are: the hydraulic diameter $D$ and the flow cross-sectional area $A_f$. Both parameters have influence on the heat transfer performance of the HEX since they affect the Nusselt and Reynolds number:

$$Nu = \frac{hD}{k} \qquad Re = \frac{mD}{A_f \mu} \tag{4.8}$$

where $k$ is the fluid thermal conductivity, μ is the cinematic viscosity, and $h$ is the convective heat transfer coefficient.

Moreover, $D$ is a measure of the compactness of the HEX since commonly the flow volume is associated with the HEX volume:

$$D = \frac{4A_f}{P} = \frac{4A_f L}{A} = \frac{V}{A} \tag{4.9}$$

Where $P$, $L$ are the channel wetted perimeter and Length, $V$ is the flow volume and $A$ the surface (heat transfer area) .Therefore it is clear that adopting a smaller $D$ means having a more compact (and usually cheaper) HEX with the same heat transfer area, although this means increasing the pressure drops. The heat transfer area is strictly related to the global heat transfer coefficient $U$ by the formula:

$$Q = UA\Delta T_{ml} \tag{4.10}$$

where $\Delta T_{ml}$ is the logarithmic mean temperature difference between hot and cold stream. The global heat transfer coefficient $U$ is a function of the two stream heat convective transfer coefficients $h_h$ and $h_c$:

$$UA_{ext} = \left(\frac{1}{h_h A_{int}} + R_{cond} + \frac{1}{h_c A_{ext}}\right)^{-1} \tag{4.11}$$

where $R_{cond}$ is the tube walls conductive resistance and $A_{ext}$ ,$A_{int}$ are the tube external and internal area. Note that fouling effects are here neglected. Is important to underline that $U$ is referred in the model to the external area $A_{ext}$ (in the following will be denoted as simply $A$).

To calculate the heat transfer coefficients, heat transfer correlations are used which correlate *Nu*, *Re* and Prandtl (*Pr*) numbers. The choice of the correlation depends on the flow regime that can be laminar or turbulent. For laminar regime in forced convection in pipes *Nu* is a constant which depends on the pipe cross section shape. In this case *h* is inversely proportional to *D* and does not depend on the *Re*. In the work of Farres and Laughlin [1], [9] which adopted Printed circuit HEX and shell and tube HEX respectively, the flow was chosen to be laminar (Re<2100) [1] or just above the turbulence threshold (Re=6000)[9], simply because *D* was chosen to be very small 1.5mm [9]and below 0.2 mm [1]. Using such small diameter has the advantage of having a good heat transfer performance but it has the disadvantage of increasing the pressure drops and of employing diameters that require special manufacturing techniques and so increase the cost of the heat exchanger. Therefore, in this model the tube side hydraulic diameter *D* was set to be 10 mm which is a common value for commercial shell and tube HEX [1] and HEXs were chosen to operate in turbulent regime.

Heat transfer correlation on the shell side were taken in the form of:

$$Nu = cRe^{a}Pr^{n} \tag{4.12}$$

For the molten-salts experimental values for *a* and *n* were found from [72] and are while for methanol *c,n* were taken from the common Dittus-Boelter correlation,

Table 4.2 reports the coefficient taken.

*Table 4.2 Coefficient for the shell side correlation*

| | **c** | **n** |
|---|---|---|

| | | |
|---|---|---|
| **Methanol** | 0.023 | 0.4 or 0.3[14] |
| **Molten salts** | 0.0197 | 0.4 |

For tube-side, i.e. the gas-side the Gnlielinski correlation was used:

$$Nu = \frac{\left(\frac{f}{8}\right)(Re - 1000)Pr}{1 + 12.7\left(\frac{f}{8}\right)^{0.5}(Pr^{\frac{2}{3}} - 1)} \quad (4.13)$$

Where f is the friction factor, calculated with the Swamee-lee direct equation [9]:

$$f = 0.25\left[\log_{10}\left(\frac{\varepsilon}{3.7D} + \frac{5.74}{Re^{0.9}}\right)\right] \quad (4.14)$$

where ε is the tube roughness.

The same procedure emplyed in 4.3.1 is used to calculate the heat transfer area, the HEX is divided in *n* parts and for each part *U* and $\Delta T_{ml}$ and *Q* are evaluated and heat transfer area is calculated using (4.10). Then the tube length and pressure drop on the gas side are computed:

$$L = \frac{A}{\pi D_{out} * N_t} \quad (4.15)$$

$$\Delta p = f\frac{L}{D}\rho\frac{v^2}{2} \quad (4.16)$$

Where $N_t$ is the number of tubes, which is calculated once the cross-sectional flow area $A_f$ is known. Once the pressure drop on the gas side is computed, the function is iterated on the $A_f$ in order to get the desired relative pressure drop, given as input.

### 4.3.3. OFF DESIGN CONSIDERATIONS

Since heat exchangers design point is modelled in the charge phase, it is clear that in the discharge phase they work in off-design condition. Concerning the off-design procedure for HEX is the same for the design, unlike that in this case the geometry of the HEXs is fixed, so *A*, $A_f$, *D* and *L* are known, the variation of *U* is computed and the $\Delta T_{ml}$ will change according to equation (4.10).

Concerning the pressure drop, for the off-design the variation will be accounted for by the following equation:

[14] 0.4 for the fluid being heated and 0.3 for the fluid being cooled

$$\Delta p_{off} = \Delta p_{design} \left( \frac{m_{off}}{m_{design}} \right)^2 \left( \frac{\rho_{design}}{\rho_{off}} \right) \quad (4.17)$$

that is derived from equation (4.17).

## 4.4.REGENERATOR

The regenerator modelling procedure is similar to the hot and cold HEX, only that in this case the regenerator is a printed circuit HEX. The model is based on the HEX model that can be found in [14].

Unlike for hot and cold HEXs, in this case the location of $\Delta T_{pp}$ is known a priori, since it depends only on the specific heat capacity of cold and hot stream and since: $c_{hot} > c_{cold}$, the pinch point is located at the inlet of the hot stream, hence $\Delta T_{pp} = T_{2R} - T_1$. Now $T_{2R}$ is the output of the hot HEX model and $T_1$ is fixed by fixing $\beta_{comp}$ for the charge cycle, therefore the regenerator performance is fixed and cannot be set like it was done for the hot and cold HEXs.

## 4.5.COMPRESSOR AND EXPANDER

As anticipated in 3.2 compressors and expanders are modelled using the polytropic efficiency. Polytropic efficiency is commonly defined as infinitesimal stage efficiency:

$$\eta_{comp} = \frac{\delta w_{comp,rev}}{\delta w_{comp}} = \frac{v \mathrm{d}p}{\mathrm{d}h} \quad (4.18)$$

$$\eta_{exp} = \frac{\delta w_{exp}}{\delta w_{exp,rev}} = \frac{\mathrm{d}h}{v \mathrm{d}p} \quad (4.19)$$

Where *h*,*v*,*p* are the fluid enthalpy, specific volume and pressure respectively. In the model the pressure ratio is given as input while the total enthalpy change is calculated via numerical integration of equations (4.18) and (4.19), in order to integrate, the pressure drops is dived in *n* stages between outlet and inlet condition, starting from the inlet the conditions at each stage outlet are computed from (for an expander):

$$h_{i+1} = h_i + v_i (p_{i+1} - p_i) * \eta_{exp} \quad (4.20)$$

$$v_{i+1} = v(h_{i+1}, p_{i+1}) \quad (4.21)$$

Note that in equation (4.20) $v_i$ is used, since $v_{i+1}$ is not known a priory. To solve this after $v_{i+1}$is evaluated $h_{i+1}$ is evaluated again using $\bar{v} = 0.5(v_i + v_{i+1})$. For the model calculation a value of $\eta_{comp} = \eta_{exp}$ =0.9 is used, which can be consider a realistic value for today state of the art turbomachinery [1].

### 4.5.1. OFF DEISGN MODEL

Unlike for HEXs, for the design model of turbomachines, two set of compressor and expander will be used, one for charge and one for discharge. However, it is still important to investigate the off-design performance of turbomachines in the case of part-load operation of the system. This is an important aspect to be investigated especially if the PHES system is coupled with a solar PV or wind turbines and has to be operated to level the production to ensure the delivery of a constant output power of the system. In this case the PHES would always work varying its charge and discharge net power to balance the production of the PV system.

The off design model used is taken from [16], with the characteristics maps of turbine and compressor expressed as a function of the reduced mass flow ratio reduced rotational speed ratio, beta ratio and isentropic efficiency ratio (the ratio is intended with respect to the design point) :

$$\dot{G} = \frac{(m\sqrt{T_{in}}/p_{in})_{off}}{(m\sqrt{T_{in}}/p_{in})_{design}} \qquad \dot{n} = \frac{(n/\sqrt{T_{in}})_{off}}{(n/\sqrt{T_{in}})_{design}} \tag{4.22}$$

$$\dot{\pi} = \frac{\beta_{off}}{\beta_{design}} \qquad \dot{\eta} = \frac{\eta_{off}}{\eta_{design}} \tag{4.23}$$

In Figure 4.9 the characteristic maps for axial expanders and compressors are presented as a function of

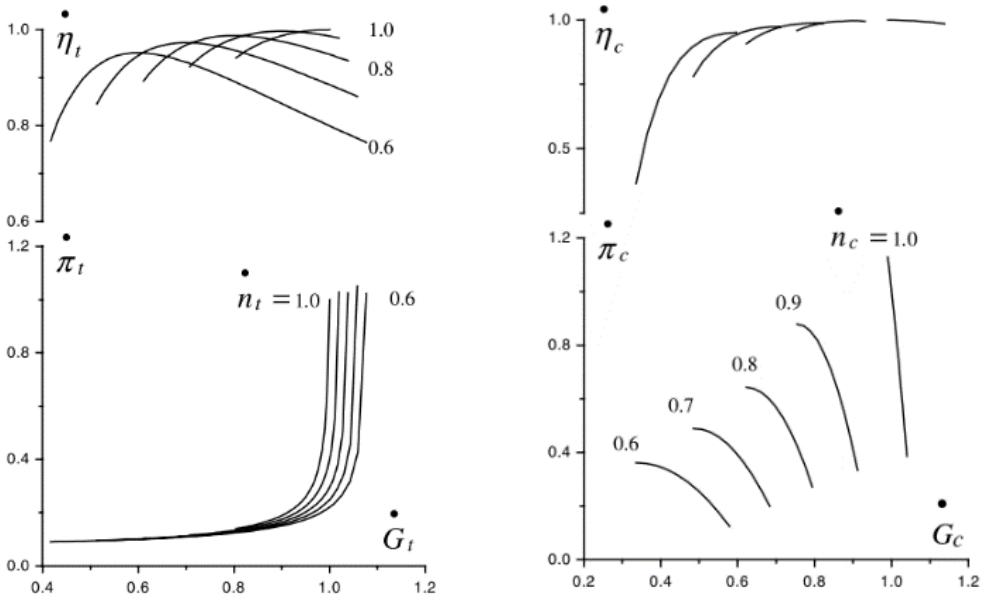


*Figure 4.9 Turbine and compressor characteristic maps* [16]

The off-design model for turbomachinery is integrated in the model only for the discharge phase, since here the scope of the off-design analysis is to understand the cycle performance at part load operation.

In the off-design of the discharge cycle turbomachines must follow their characteristic map, therefore in this case two additional variables must be used to satisfy these two constraints (compared to the design one ). The two additional variables are the discharge cycle the pressurization and the discharge temperature of the hot TES $T_b$.

The characteristics map presented before are for axial turbomachines. The choice of axial turbomachines was made based on considerations obtained from the Balje diagrams [73] which gives a general estimation on the turbomachines performance and type based on two dimensionless numbers that are the specific speed $n_s$ and the specific diameter $d_s$ :

$$d_s = \frac{D * \Delta H_{is}^{0.25}}{\dot{V}^{0.5}} \qquad n_s = \frac{n * \dot{V}^{0.5}}{\Delta H_{is}^{0.75}} \tag{4.24}$$

Where $\dot{V}$ is the outlet volumetric flow rate, calculated at the inlet for the compressor and at the outlet for the expander, $\Delta H_{is}$ is the isentropic enthalpy difference, $D$ is the diameter and $n$ is the shaft rotational speed. To reach the desired turbomachinery efficiency only specified values of $n_s$ and $d_s$ are suitable and these values differs based on the type of turbomachines as can be seen in Figure 4.10.

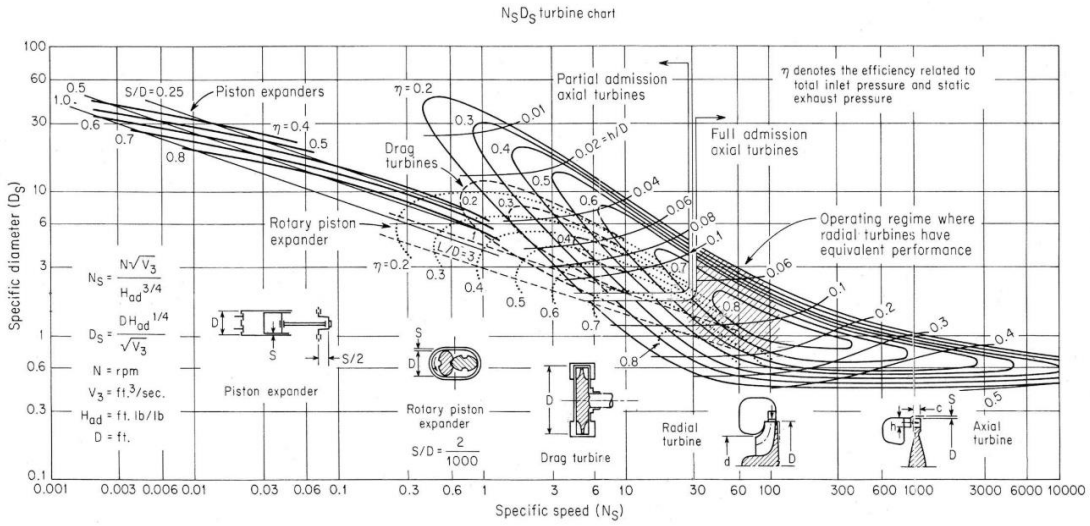


*Figure 4.10 Baljie diagram for turbines source:*[73]

The approach followed was to divide the compression/expansion in *N* number of stages with equal enthalpy difference ($\Delta H_{is,stage}$). From the Balje diagram the values of $n_s$ and $d_s$ to reach the desired efficiency were obtained and these were used in equation (4.24) to calculate the *n* and *D* for the stage which was in the middle of the turbomachine.

The comparison for the charge set of turbomachines is presented in Table 4.3 for a 18 MW rated net charge power, in this case the Balje diagram was used to optimize *n* and *D* for the charge compressor while the expander was assumed to operate with the same rotational speed of the compressor.

It can be seen that if radial turbomachines are used the charge compressor should have three radial stages, because the rotor speed at the medium diameter *D* must be kept below the limit of 250 m/s due to mechanical constraints [74]. Having more than one radial stage outweigh the cost reduction (related to machine compactness) which would be the advantage of using radial turbomachines. This reason plus the fact that radial turbomachines are normally used for rated power up to 5 MW [73], suggests that for this particular application the use of multistage axial turbomachines it is the better choice.

It must be underlined that the comparison presented is a preliminary analysis, to have a better understanding of the best turbomachines choice a more detailed study in the field of turbomachines should be developed.

From Table 4.3 it must be noted that for a charge power size of 18 MW the rotational speed is around 32 krpm and therefore a gearbox will have to be used to couple the motor shaft and the electric generator that has to rotate at 3000rpm to deliver a grid frequency of 50Hz.

*Table 4.3 Comparison of turbomachinery type for the charge of PHES with indirect TES, results obtained from the Balje diagram Dm and U calculated from the assumption on $n_s$ and $d_s$, are computed for the second and fourth stage for the two compressors.*

| | | N° stages | beta | ns | ds | n [rpm] | $D_m$ [m] | U [m/s] |
|---|---|---|---|---|---|---|---|---|
| **Axial** | compressor | 7 | 3.88 | 300 | 0.8 | 32087 | 0.22 | 370 |
| | expander | 1 | 3.72 | 107 | 1 | 32087 | 0.19 | 288 |
| **Radial** | compressor | 3 | 3.88 | 100 | 1.8 | 20764 | 0.18 | 254 |
| | expander | 1 | 3.72 | 91 | 1 | 20764 | 0.17 | 186 |

## 4.6.COST MODEL

Since economic performance of the storage plays a significant role it is important to develop an economic analysis of the system. Normally for a storage system the capital expenditure (CAPEX) cost is divided in power based cost in (€/kW) and energy based cost in (€/kWh). The first is representative of the cost of the power cycle like turbomachinery and heat exchangers while the second gives an indication of the cost of the storage system, which in this case is the hot and cold TES. These two parameters are used in PHES literature to evaluated the potential of the technology [1], [9], this is done because in emerging technology there is a lot of uncertainty on the operational cost (OPEX) and the lifetime of the plant in the absence of long term utilisation of the ESS and field experience. Even if this is the case for PHES it is important to estimate the parameter that allows to evaluated the financial feasibility of a storage plant, which is the levelized cost of storage (LCOS) in $/kWh, which can be seen as the cost to deliver one kWh of stored electricity. In the following the cost model for the different components will be presented, at the end the method for the calculation of the LCOS is shown.

### 4.6.1. CAPEX POWER BASED COST

Power based cost is usually expressed as:

$$Z^*_{power} = \frac{Z_{power}}{W_{net,discharge}} \tag{4.25}$$

Where $Z_{power}$ is the total investment cost (in $) which is divided by the net discharge power (in kW).

The power cost of turbomachines $Z_{comp/exp}$ is calculated by the following formula proposed by Laughlin and Farres [1]:

$$Z_{comp/exp} = \frac{C_{comp/exp}\, m\, \ln\beta}{\eta_{max} - \eta} * \frac{\rho_{ref}}{\rho} \tag{4.26}$$

Where the first part of the formula is the one proposed by Valero et al. [17] for common gas turbines:

- m is the mass flow, the mass flow is representative of the size and power rating of the machine
- $C_{comp/exp}$ is the cost per unit of mass flow
- β is the pressure ratio, which represents the number of stages of the machine, the higher it is the higher the cost
- $\eta$ is the polytropic efficiency, and this dependency accounts for the fact that to reach a higher efficiency the cost of the machine increases, $\eta_{max}$ is set to 92%.

Farres and Laughlin then proposed to add for a closed Brayton cycle the second term of the equation to account for the closed cycle pressurization. If the cycle is pressurized this means that the same power can be delivered with a more compact device, since the flow rate in the machine will be lower. To account for that they multiplied the equation by the ratio of the reference density $\rho_{ref}$ at which the $C_{comp/exp}$ is evaluated and the density of the cycle. In Table 4.4 the cost parameters used are presented.

*Table 4.4 Cost Parameters used for turbomachinery* [1]

| | |
|---|---|
| **Compressor** | $C_{comp}$=670 \$/(kg/s) $\boldsymbol{\rho_{ref}}$= 1.2 kg/m$^3$ |
| **Expander** | $C_{exp}$=1100 \$/(kg/s) $\rho_{ref}$= 0.5 kg/m$^3$ |

For hot and cold heat exchangers the cost equation was taken from Hall et al. [18]

$$Z_{hot/cold} = (30800 + 1438\, A^{0.81}) \qquad (4.27)$$

Where *A* is the heat transfer area, this equation is proposed for a pressure of 60 bar on shell and tube side and it is used for the cold and hot heat exchanger even though the pressure in the hot HEX is around 100 bar and in the cold HEX is around 20 bar, in design operation.

Concerning the auxiliary heat exchanger with the environment the cost equation was taken from [19], proposed for air cooled heat exchangers:

$$Z_{AUX} = 5443 A^{0.395} \qquad (4.28)$$

Regarding the regenerator another formula was used that relates the cost to the total metal volume of the heat exchanger, taken from Farres [1] :

$$Z_{REG} = C_{HEX}\, \rho_{metal} V_{metal} \tag{4.29}$$

Where $\rho_{metal}$= 8000 kg/m$^3$ which is the density of stainless steel, $V_{metal}$ is the HEX metal volume and $C_{hex}$ is the heat exchanger cost per unit of metal mass, which for printed circuit HEX is around 30 $/kg.

### 4.6.2. CAPEX ENERGY BASED COSTS

The energy cost is commonly expressed as:

$$Z^*_{ENERGY} = \frac{Z_{energy}}{E_{el,charge}} \tag{4.30}$$

Where Z is the total investment cost of the storage system, which in this case contains the storage material costs and the tanks cost, and $E_{el,charge}$ is stored electrical energy in the tanks, which is simply the product of the charge time and the net electric power output

In Table 4.5 the cost parameter used for the molten salts and methanol and for the hot and colt tanks are presented. The total cost is the is the sum of the storage medium, the cost for the four tanks plus the cost of insulation of the tanks.

| | **Material cost [$/kg]** | **Tank cost [$/m$^3$]** | **Insulation cost %** |
|---|---|---|---|
| **HOT TES** | 0.5 | 150 | 20% |
| **COLD TES** | 0.3 | 50 | 20% |

*Table 4.5 Cost parameter for the energy based costs estimation* [1]

### 4.6.3. LEVELIZED COST OF STORAGE

Levelized cost of storage is the most important parameter when comparing two storage technology because it gives from an ownership perspective, the cost needed to run the energy storage plant: the CAPEX cost , operation and maintenance cost (OPEX) including the repayment of the loan and upfront of the CAPEX, plus the cost for the charged electricity.

The LCOS is computed by the following formula [20]:

$$LCOS = \frac{CAPEX + \sum_{t=1}^{t=L} \frac{A_t}{(1+i)^t}}{\sum_{t=1}^{t=L} \frac{E_{out}}{(1+i)^t}} \tag{4.31}$$

$$A_t = OPEX_t + c_{el}E_{in} \quad (4.32)$$

Where the CAPEX is the total investment cost which is the summation of $Z_{Power}$ and $Z_{energy}$ calculated before. $A_t$ are the annual costs which are the summation of the yearly OPEX and they yearly cost of the input electricity $E_{in}$. $E_{out}$ is the annual output electricity. The annual cost and the output electricity are both discounted by the discount factor *d* to address the time factor of the investment.

The lifetime of the system is assumed to be 20 years [20] while for the operation of the storage system, 1 cycles per day is assumed. For the OPEX accounting its value was assumed equal to the one proposed for power cycle of the CAES system in [75] which is 15 $/kW/y, because of the similar characteristics of the power cycle of CAES which employs similar cycle components to PHES.

## 4.7. ROUND TRIP EFFICIENCY AND EXERGY ANALYS OF THE SYSTEM

The round-trip efficiency in the model is computed by the following formula starting from the thermodynamic performance of the charge cycle (COP) and of the discharge cycle efficiency ($\eta_{engine}$). The COP is computed as:

$$COP = \frac{W_{net,ch}}{Q_{hot,ch}} \quad (4.33)$$

While $\eta_{engine}$ is computed as

$$\eta_{engine} = \frac{W_{net,dis} - W_{fan}}{Q_{hot,dis}} \quad (4.34)$$

Where $W_{fan}$ is the fan consumption for the auxiliary heat exchangers with the environment (assumed 1% of its thermal duty). $Q_{hot}$ and $W_{net}$ are the heat power exchanged with the hot TES and the net cycle power respectively. The RTE is then calculated:

$$RTE = \eta_{engine} * COP * {\eta_{e,m}}^2 \quad (4.35)$$

Where $\eta_{e,m}$ is the electromechanical generator efficiency (assumed to be 97%). In the results chapter an exergy analysis will also be presented, this allows to evaluate the impact of each components irreversibilities on the overall round trip efficiency. Here it will be briefly explained how this analysis is performed. The exergy losses (also called “lost-work”) are calculated with the following relation:

$$W_{irr}^{i} = T_0 S_{irr}^{i} \tag{4.36}$$

where $S^{i}_{irr}$ is the entropy generation in the single component (per unit of time) and $T_0$ is the ambient temperature (293.15 K). In Table 4.6 the formula for the calculation of the exergy losses are summarised.

| **Component** | $\mathbf{S^{i}_{irr}}$ |
|---|---|
| **Compressor/expander** | $m(s_{out} - s_{in})$ |
| **Heat exchangers** | $[m(s_{out} - s_{in})]_{hot,stream} + [m(s_{out} - s_{in})]_{cold,stream}$ |
| **Auxiliary heat exchanger** | $m[(s_{out} - s_{in}) - (h_{out} - h_{in})/T_0]_{hot,stream}$ |

*Table 4.6 Entropy generation formulas*

Other sources of losses such the fun consumption, the electrical losses in the generator or the mechanical losses, will be treated as a pure exergy loss.

It is important to note that the exergy losses are related to the RTE through the exergy balance of the system:

$$RTE = 1 - \frac{\sum W_{irr}^{i}}{W_{el,ch}} \tag{4.37}$$

where $W_{el,ch}$ is the net electrical input during charge. The RTE computed in this way must be identical to the one calculated from equation (4.35), based on a first law balance of the system, therefore providing a check on the model coherence.

# 5. RESULTS

## 5.1. THERMODINAMIC CONSIDERATIONS

At first to address the validity of the proposed model, a comparison with the model of Farres [1] will be done. Taking the same input condition of his model, the model gives a round trip efficiency of 66% with an energy density of 44.4 kWh/m$^3$ which is similar to the 65% RTE and 46 kWh/m$^3$ obtained by Farres. The main assumption made in the model of Farres are: relative pressure drop in HEX of 1%, HEXs effectiveness of 97% and polytropic efficiency of turbomachines of 90% and equal charge and discharge time.

In Table 5.1 the model first results are presented for a system with equal charge and discharge time of 6 h, for this reason in this case the four control variables of the discharge cycle are kept equal to the charge cycle values. This is done to simplify the thermodynamic analysis, later on in 5.1.2 other cases, in which the discharge time and charge time are different will be presented.

The model inputs are the one of Table 5.2, the input parameters were chosen based on the considerations done in chapter 3, therefore the relative pressure drop in the HEXs is taken as 1% and the polytropic efficiency of turbomachines is 90%, for the heat exchangers the $\Delta T_{pp}$ in hot and cold HEX and the charge pressure ratio ($\beta_{comp,ch}$) were chosen in order to keep heat exchangers effectiveness at 96%, concerning the discharge temperature of the hot TES ($T_b$) in the next paragraph an analysis will explain the choice of the input value taken. The reached RTE with these inputs is 56.0 % with an energy density of 31 kWh/m$^3$ which is and order of magnitude greater than that of pumped hydro energy storage[15]. Another result to be underlined is the power density of 2.1 MW/(m$^3$/s) that, compared to PHES with packed-bed TES with $\rho_{power}$ =0.24 MW/(m$^3$/s), is an order of magnitude greater resulting in a lower cost of turbomachines. This is the reason why the maximum charge cycle pressure was set to be 100 bar.

*Table 5.1 System specification of the Brayton PHES with 6 h storage*

| **Model results** | | |
|---|---|---|
| **$t_{charge}=t_{disscharge}$** | 6 | h |
| **Charge net power** | 18.9 | MW |
| **Discharge net power** | 10.6 | MW |
| **RTE** | 56.0 | % |
| **$\rho_{energy}$**[16] | 31 | kWh/m$^3$ |
| **$\rho_{power}$** | 2.1 | MW/(m$^3$/s) |

[15] At a height of 550m the energy density is 1.5 kWh/m$^3$

[16] Energy density in the table is calculated considering the volume of the four tanks of the TES system, in Farres [1] this parameter was calculated considering only the storage material volume

*Table 5.2 Input parameters of the model used in the exergy analysis*

| $T_{3,ch}$ | $T_{2,ch}$ | $p_{2,ch}$ | $T_a$ | $T_b$ | $f_p$ | $\eta_{comp/exp}$ | $\Delta T_{pp,hot}$ | $\Delta T_{pp,cold}$ | $\beta_{comp,ch}$ |
|---|---|---|---|---|---|---|---|---|---|
| 40°C | 575°C | 100 bar | 565°C | 290°C | 1% | 90% | 10°C | 2.5°C | 3.88 |

In Figure 5.1 a pie chart of the relative exergy losses (see 4.7 for explanation) of the system is presented, as expected for a Brayton based PHES the biggest source of irreversibilities are the ones linked to turbomachines, which account for more than 50% of the overall lost work, while heat exchangers account for almost 25%. Note that between the three HEXs the regenerator is the one with the highest exergy loss, this suggests that to increase the RTE it would be most beneficial to increase its effectiveness rather than intervening on the hot and cold HEXs. The sum of the overall exergy losses accounts for 44.0% of the charged input electricity, therefore respecting the exergy balance of equation (4.37).

It can be noted that the heat rejection to the environment in the auxiliary HEX is an important source of exergy loss, the heat rejected to the environment, from $T_{4R'}$ =124°C to $T_5$=35°C and the heat rate is 7.5 MW for a rated discharge net power of 10.6 MW , this heat could be recovered if the PHES is coupled with an organic Rankine cycle [76] that used this waste heat to increase the net power output.

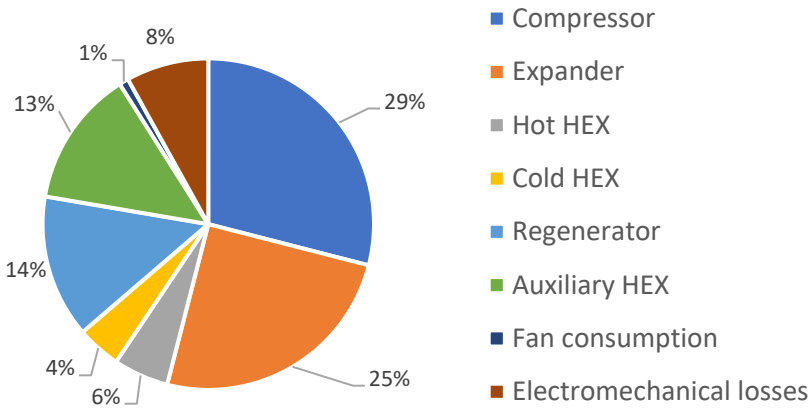


*Figure 5.1 Relative exergy losses of a regenerative PHES with liquid storage, the sum of the exergy losses accounts for 44 % of the charged net power input*

### 5.1.1. EFFECT OF THE HOT TES DISCHARGE TEMPERATURE $T_B$

In chapter 3 it was shown that turbomachinery and heat transfer irreversibilities had and opposite trend with respect to the charge compression temperature ratio ($\tau$) or equivalently to the charge compression pressure ratio. This trend was verified also in the numerical model, by varying the discharge temperature of the hot TES $T_b$. In fact, in the model basically a variation on $T_b$ means varying the charge compression

pressure ratio if the regenerator effectiveness is kept the same. This is shown in Figure 5.2 where two T-s diagram for the charge cycle are plotted for two different temperatures $T_b$, it can be seen that the dashed one with a higher $T_b$ has a lower $\beta$ in order to have the same regenerator effectiveness of 96%

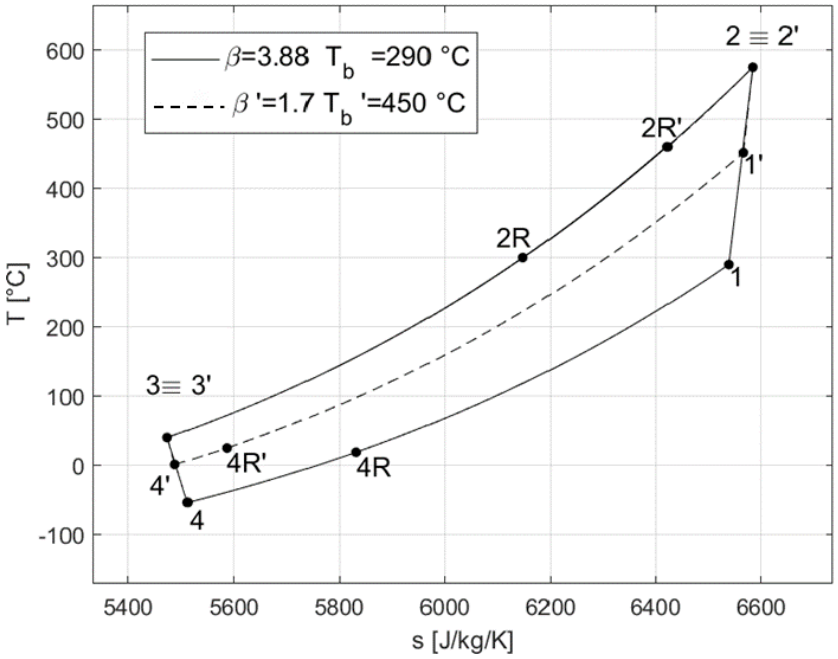


*Figure 5.2 T-s diagrams of Brayton regenerative PHE with indirect TES charge cycle at two different beta and different discharge temperature of the hot TES*

In Figure 5.3 the exergy distribution of irreversibilities to the change of $T_b$ is presented, the chart is calculated from the model with the input parameters presented in Table 5.2 note that also in this case the four control variables for the discharge cycle are set equal to the charge cycle. As expected, when $T_b$ is lower turbomachinery losses are higher and heat transfer losses are lower. As can be seen from the exergy analysis the lost work is minimum (i.e. the RTE is maximum) when $T_b$ is the lowest possible. Increasing $T_b$ has the disadvantage of increasing the losses in the regenerator which outweigh the decrease of the turbomachinery losses. Adopting a low $T_b$ is also beneficial for the energy density of the system because it allows to use all the temperature range of the hot TES and therefore lowers the required mass flow rate of solar salts.

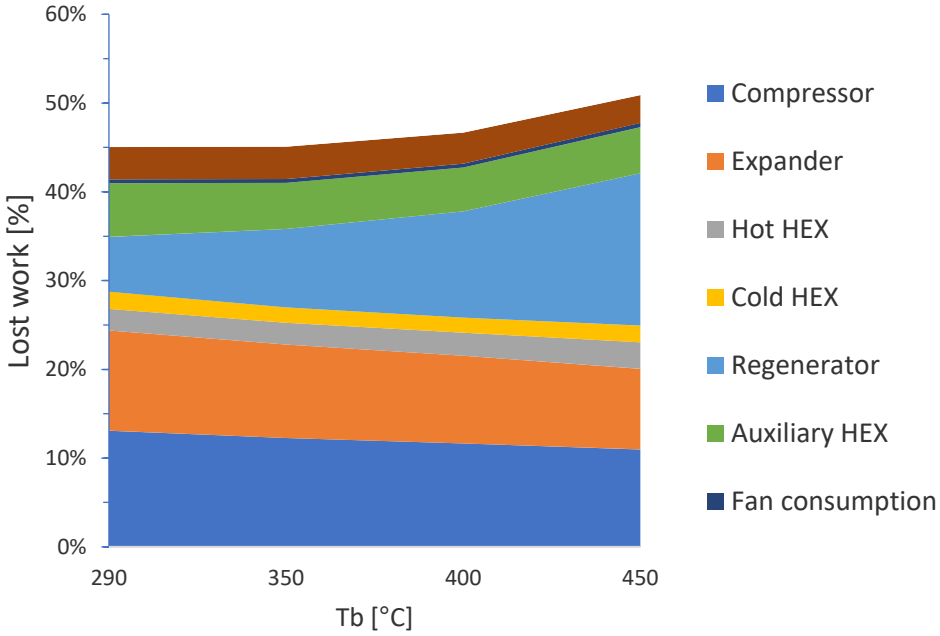


*Figure 5.3 Lost work/exergy losses distribution in a regenerative Brayton PHES with liquid TES as function of the hot storage lower temperature*

### 5.1.2. EFFECT OF THE DESIGN POWER RATIO

Beside the round-trip efficiency another important parameter to be considered for the design of the PHES system are the power ratio between charge and discharge and the charge/discharge time. These parameters are very important because usually an energy storage system is charged during off-peak periods and is discharged in a very short period when there is a peak in the electricity price on the market. If this is the case it means that in the discharge phase the output power must be greater than the charge power in order to discharge the stored electricity in a shorter time. The variables which could be changed in the design of the discharge phase to increase the output power are:

- the mass flow rate of the working fluid ($m_{wf,dis}$)
- the mass flow rate of the hot and cold TES ($m_{hot,dis}$ ,$m_{cold,dis}$)
- the cycle pressurization

It must be underlined that the three mass flow rates are all related together, in the sense that when increasing the net discharge power by increasing the $m_{wf,dis}$ also $m_{hot,dis}$ and $m_{cold,dis}$ must be increased so that the HEXs are operated with balanced flows also in the discharge phase, otherwise the temperature difference in the HEXs would increase reducing drastically the RTE without any real advantage. Therefore, practically when deciding to increase design net discharge power this means also reducing the discharge time. Therefore, in the discharge model the three mass flow

rates are all changed with the same percentage variation with respect to the charge phase.

In Table 5.3 it is shown the comparison between three cases chosen to show what is the effect of increasing the power ratio on the RTE:

- CASE A where $p_{4.dis}$ and $m_{wf,dis}$ are kept the same as in the charge cycle (same case as the one presented in Table 5.1)
- CASE B in which $m_{wf,dis}$ is doubled
- CASE C in which $m_{wf,dis}$ is doubled and $p_{4,dis}$ is increased

It is important to underline that the three cases presented in Table 5.3 are different design scenarios for the discharge cycle and are not off design conditions of the cycle.

For CASE B it can be seen that doubling the working fluid mass flow rate does not double the net power output, due to the fact that the RTE decreases with respect to CASE A. This is mainly related to the off-design of the heat exchangers, in fact increasing the mass flow rate of the fluid will also increases the relative pressure drop as explained in 4.3.3 and this negative effect outweighs the positive effect of the increase of the global heat transfer coefficient of the HEXs, as shown in Table 5.3.

Regarding CASE C this could be a solution to double the power ratio with respect to case A and also to avoid losing 7 % points on the RTE like in case B. A higher pressure has the positive effect of reducing the relative pressure drop in the HEXs and also of increasing the HEXs global heat transfer coefficient, although this would results in an increased cost for the HEX because of the increased operating pressure. Plus increasing the cycle pressure would also mean having more compact discharge turbomachines but also having a casing and sealing that should sustain higher pressures. Note that in CASE C the maximum pressure is around 188 bars compared to 130 bar of the base case.

*Table 5.3 Relative pressure drop in the discharge cycle of a regenerative PHES system with different power ratio, CASE A*

| | CASE A | CASE B | CASE C |
|---|---|---|---|
| **Discharge cycle control variables** | | | |
| $m_{wf,dis}/m_{wf,ch}$<br>$m_{hot,dis}/m_{hot,ch}$<br>$m_{cold,dis}/m_{cold,ch}$ | **1** | **2** | **2** |
| $p_{min.dis}/p_{min.ch}$ | 1 | 1 | 1.6 |
| **Results** | | | |
| **$W_{net,dis}/W_{net.ch}$ (power ratio)** | **0.56** | **0.97** | **1.12** |
| **$W_{net,dis}$ [$MW_{el}$]** | 10.6 | 18.5 | 20.4 |
| **Heat exchanger** | **Δp/p [%] discharge cycle** | | |
| Hot HEX | 0.8 | 2.4 | 1.1 |
| Regenerator cold stream | 0.7 | 5.2 | 2.1 |

| | | | |
|---|---|---|---|
| Regenerator hot stream | 1.1 | 3.2 | 1.5 |
| Cold HEX | 1.2 | 5 | 1.9 |
| **Heat exchanger** | **Global heat transfer coefficient $U_{dis}$ [W/m$^2$/K]** | | |
| Hot HEX | 368 | 660 | 697 |
| Regenerator | 854 | 1680 | 1700 |
| Cold HEX | 768 | 1407 | 1466 |
| **RTE [%]** | 56.0 | 49.1 | 54.5 |

## 5.2. OFF DESIGN OPERATION OF THE DISCHARGE CYCLE

Off-design operation is an important aspect to be investigated in an energy storage system, since in real operation the plant cannot always work at the design conditions because of market requirements, for example in some periods it could be advantageous to discharge the PHES in a longer time. It is important to underline that for the PHES using indirect TES system when referring to off-design of the discharge cycle it is meant the off design of turbomachines, because the heat exchangers operate already in an off design condition between the charge and discharge cycle.

As already mentioned in 4.5.1 in the off design cycle, pressurization and discharge temperature of the hot TES ($T_b$) are the two additional variables that the model uses to ensure that the operating point of turbomachines respect the characteristics maps.

The results of the off-design operation are presented in Figure 5.6, in the graph the efficiency of the discharge cycle and the net power output are plotted as function of the cycle maximum pressure. Note that this off-design analysis is done with respect to a discharge design equal to CASE C presented in Table 5.1. The off-design method employed in the model is called in literature *inventory control* [21], basically it consists of reducing the working fluid mass flow rate and the pressurization of the cycle simultaneously by reducing the total amount of working fluid in the cycle and storing into a pressurized tank, when the net power output must be decreased. Note that as the working fluid mass flow rate is reduced also the hot and cold TES mass flow rates are reduced too to operate the HEXs with balanced flows and avoid reducing the discharge cycle efficiency.

In Figure 5.4 it is presented the T-s diagram of the off-design discharge cycle with a load reduction of 30% (in blue) compared to the design one. It can be noted that basically the cycle is translated to the right because of the decreased pressurization, while cycle temperatures remain almost constant to the design ones.

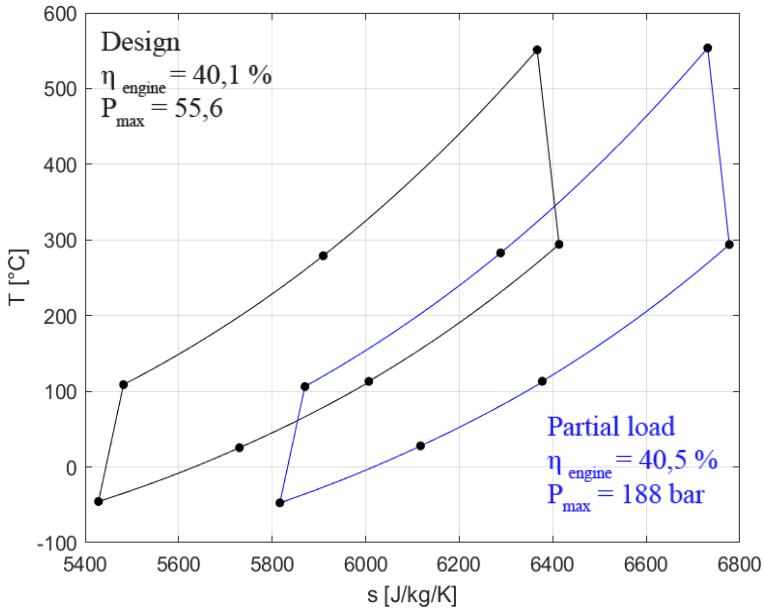


*Figure 5.4 T-s diagrams of discharge cycle of a regenerative Brayton PHES, in black the diagram of design discharge cycle, in blue the diagram in off-design operation with net discharge power of 30% of design power, inventory control mode used: working fluid mass flow rate and cycle pressure reduced of 30%, turbomachines at constant rotational speed.*

In Table 5.4 the relevant parameters of turbine and compressor are reported and compared to an off-design condition of partial load at 30% of the design power. The first three parameters are the parameters employed in the characteristics maps presented in 4.5.1. It can be noted that in the off-design condition both machines does not move far away from the design point, as a matter of fact $\dot{\boldsymbol{G}}$ and $\dot{\pi}$ are near 1. There is a slight variation of the pressure ratios which is due to the decreases of the pressure drops in the heat exchangers (because the reduced mass flow rate ). As example the off design point in the compressor map is presented in Figure 5.5, it can be seen that the operating point moves to a curve with a slightly higher $\dot{\boldsymbol{n}}$, this is due to the variation of the compressor inlet temperature (CIT) while the rotational speed is kept constant. Because of these considerations the turbomachines maintain the same efficiency as the design point.

This is advantageous for the cycle efficiency and since that the regulation can be assured only by varying the cycle pressure and mass flow rate, the turbomachines can be operated at constant rotational speed.

*Table 5.4 Off-design operation of compressor/expander in the discharge cycle of a PHES system with liquid TES, characteristics parameters of the compressor and expander*

| **Partial load ($m_{wf,dis}$=30%$m_{wf,dis,\ DESIGN}$)** | **Compressor** | | **Expander** | |
|---|---|---|---|---|
| | DESIGN | OFF DESIGN | DESIGN | OFF DESIGN |
| $\dot{\pi}$ | 1 | 1.02 | 1 | 1.02 |
| $\dot{G}$ | 1 | 1.02 | 1 | 0.99 |
| $\dot{n}$ | 1 | 1.01 | 0.99 | 1 |
| **$Wnet_{dis}$ [MW]** | 12.6 | 7.6 | 23.6 | 13.9 |
| **$m_{wf,dis}$ [kg/s]** | 160 | 48 | 160 | 48 |
| $\beta$ | 4.96 | 5.05 | 4.6 | 4.68 |
| TIT/CIT [17] [K] | 228 | 226 | 824 | 827 |
| $p_{in}$ [bar] | 38 | 11 | 184 | 55 |
| $\eta_{isoentropic}$ [%] | 87.4 | 87.4 | 91.9 | 91.9 |

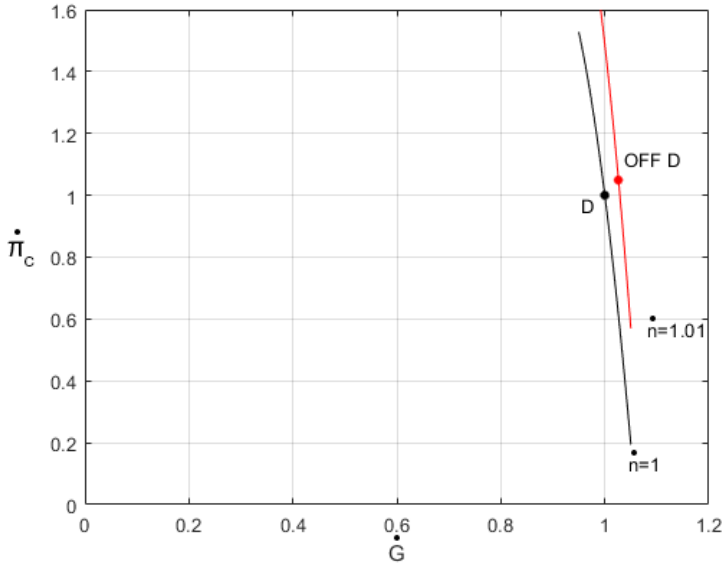


*Figure 5.5 Compressor characteristics map, design point D in black, off design partial load point OFF D in red, beta, G and n are the dimensionless parameters used in the characteristic map taken from* [16]

Since the turbomachines efficiency remain constant, the discharge cycle efficiency reported in Figure 5.6 does not change significantly as the net power decreases, this is coherent with results found in literature for Closed Brayton cycles [14], [21].

The fact that the cycle efficiency remains almost constant, is also because the working fluid behaves as an ideal gas so that the specific heat does not depend on pressure, this is true for nitrogen in PHES cycle because the operating temperature and pressures are far from the critical point (−147,14 °C a 33.9 bar) , e.g. minimum

[17] Turbine inlet temperature/ Compressor inlet temperature

cycle temperature is -45°C at 38 bar, plus if we look to the compressibility factor of the working fluid it ranges 0.96 to 1.04.

Regarding the heat exchangers, the global heat transfer decreases linearly with the reduction of the working fluid mass flow rate (i.e. as the cycle pressure decreases) and also with the reduction of the hot and cold storage mass flow rates as can be seen in Figure 5.7. Regarding the relation between the mass flow rate and global heat transfer coefficient in off-design condition, looking at the equation to calculate $U$, if the ratio between the two mass flow rate remains constant and the effect of conduction is negligible, the relation between the mass flow ration and $U$ can be simplified [67] to :

$$\frac{U_{off}}{U_{design}} = \left(\frac{m_{off}}{m_{design}}\right)^{n} \qquad (5.1)$$

This simplification can be done because since $h \propto Nu$, $Nu \propto Re^{n}$ and $Re \propto m$ then $h \propto m^{n}$. In this model since different correlation are used for the hot and cold stream of the HEXs, the exponent cannot be analytically derived. For the hot and cold heat exchangers $n$ is around 0.67 while for the Regenerator $n=0.96$. In Figure 5.7 the plot of $U$ as a function of the discharge mass flow rate is shown, the regenerator which has the high $n$ is the steepest line.

This means that $U$ does decrease with a lower rate with respect to the mass flow rate and therefore as heat exchanged drops at the same rate as $m_{wf}$ , the temperature differences in the HEXs slightly decreases in the off-design leading to a slight increase of the cycle efficiency.

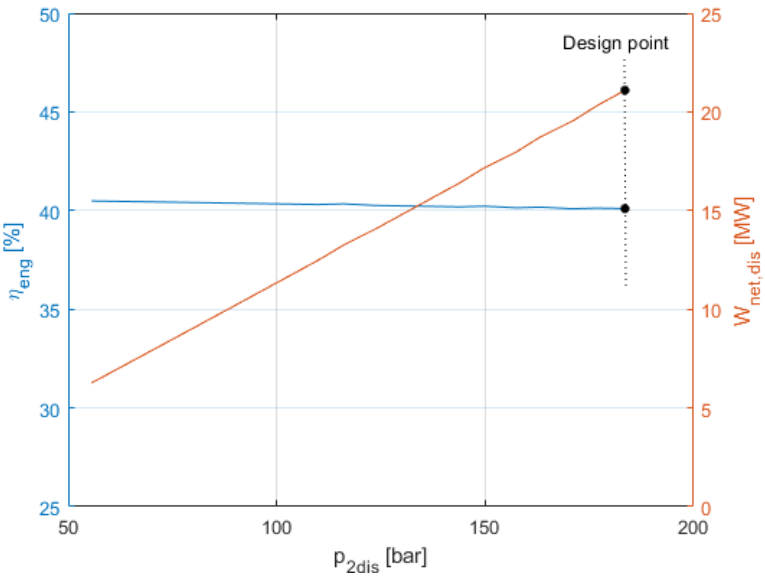


*Figure 5.6 Partial load performance of the discharge cycle for a regenerative PHES system with liquid TES, cycle efficiency on the left axis, net discharge power on the right y-axis, discharge cycle maximum pressure on the x-axis*

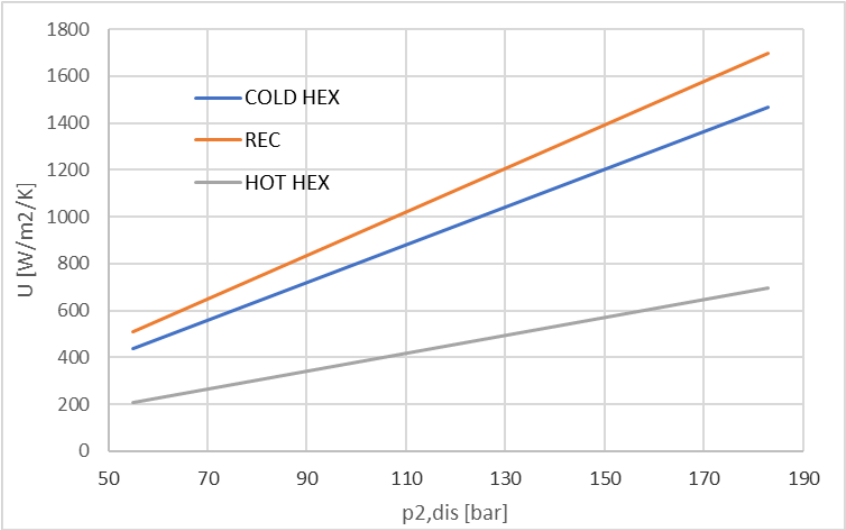


*Figure 5.7 Off-design analysis of the global heat transfer coefficient of the heat exchangers of PHES as the cycle pressure is reduced to reduce the net power output*

## 5.3.ECONOMONIC RESULTS

To simulate the operation in a real case scenario, a real case study was developed assuming to operate PHES system in the Californian electricity day-ahead market. As shown in Figure 5.8 which reports the hourly wholesale electricity prices in the day-ahead market, the price has an off-peak periods that goes from 10:00 to 16:00 and has a peak period from 18:00 to 21:00. The trend in the electricity price that California is experiencing, is also called the *duck curve*, which is a situation that happens when there is high share of solar PV electricity production. Because of this during the afternoon solar production drops off and therefore thermal power plants have to rump up quickly and provide the energy in the peak hours. This situation was reached in California with a solar PV generation share of 11% [77], but is likely to be the new standard in the electricity markets of regions with a high share of solar PV generation. This is an important scenario to investigate because it highlights the challenge the electric system have to face when in a region the share of solar PV is increasing, and it is in this scenario that energy storage systems are more likely to become a viable solution, to avoid the new installation of thermal power plants and therefore reducing the carbon footprint of electricity generation during peak periods.

To simulate the operation in the Californian market it was chosen to charge the plant for the 6 hours of off-peak period and discharge all the stored electricity at the 3 hours of peak period. Therefore, the system set up for the discharge cycle is the one shown in Table 5.3 CASE c, with a power ratio of 1.12 that allows to discharge the TES with halved discharge time. While for the charge cycle the model input data are the one of Table 5.2.

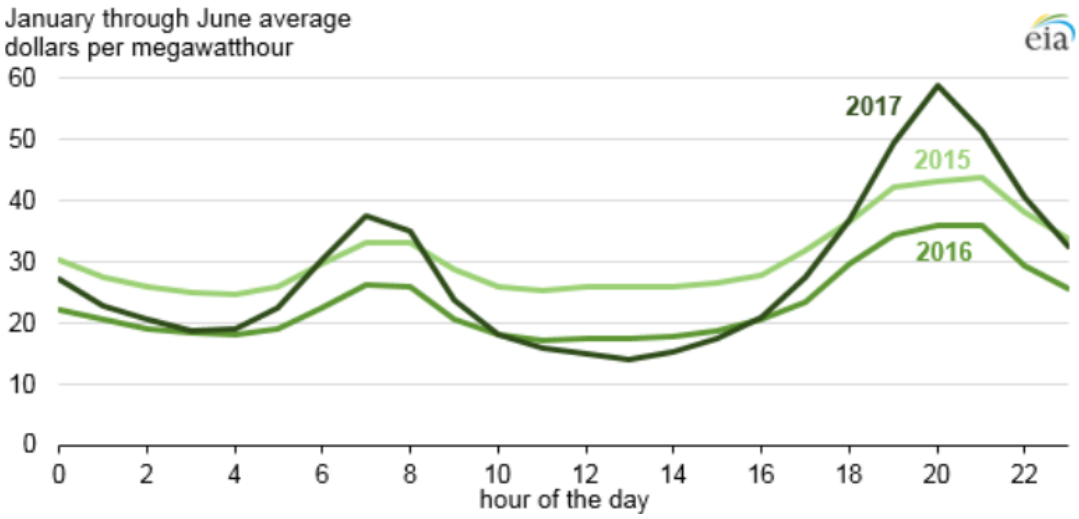


*Figure 5.8 average hourly wholesale electricity prices in California, average from June to July. source:* [22]

The system is assumed to have a storage capacity of 113 $MWh_{el}$[18] and a discharge power of 20.5 $MW_{el}$. Note that an additional cost of 400 $\$/kW_{el}$ was introduced to

[18] This is the stored electricity, to calculate the discharged electricity this value must be multiplied by the RTE

account for the electric generator/motor and all the other cost for the installation of the power plant, in the work of [20] this cost was assumed to range between 200 to 520\$/$kW_{el}$, remember that all the specific cost reported in this chapter are referred to the net discharge power. A summary of the technical specification of the PHES and the CAPEX calculation is reported in Table 5.5, the system has an overall CAPEX of 570 \$/kW for a 6h storage and an RTE of 54,5%, the result obtained for a PHES with liquid TES is in line with the calculated cost of 470\$/ $kW_{el}$ obtained by Farres [1] and of 550 \$/ $kW_{el}$ obtained by Laughlin [9].

*Table 5.5 Technical and cost parameters output of a regenerative Brayton PHES with liquid TES for a 110MWh / 20MW plant, specific cost referred to the net discharge power*

| **System technical specification** | | |
|---|---|---|
| **Charge net power** | 18.9 | $MW_{el}$ |
| **Capacity** | 113.4 | $MWh_{el}$ |
| **Discharge net power** | 20.5 | $MW_{el}$ |
| **RTE** | 54.5 | % |
| **$\rho_e$[19]** | 31 | $kWh/m^3$ |
| **Power Based CAPEX** | | |
| **Turbomachinery, ch** | 17 | $/kW_{el}$ |
| **Turbomachinery, dis** | 23 | |
| **Heat exchangers** | 80 | |
| **Generator+Extra costs** | 400 | |
| **Total** | 520 | |
| **Energy based CAPEX** | | |
| **Storage materials** | 8 | $/kWh_{el}$ |
| **Tanks** | 4 | |
| **Total** | 12 | |
| **Total CAPEX[20] (6 h storage)** | 577 | $/kW_{el}$ |
| **Total CAPEX (5 days storage)** | 1770 | $/kW_{el}$ |

From the cost analysis it can be seen that with exception of the extra cost, the cost is dominated by the heat exchangers cost, while for the turbomachinery the cost it is higher for the discharge set of turbomachines, because of the double working fluid mass flow rate in discharge and the higher pressure ratio. When comparing energy and power cost it is clear that for a storage time of 6 hours the power based cost is predominant , on the other hand if the PHES plant would have to be used for long term energy storage (charge time > 1 day) the energy base cost would be the highest part of the overall cost. It is important to underline that the PHES system is a storage

[19] Energy density in the table is calculated considering the volume of the four tanks of the TES system

[20] Total CAPEX includes the energy and power cost divided by the net discharge power

technology in which power and capacity are decoupled. Therefore, for the same plant power rating, the PHES could be used for short term energy storage or long-term energy storage by simply enlarging the thermal energy storage vessels.

In Table 5.6 and Table 5.7 the operating parameters for the turbomachinery and heat exchangers are reported, plus in appendix A a detailed report of model results is presented. It must be underlined that for the heat exchangers the parameters presented in Table 5.7 refers to the charge cycle in which HEXs design is performed. Note that the auxiliary heat exchanger is not reported since it is not modelled in detail and its cost is 120 k$ and the specific CAPEX is lower than the other HEXs and is around 6 $\$/kW_{el}$. The results found for turbomachinery and heat exchangers are in line with the cost obtained by Farres [1].

*Table 5.6 Main parameters employed in the economic model for the turbomachinery of a PHES system with liquid TES*

| **Component** | **Unit** | **Charge** | | **Discharge** | |
|---|---|---|---|---|---|
| | | Compressor | Expander | Compressor | Expander |
| **Working fluid** | - | Nitrogen | | | |
| **$T_{in}$** | [K] | 563 | 313 | 228 | 824 |
| **$T_{out}$** | [K] | 848 | 219 | 382 | 567 |
| **$p_{in}$** | [bar] | 25.7 | 98 | 38 | 183 |
| **$p_{out}$** | [bar] | 100 | 26.4 | 189 | 40 |
| **β** | - | 3.88 | 3.72 | 4.96 | 4.6 |
| **ρ[21]** | [kg/m$^3$] | 15 | 41 | 58 | 23 |
| **m** | [kg/s] | 80 | | 160 | |
| **$\eta_{polytropic}$** | % | 90 | | | |
| **W** | MW | 25.6 | 7.3 | 26 | 47 |
| **Z** | [k$] | 287 | 69 | 175 | 289 |
| **Z/Wnet_dis** | [$/kW$_{el}$] | 14 | 3.4 | 8.5 | 14 |

*Table 5.7 Main parameters employed in the economic model for the heat exchangers of a PHES system with liquid TES, the parameters refers to the design condition of HEXs, i.e. to the charge phase*

| **Component** | **Unit** | **Heat exchangers** | | |
|---|---|---|---|---|
| | | **Hot** | **Regenerator** | **Cold** |
| **Fluid1** | - | Solar Salt | Nitrogen | Nitrogen |
| **$T_{in}$** | [K] | 838 | 573 | 219 |
| **$p_{in}$** | [bar] | 1 | 99 | 26 |
| **m** | [kg/s] | 59.3 | 80 | 80 |
| **Fluid2** | - | Nitrogen | Nitrogen | Methanol |
| **Tin** | [K] | 848 | 292 | 294 |

[21] Reference density for the cost equation calculated at the inlet for compressors and at the outlet for expanders

| | | | | |
|---|---|---|---|---|
| **pin** | [bar] | 99 | 26 | 1 |
| **m** | [kg/s] | 80 | 80 | 37.8 |
| $\Delta T_{ml}$ | [K] | 10 | 10 | 2.5 |
| $(\Delta p/p)_1$ | [%] | 5 | 1 | 1 |
| $(\Delta p/p)_2$ | [%] | 1 | 1 | 5 |
| **A** | [$m^2$] | 2642 | 1968 | 4357 |
| **U** | [W/K/ $m^2$] | 916 | 851 | 438 |
| **Q** | [MW] | 24.7 | 23.2 | 6.43 |
| **Z** | [k$] | 474 | 373 | 696 |
| $Z/W_{net,dis}$ | [$/$kW_{el}$] | 23 | 18 | 34 |

To evaluate the economic feasibility of the system the levelized cost of storage for the PHES plant was calculated. In Table 5.8 the parameters used to calculate the LCOS, as described in 4.6.3, are presented, these parameters were taken from Smallbone et. al [20] who developed the LCOS for a PHES with packed beds TES. In the table the results of the LCOS are presented and the three components of the LCOS are shown.

It can be seen that the biggest component is the one related to the CAPEX while the OPEX component is very small. The electricity cost component ($C_{el}$) is the component related to the RTE of the system, on first approximation (without discounting) it is the ratio of the electricity price over the RTE. In this scenario the price for charging electricity was taken as the average of the price from 10:00 to 16:00 from Figure 5.8 which is 18 $/MWh.

| | | |
|---|---|---|
| **Lifetime** | 20 | years |
| **Discount rate** | 8 | % |
| **Cycles per year** | 365 | - |
| **Charging time** | 6 | h |
| **Discharge time** | 3 | h |
| **Electricity buy price** | 18 | $/MWh |
| **CAPEX** | 53.7 | $/MWh |
| **OPEX** | 13.7 | |
| **$C_{el}$** | 32.1 | |
| **LCOS** | 99.5 | |

*Table 5.8 Parameters used for the calculation of the levelized cost of storage calculation*

The calculated LCOS was 99 $/MWh, comparing this result with the average selling price which is around 50$/MWh it is clear that is not financially feasible to run the system in the day-ahead without any incentives. Even if the electricity cost in the off-peak period would be zero, the LCOS would be still 67$/MWh which is still above the sell price electricity.

This result is in line with other LCOS studies on PHES ([20], [32]), plus as shown by Frate in [43] this result must not be seen as a negative aspect because currently no other energy storage technology can economically self-sustain in the day-ahead market without any incentives.

Buy prices greater than 100$/MWh have not to be seen as unrealistic, because the prices of peak periods is increasing in regions with a high share of renewable energies [78]. To do a better evaluation of the profitability of an energy storage system, in a more detailed study it should also be investigated the participation of the storage system in the ancillary services market, in which prices can reach values above 100$/MWh [23].

To better understand the influence of the design of the heat exchangers on the LCOS a sensitivity analysis was developed. In one case the HEXs relative pressure drop is changed and in the other the HEXs temperature differences are varied, the variations are done with respect to the design parameters of Table 5.7. In Table 5.9 it is shown how the variation of the parameters influence the CAPEX and the RTE. It can be noted that concerning the CAPEX it would be more beneficial to increase the temperature difference in the HEXs to reduce their cost even though the RTE would drop, the same cannot be said for the relative pressure drops in fact a increase in the pressure drops would allow to reduce heat exchangers cost but not enough to outweigh the reduction of the RTE and therefore the CAPEX increases.

Looking at the LCOS variation plotted in Figure 5.9 it can be noted that in the case of increased $\Delta T$, even though the CAPEX was lower the LCOS increased, because the increase of the electricity cost component (due to the reduced RTE) outweighs the reduction of the CAPEX. The opposite situation occurs for the case of the reduced $\Delta p/p$, in this case the increase on the RTE was enough to counterbalance the increased CAPEX bringing to a slight reduction of the LCOS.

*Table 5.9 Sensitivity analysis on the CAPEX and RTE of PHES for different heat exchangers temperature differences and for different relative pressure drops, variation referred to the design parameters presented in Table 5.7*

| **$\Delta$T sensitivity analysis** | | | |
|---|---|---|---|
| $\Delta T_{ml}$ | **-50%** | **0%** | **+100%** |
| CAPEX [$/kW$_{el}$] | 626 | 577 | 556 |
| RTE | 56.9 | 54.5 | 46.17 |
| **Relative pressure losses sensitivity analysis** | | | |
| $\Delta p/p$ | **-50%** | **0%** | **+100%** |
| CAPEX [$/kW$_{el}$] | 580 | 577 | 587 |
| RTE | 57.3 | 54.5 | 48.6 |

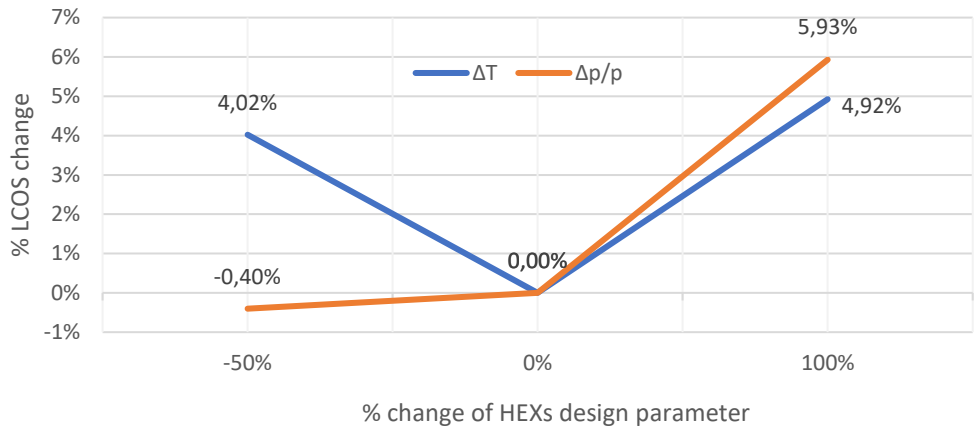


*Figure 5.9 Sensitivity analysis of LCOS, varying the design parameters of heat exchangers, in blue the temperature difference, in orange the relative pressure drops*

In Figure 5.9 another sensitivity analysis is presented for the main input parameters of LCOS calculation. The most sensitive parameter is the yearly cycles of the plant, a decrease of 20% would result in an increase of 17%. Clearly if the system would be used for delivering electricity also in the lower morning peak from 6:00 to 8:00, an increase of the yearly cycles of the plant could be reasonable. The other parameter which is very important is the cost of the charged electricity, the lower the RTE the higher the impact of this parameter will be on the LCOS.

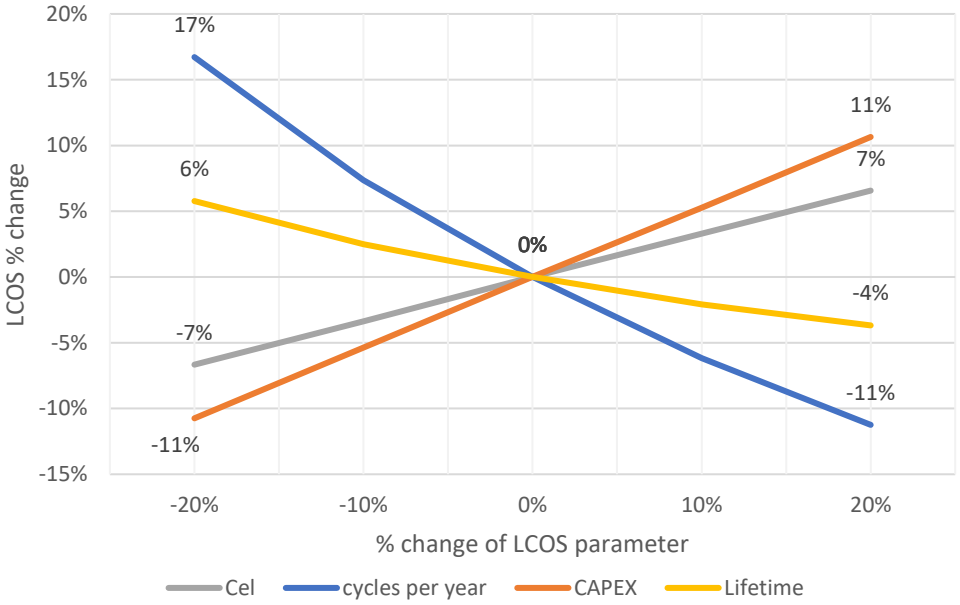


*Figure 5.10 Sensitivity analysis of LCOS for PHES with main parameters. Reference case for 1 cycle per day, 20 years lifetime, electricity cost of 18$/MWh and CAPEX of 577$/KW*

# 6. CONCLUSIONS

In recent years the generation of renewable energy sources has rapidly increased, introducing new challenges that the electricity system must solve, in order to increase the RES generation. RES generation is in fact non dispatchable like the generation from thermal power plants and Energy storage technologies are a key solution to enable the integration of RES into the electricity system.

This thesis has investigated the thermodynamic and economic analysis of a new energy storage technology called pumped heat electricity storage (PHES). PHES takes electricity from the grid to drive a heat pump that stores thermal energy in a hot and a cold reservoir during charging, during discharge the hot reservoir is cooled down while the cold one is heated up to drive a heat engine that generates electricity and gives it back to the grid. PHES is categorized depending on the power cycles adopted for the heat pump and heat engine, which can be Rankine-cycle or Brayton cycles, in this thesis the focus was on PHES based on Brayton cycles. In literature the most studied PHES based on Brayton cycles are the ones employing packed beds as thermal energy storage (TES) even though packed-bed have not been yet been tested for the large scale TES application, therefore in this paper it was chosen to investigate a different case which is a TES with liquid storage , with molten salts (widely used TES for CSP application) as the hot TES and methanol as the cold TES.

After developing a literature review on PHES and on TES system, an analytical thermodynamic analysis of PHES was developed to understand how the different components irreversibilities influenced the overall round trip efficiency. It was shown that the turbomachinery irreversibilities has the highest impact on the RTE and that in the best cycle configuration, with a polytropic efficiency of turbomachines of 90% and a maximum temperature of 565°C the RTE highest achievable RTE is 71%, if only irreversibilities in the turbomachines are considered. Plus, it was shown that to avoid having a very poor RTE heat exchangers effectiveness should be kept above 95% and relative pressure drops below 1%.

After the preliminary analysis, a numerical model was developed to evaluate the real performance of the system. Due to the compatibility with liquid storage operating temperatures a regenerator was introduced, the molten salts are operated between 560°C and 290 °C while the methanol works between -50°C to 20°C. For the working fluid nitrogen was chosen because of a trade-off between turbomachinery costs and heat exchangers cost. The PHES modelled, employs the same heat exchangers between charge and discharge phase, and instead a different turbomachinery set between charge and discharge is used, meaning that in the discharge phase the heat exchangers operates in off-design condition, while the turbomachines operates in a design condition.

The results obtained by the numerical model was a RTE of 56.0 %[22] and an energy density of 31 kWh/m$^3$ for a system with 11 $MW_{el}$ rated discharge power, a storage time of 6 hours and a power ratio of 0.56. An exergy analysis of the system was performed, and it showed that the 55% of the exergy losses are related to the turbomachines, highlighting the importance of having a high efficiency of these components. The effect of the power ratio[23] between charge and discharge was also investigated, to operate the storage system with a different charge and discharge time. The result was that the increase of the PHES discharge power has a negative effect on the RTE because of the off-design of HEXs and the increase of the pressure drops. The RTE calculated with a power ratio of 0.97 , dropped from 56.0% to 49%. To contain this negative effect, it was shown that by increasing the discharge cycle pressurization of 60% the system had an RTE of 54.5 % with a power ratio of 1.12. This problematic highlighted the fact that the heat exchangers off-design has a negative impact on the system operation, therefore to better account for this, HEXs design should be done in the discharge phase which it is most likely to be the condition in which they operate with the highest thermal duty. Another approach could be simply to oversize the heat exchangers if their design is done in the charge phase like in this thesis.

The partial load operation of the discharge cycle was also investigated to understand how it affects the RTE. The off-design control strategy employed was the *inventory control* strategy which consists of reducing the total amount of fluid in the system and storing into a pressurized tanks, to decrease the cycle pressurization and the working fluid mass flow rates. This allows the turbomachines to operate very close to their design point with the same efficiency of the design condition, plus it allows to have a constant rotational speed. Cycle efficiency then resulted to be almost constant as the net power of the cycle is reduced and therefore allowing the operation of the PHES without reducing the RTE.

Finally the economics and cost of the PHES was investigated and the overall CAPEX was calculated to be 577 \$/kW[24] for a 20.5 MW/113MWh[25] system with a RTE of 54.5%, with 80 \$/kW related to HEXs, 40 \$/kW to turbomachinery, 400\$/kW for the generator and installation cost and 57 \$/kW for the hot and cold TES. To evaluate the economic feasibility of the system a levelized cost of storage analysis was developed assuming to operate the system in the Californian market to provide electricity in the peak hours, the calculated LCOS was found around 99\$/MWh, which underlines that without any incentives this kind of operation of the ESS is not financially feasible.

Compared to other storage technology PHES is a promising solution because it has a power-based cost comparable to PHS and CAES and because it is a ESS with no

[22] $\Delta p/p$=1%, HEXs effectiveness =96% and $\eta_{pol}$=90% and $\eta_{em}$=97%
[23] Ratio between the discharge net power and the charge net power
[24] Referred to the discharge net power
[25] System Capacity defined as the product of the net charge power and the charge time

specific geographical requirements, even though efforts must be made to increase the RTE and a achieve the best cost effective solution. Concluding with a quote form Laughlin all that is needed to make this technology prevail are " no laboratory breakthroughs or discovery but only fine engineering and assiduous attention to detail" [9].

## FUTURE DEVELOPMENTS

Regarding the power block side alternative layouts should be investigated, in appendix B an alternative discharge cycle with a double stage intercooled compression is presented. Another future development could be the optimisation of the cycle LCOS in order to see what is the most cost effective solution for the HEXs design. Regarding the thermal energy storages, the employment of a cascade thermal energy storage system to store the heat for a longer-term storage could be investigated. Another aspect could be instead to substitute the liquid TES with un indirect unpressurized packed-bed TES that would store heat using a secondary heat transfer fluid that could link the TES with the power cycle. This could merge the advatnages of indirect TES and packed-bed TES allowing for a cheap TES, operating with a high temperature range, eliminating the use of the regenerator but still having the power cycle with a high power density, the only drawback would the increase plant complexity.

# Bibliography


[1] P. Farres-Antunez, “Modelling and development of thermo-mechanical energy storage,” no. September, 2018, doi: 10.17863/CAM.38056.

[2] F. Marguerre, “‘Ueber ein neues verfahren zur aufspeicherung elektrischer energie,’” vol. Mitteilung.

[3] Weissenbach B., “Thermischer kraftspeicher thermal power storage.,” 1979.

[4] A. White, G. Parks, and C. N. Markides, “Thermodynamic analysis of pumped thermal electricity storage,” *Appl. Therm. Eng.*, vol. 53, no. 2, pp. 291–298, 2013, doi: 10.1016/j.applthermaleng.2012.03.030.

[5] T. Desrues, J. Ruer, P. Marty, and J. F. Fourmigué, “A thermal energy storage process for large scale electric applications,” *Appl. Therm. Eng.*, vol. 30, no. 5, pp. 425–432, 2010, doi: 10.1016/j.applthermaleng.2009.10.002.

[6] A. Thess, “Thermodynamic Efficiency of Pumped Heat Electricity Storage ´,” vol. 110602, no. SEPTEMBER, pp. 1–5, 2013, doi: 10.1103/PhysRevLett.111.110602.

[7] J. Howes, “Concept and development of a pumped heat electricity storage device,” *Proc. IEEE*, vol. 100, no. 2, pp. 493–503, 2012, doi: 10.1109/JPROC.2011.2174529.

[8] J. Howes and J. S. Macnaghten, “CA2701526A1.pdf,” CA2701526A1, 2009.

[9] R. B. Laughlin, “Pumped thermal grid storage with heat exchange,” *J. Renew. Sustain. Energy*, vol. 9, no. 4, pp. 1–16, 2017, doi: 10.1063/1.4994054.

[10] J. D. McTigue, A. J. White, and C. N. Markides, “Parametric studies and optimisation of pumped thermal electricity storage,” *Appl. Energy*, vol. 137, pp. 800–811, 2015, doi: 10.1016/j.apenergy.2014.08.039.

[11] H. Singh, R. P. Saini, and J. S. Saini, “A review on packed bed solar energy storage systems,” *Renew. Sustain. Energy Rev.*, vol. 14, no. 3, pp. 1059–1069, 2010, doi: 10.1016/j.rser.2009.10.022.

[12] G. Peiró, C. Prieto, J. Gasia, A. Jové, L. Miró, and L. F. Cabeza, “Two-tank molten salts thermal energy storage system for solar power plants at pilot plant scale: Lessons learnt and recommendations for its design, start-up and operation,” *Renew. Energy*, vol. 121, pp. 236–248, 2018, doi: 10.1016/j.renene.2018.01.026.

[13] “Matlab R 2019b.” [Online]. Available: https://it.mathworks.com/products/matlab.html.

[14] P. H. V Dostal, MJ Driscoll, “A supercritical carbon dioxide cycle for next generation nuclear reactors,” 2004.

[15] J. D. McTigue, “ANALYSIS AND OPTIMISATION OF THERMAL ENERGY STORAGE,” 2016.

[16] N. Zhang and R. Cai, “Analytical solutions and typical characteristics of part-load performances of single shaft gas turbine and its cogeneration,” *Energy Convers.*

*Manag.*, vol. 43, no. 9–12, pp. 1323–1337, 2002, doi: 10.1016/S0196-8904(02)00018-3.

[17] M. R. V. S. A. Valero, M. A. Lozano, L. Serra, C. Frangopoulos, “CGAM problem: Definition and conventional solution,” 1994.

[18] R. Hall, S.G., Ahmad, S.& SMith, “Capital cost targes for heat exchanger networks comprising mixe materials of construction, pressure raiting and exchanger types,” 1990.

[19] A. R. Doodman, M. Fesanghary, and R. Hosseini, “A robust stochastic approach for design optimization of air cooled heat exchangers,” *Appl. Energy*, vol. 86, no. 7–8, pp. 1240–1245, 2009, doi: 10.1016/j.apenergy.2008.08.021.

[20] A. Smallbone, V. Jülch, R. Wardle, and A. P. Roskilly, “Levelised Cost of Storage for Pumped Heat Energy Storage in comparison with other energy storage technologies,” *Energy Convers. Manag.*, vol. 152, no. September, pp. 221–228, 2017, doi: 10.1016/j.enconman.2017.09.047.

[21] Z. Li, X. Yang, J. Wang, and Z. Zhang, “Annals of Nuclear Energy Off-design performance and control characteristics of space reactor closed Brayton cycle system,” *Ann. Nucl. Energy*, vol. 128, pp. 318–329, 2019, doi: 10.1016/j.anucene.2019.01.022.

[22] “California wholesale electricity prices are higher at the beginning and end of the day.”

[23] Terna, “Rapporto Mensile Ottobre 2020,” 2020.

[24] D. O. Akinyele and R. K. Rayudu, “Review of energy storage technologies for sustainable power networks,” *Sustain. Energy Technol. Assessments*, vol. 8, pp. 74–91, 2014, doi: 10.1016/j.seta.2014.07.004.

[25] R. Morgan, S. Nelmes, E. Gibson, and G. Brett, “Liquid air energy storage - Analysis and first results from a pilot scale demonstration plant,” *Appl. Energy*, 2015, doi: 10.1016/j.apenergy.2014.07.109.

[26] IPCC, “Sommario per i Decisori Politici.”

[27] “No Title.” [Online]. Available: https://ec.europa.eu/clima/policies/strategies/2030_en.

[28] E. D. Ministry, N. Resources, and T. December, “INTEGRATED NATIONAL ENERGY AND CLIMATE Ministry of Economic Development,” no. December, 2019.

[29] IEA, “Energy storage report.”

[30] A. Benato and A. Stoppato, “Pumped Thermal Electricity Storage: A technology overview,” *Therm. Sci. Eng. Prog.*, vol. 6, pp. 301–315, 2018, doi: 10.1016/j.tsep.2018.01.017.

[31] “No Title.”

[32] G. F. FRATE, “ANALYSIS OF A PUMPED THERMAL ELECTRICITY STORAGE SYSTEM WITH THE INTEGRATION OF LOW TEMPERATURE HEAT SOURCES,” University of

Pisa, 2019.

[33] H. Zhang, L. Wang, X. Lin, and H. Chen, “Combined cooling, heating, and power generation performance of pumped thermal electricity storage system based on Brayton cycle,” *Appl. Energy*, vol. 278, no. July, p. 115607, 2020, doi: 10.1016/j.apenergy.2020.115607.

[34] M. Abarr, B. Geels, J. Hertzberg, and L. D. Montoya, “Pumped thermal energy storage and bottoming system part A: Concept and model,” *Energy*, 2017, doi: 10.1016/j.energy.2016.11.089.

[35] “Newcastle University connects first grid-scale pumped heat energy storage system,” 2019. [Online]. Available: https://www.theengineer.co.uk/grid-scale-pumped-heat-energy-storage/.

[36] Xabier Peña, “Compressed Heat Energy Storage for Energy from Renewable Sources (CHESTER),” *European Union’s Horizon 2020 research and innovation programme*, no. 764042. 2018.

[37] B. F. Chen H., Ding Y., Peters T., “A method of storing energy and a cryogenic energy storage system.,” CA 2,643,742, 2007.

[38] R. J., “Installation et procedes de stockage et restitution d’energie electrique.,” CA 2,686,417, 2008.

[39] W. B., “Verfahren zur speicherung und rückgewinnung von energie a method for storage and recovery of energy,” DE200,610,007,119, 2007.

[40] A. Benato, “Performance and cost evaluation of an innovative Pumped Thermal Electricity Storage power system,” *Energy*, vol. 138, pp. 419–436, 2017, doi: 10.1016/j.energy.2017.07.066.

[41] W. D. Steinmann, “The CHEST (Compressed Heat Energy STorage) concept for facility scale thermo mechanical energy storage,” *Energy*, 2014, doi: 10.1016/j.energy.2014.03.049.

[42] D. Laing *et al.*, “Combined storage system developments for direct steam generation in solar thermal power plants,” *30th ISES Bienn. Sol. World Congr. 2011, SWC 2011*, vol. 2, pp. 1226–1237, 2011, doi: 10.18086/swc.2011.09.04.

[43] R. B. Peterson, “A concept for storing utility-scale electrical energy in the form of latent heat,” *Energy*, vol. 36, no. 10, pp. 6098–6109, 2011, doi: 10.1016/j.energy.2011.08.003.

[44] W. D. Steinmann, “Thermo-mechanical concepts for bulk energy storage,” *Renew. Sustain. Energy Rev.*, vol. 75, no. November 2016, pp. 205–219, 2017, doi: 10.1016/j.rser.2016.10.065.

[45] M. Mercangöz, J. Hemrle, L. Kaufmann, A. Z’Graggen, and C. Ohler, “Electrothermal energy storage with transcritical CO2 cycles,” *Energy*, 2012, doi: 10.1016/j.energy.2012.03.013.

[46] W. D. Steinmann, H. Jockenhöfer, and D. Bauer, “Thermodynamic Analysis of High-Temperature Carnot Battery Concepts,” *Energy Technol.*, vol. 8, no. 3, 2020, doi:

10.1002/ente.201900895.

[47] “International Energy Agency.” [Online]. Available: https://www.iea.org/.

[48] T. Desrues, J. Ruer, P. Marty, and J. F. Fourmigué, “A thermal energy storage process for large scale electric applications,” *Appl. Therm. Eng.*, 2010, doi: 10.1016/j.applthermaleng.2009.10.002.

[49] F. Ni and H. S. Caram, “Analysis of pumped heat electricity storage process using exponential matrix solutions,” *Appl. Therm. Eng.*, vol. 84, pp. 34–44, 2015, doi: 10.1016/j.applthermaleng.2015.02.046.

[50] A. Benato and A. Stoppato, “Heat transfer fluid and material selection for an innovative Pumped Thermal Electricity Storage system,” *Energy*, 2018, doi: 10.1016/j.energy.2018.01.045.

[51] L. Wang, X. Lin, L. Chai, L. Peng, D. Yu, and H. Chen, “Cyclic transient behavior of the Joule–Brayton based pumped heat electricity storage: Modeling and analysis,” *Renew. Sustain. Energy Rev.*, vol. 111, no. March, pp. 523–534, 2019, doi: 10.1016/j.rser.2019.03.056.

[52] A. Dietrich, “Assessment of Pumped Heat Electricity Storage Systems through Exergoeconomic Analyses,” no. August, 2017.

[53] T. Bauer, W.-D. Steinmann, D. Laing, and R. Tamme, “Thermal Energy Storage Materials and Systems,” *Annu. Rev. Heat Transf.*, vol. 15, no. 15, pp. 131–177, 2012, doi: 10.1615/annualrevheattransfer.2012004651.

[54] T. R. Davenne, S. D. Garvey, B. Cardenas, and M. C. Simpson, “The cold store for a pumped thermal energy storage system,” *J. Energy Storage*, 2017, doi: 10.1016/j.est.2017.03.009.

[55] A. Gil *et al.*, “State of the art on high temperature thermal energy storage for power generation. Part 1-Concepts, materials and modellization,” *Renew. Sustain. Energy Rev.*, vol. 14, no. 1, pp. 31–55, 2010, doi: 10.1016/j.rser.2009.07.035.

[56] H. Peng, H. Dong, and X. Ling, “Thermal investigation of PCM-based high temperature thermal energy storage in packed bed,” *Energy Convers. Manag.*, vol. 81, pp. 420–427, 2014, doi: 10.1016/j.enconman.2014.02.052.

[57] M. M. Farid, A. M. Khudhair, S. A. K. Razack, and S. Al-Hallaj, “A review on phase change energy storage: Materials and applications,” *Energy Convers. Manag.*, vol. 45, no. 9–10, pp. 1597–1615, 2004, doi: 10.1016/j.enconman.2003.09.015.

[58] I. Sarbu and C. Sebarchievici, “A comprehensive review of thermal energy storage,” *Sustain.*, vol. 10, no. 1, 2018, doi: 10.3390/su10010191.

[59] SaltX Technologies, “No Title.” [Online]. Available: https://saltxtechnology.com/technology/.

[60] J. P. Deane, B. P. Ó Gallachóir, and E. J. McKeogh, “Techno-economic review of existing and new pumped hydro energy storage plant,” *Renew. Sustain. Energy Rev.*, vol. 14, no. 4, pp. 1293–1302, 2010, doi: 10.1016/j.rser.2009.11.015.

[61] S. Rehman, L. M. Al-Hadhrami, and M. M. Alam, “Pumped hydro energy storage

system: A technological review," *Renew. Sustain. Energy Rev.*, vol. 44, pp. 586–598, 2015, doi: 10.1016/j.rser.2014.12.040.

[62] S. Georgiou, N. Shah, and C. N. Markides, "A thermo-economic analysis and comparison of pumped-thermal and liquid-air electricity storage systems," *Appl. Energy*, vol. 226, no. November 2017, pp. 1119–1133, 2018, doi: 10.1016/j.apenergy.2018.04.128.

[63] "Highview Power." [Online]. Available: https://highviewpower.com/join-us/.

[64] "No Title." [Online]. Available: https://www.behance.net/simonedifuria.

[65] H. Xue, "A comparative analysis and optimisation of thermo-mechanical energy storage technologies," no. September, 2018.

[66] "Refprop 9.1." [Online]. Available: https://www.nist.gov/srd/refprop.

[67] A. Giostri, M. Binotti, M. Astolfi, P. Silva, E. Macchi, and G. Manzolini, "Comparison of different solar plants based on parabolic trough technology," *Sol. Energy*, vol. 86, no. 5, pp. 1208–1221, 2012, doi: 10.1016/j.solener.2012.01.014.

[68] S. S. Mostafavi Tehrani, Y. Shoraka, K. Nithyanandam, and R. A. Taylor, "Shell-and-tube or packed bed thermal energy storage systems integrated with a concentrated solar power: A techno-economic comparison of sensible and latent heat systems," *Appl. Energy*, vol. 238, no. January, pp. 887–910, 2019, doi: 10.1016/j.apenergy.2019.01.119.

[69] J. L. Mason, "AG-81 WORKING GAS SELECTION FOR THE CLOSED BRAYTON CYCLE."

[70] J. Tarlecki and N. Lior, "Analysis of thermal cycles and working fluids for power generation in space Author ' s personal copy," vol. 48, pp. 2864–2878, 2007, doi: 10.1016/j.enconman.2007.06.039.

[71] G. Peiró, J. Gasia, L. Miró, C. Prieto, and L. F. Cabeza, "Influence of the heat transfer fluid in a CSP plant molten salts charging process," *Renew. Energy*, vol. 113, pp. 148–158, 2017, doi: 10.1016/j.renene.2017.05.083.

[72] Y. L. He, Z. J. Zheng, B. C. Du, K. Wang, and Y. Qiu, "Experimental investigation on turbulent heat transfer characteristics of molten salt in a shell-and-tube heat exchanger," *Appl. Therm. Eng.*, vol. 108, pp. 1206–1213, 2016, doi: 10.1016/j.applthermaleng.2016.08.023.

[73] K. E. N. P. E, "How to Select Turbomachinery For Your Application How to Select Turbomachinery For Your Application."

[74] T. El Samad, J. A. Teixeira, and J. Oakey, "Investigation of a radial turbine design for a utility-scale supercritical CO2 power cycle," *Appl. Sci.*, vol. 10, no. 12, pp. 1–26, 2020, doi: 10.3390/APP10124168.

[75] B. Zakeri and S. Syri, "Electrical energy storage systems : A comparative life cycle cost analysis," *Renew. Sustain. Energy Rev.*, vol. 42, pp. 569–596, 2015, doi: 10.1016/j.rser.2014.10.011.

[76] L. Xiang, P. Hu, P. Pan, M. Na, and F. Xiang, "Thermodynamic analysis of a High Temperature Pumped Thermal Electricity Storage ( HT-PTES ) integrated with a

parallel organic Rankine cycle ( ORC ),” *Energy Convers. Manag.*, vol. 177, no. July, pp. 150–160, 2018, doi: 10.1016/j.enconman.2018.09.049.

[77] CAISO, “Annual report on market issues & performance,” 2017.

[78] M. Analysis, “CAISO Energy Markets Price Performance Report,” 2019.

# Appendix A: Model output

| Closed Brayton cycle points, Working fluid: Nitrogen | | | | | |
|---|---|---|---|---|---|
| **Charge** | T [K] | p [bar] | h [J/kg/K] | s[J/kg/K] | m [kg/s] |
| **1** | 563.1 | 25.8 | 587150 | 6538 | 80 |
| **2** | 848.2 | 100.0 | 906414 | 6584 | 80 |
| **2R** | 573.2 | 99.0 | 597991 | 6148 | 80 |
| **3** | 313.2 | 98.1 | 307827 | 5474 | 80 |
| **4** | 219.4 | 26.4 | 216819 | 5513 | 80 |
| **4R** | 291.9 | 26.0 | 296986 | 5832 | 80 |
| **Discharge** | T [K] | p [bar] | h [J/kg/K] | s[J/kg/K] | m [kg/s] |
| **1** | 565.3 | 40.0 | 589404 | 6410 | 160 |
| **2** | 823.5 | 185.6 | 883201 | 6362 | 160 |
| **2R** | 551.4 | 187.8 | 574778 | 5904 | 160 |
| **3** | 393.6 | 190.6 | 394542 | 5514 | 160 |
| **4** | 233.7 | 38.0 | 228729 | 5460 | 160 |
| **4R** | 397.6 | 39.2 | 409169 | 6038 | 160 |
| **5** | 305.2 | 38.8 | 308896 | 5754 | 160 |

| HOT TES : Molten-salts | | | | | | |
|---|---|---|---|---|---|---|
| | point | T [K] | p [bar] | h [J/kg/K] | s[J/kg/K] | m [kg/s] |
| **charge** | a | 838.2 | 1 | 1.23E+06 | 9.54E+03 | 59.3 |
| | b | 563.2 | 1 | 8.13E+06 | 8.94E+03 | 59.3 |
| **discharge** | a | 838.2 | 1 | 1.23E+06 | 9.54E+03 | 118.6 |
| | b | 563.2 | 1 | 8.13E+06 | 8.94E+03 | 118.6 |
| **COLD TES: Methanol** | | | | | | |
| | point | T [K] | p [bar] | h [J/kg/K] | s[J/kg/K] | m [kg/s] |
| **charge** | c | 294.3 | 1 | -1.12E+05 | -3.65E+02 | 37.8 |
| | d | 222 | 1 | -2.85E+05 | -1.03E+03 | 37.8 |
| **discharge** | c | 294.3 | 1 | -1.12E+05 | -3.65E+02 | 75.6 |
| | d | 222 | 1 | -2.85E+05 | -1.03E+03 | 75.6 |

## First law Balance

| Charge | | |
|---|---|---|
| **Net power input** | 18.9 | MW |
| **Heat to hot TES** | 24.7 | |
| **Heat from cold TES** | 6.4 | |
| **Electro-mechanical losses** | 0.6 | |
| **Charge time** | 6 | h |
| **Discharge** | | |
| **Net power output** | 20.5 | MW |
| **Heat from hot TES** | 49.5 | |
| **Heat to cold TES** | 12.9 | |
| **Het to environment** | 15.3 | |
| **Fan consumption** | 0.2 | |
| **Electro-mechanical losses** | 0.6 | |
| **Discharge time** | 3 | h |
| **Round trip efficiency** | 54.5 | % |

## Exergy analysis

| CHARGE | |
|---|---|
| **Component** | Exergy loss [%][26] |
| **Compressor** | 5.9 |
| **Expander** | 4.9 |
| **Hot HEX** | 1.2 |
| **Regenerator** | 4.2 |
| **Cold HEX** | 0.9 |
| **DISCHARGE** | |
| **Compressor** | 6.9 |
| **Expander** | 6.0 |
| **Hot HEX** | 1.5 |
| **Regenerator** | 2.6 |
| **Cold HEX** | 1.3 |
| **Auxiliary HEX** | 6.2 |
| **Fan consumption** | 0.0 |
| **Electromechanical losses** | 3.8 |
| **∑ exergy losses** | 45.5 |
| **RTE** | 54.5 |

[26] Percentage value referred to the total net electricity charged

# Appendix B: Alternative discharge layout

In this chapter an alternative discharge layout is investigated, in which the compression is divided in two stage compression with an intercooler in between. In Figure 0.1 and Figure 0.2 the plant scheme and the T-s diagram of the alternative discharge layout are presented. Dividing the compression has the advantage of reducing the compression work required and also reducing the average temperature at which heat is rejected to the environment. This is proofed also by the exergy analysis presented in **Error! Reference source not found.**, the Auxiliary heat exchanger exergy loss goes from 5.9% in the base case to 4,2% in the intercooled case. Compared to the basic discharge layout, this layout has a higher RTE which is 57.2% compared to 56.0% of the cycle with a discharge design as the in CASE A of Table 5.3, with a power equal to the RTE. The two RTE are calculated with the input data of Table 5.2Table 5.2 Input parameters of the model used in the exergy analysis

*Table 1 Comparison of exergy analysis for basic Brayton cycle regenerative PHES and of regenerative cycle PHES with two stage intercooled compression*

| **EXERGY ANALYSIS** | | |
|---|---|---|
| **Charge cycle** | Exergy Loss [%] | |
| Compressor | 5.9 | |
| Expander | 4.9 | |
| Hot HEX | 1.2 | |
| Cold HEX | 0.9 | |
| Regenerator | 4.2 | |
| **Discharge cycle** | Base | Intercooled |
| Compressor | 6.8 | 6.7 |
| Expander | 6.1 | 6.0 |
| Hot HEX | 1.2 | 1.2 |
| Cold HEX | 1.0 | 1.0 |
| Regenerator | 1.9 | 2.5 |
| Auxiliary HEX | 5.9 | 4.2 |
| Fan consumption | 0.4 | 0.4 |
| Electromechanical | 3.5 | 3.6 |
| RTE | 56.0 | 57.2 |

The compression is divided using a parameter A such as:

$$\beta_{comp,1} = \beta_{comp,total}^{A} \qquad \beta_{comp,2} = \beta_{comp,total}^{(1-A)} \qquad (0.1)$$

where $\beta_{comp,1}$ and $\beta_{comp,2}$ are the compression ratio for the first and second compressor. The parameters $A$ was optimised with respect to the RTE, and the optimal value was found to be $A$=0.72. This is the value which allows to reject 60% of the heat to the environment through the intercooler and 40% through the auxiliary heat exchanger. The intercooler was modelled in the same way as the auxiliary heat exchanger.

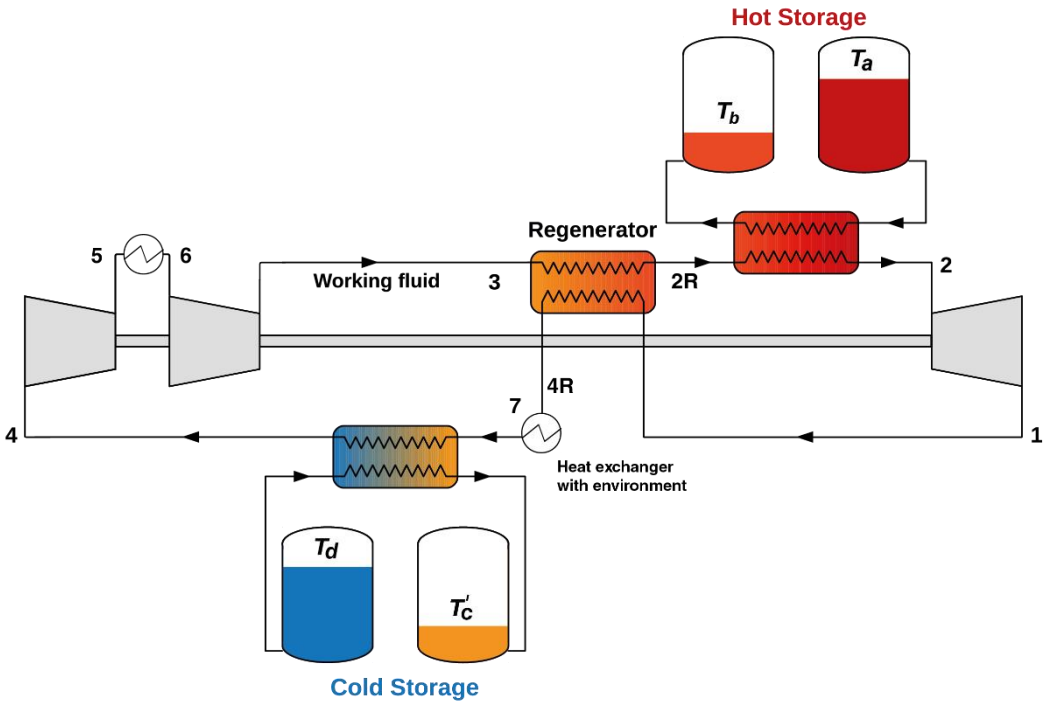


*Figure 0.1 Plant scheme of a regenerative Brayton PHES with liquid TES, discharge cycle with intercooled compression*

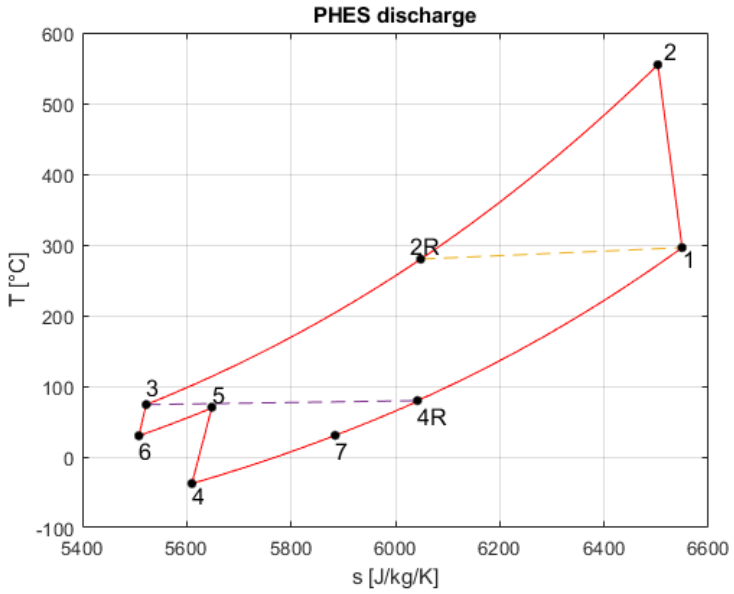


*Figure 0.2 T-s diagram of the discharge cycle for a regenerative PHES with intercooled two stage compression*

Clearly this solution has an increased overall installation cost and also it complicates the plant scheme. Due to the low increase of the RTE and because of the increased complexity of the plant this solution results to be not effective and therefore is not further investigated.